Spring 5-7-2011

Study of Innate Immune Response Components in West Nile Virus Infected Cells

Husni M. Elbahesh
Georgia State University

STUDY OF INNATE IMMUNE RESPONSE COMPONENTS IN WEST NILE VIRUS INFECTED CELLS

by

HUSNI MUHAMMAD HISHAM ELBAHESH

Under the direction of Margo A. Brinton

ABSTRACT

Two cellular innate responses, the dsRNA protein kinase (PKR) pathway and the 2'-5' oligoadenylate synthetase (OAS)/RNase L pathway, are activated by dsRNAs produced by viruses and reduce translation of host and viral mRNAs. PKR activation results in eIF2a phosphorylation. As a consequence of eIF2a phosphorylation, stress granules (SGs) are formed by the aggregation of stalled SG proteins with pre-initiation complexes and mRNA. West Nile virus (WNV) infections do not induce eIF2a phosphorylation despite upregulation of PKR mRNA and protein suggesting an active suppression of PKR activation. Assessment of the mechanism of suppression of PKR activation in WNV-infected cells indicated that WNV infections do not induce PKR phosphorylation so that active suppression is not required.

In contrast to infections with "natural" strains of WNV, infections with the chimeric W956 infectious clone (IC) virus efficiently induce SGs in infected cells. After two serial passages, the IC virus generated a mutant (IC-P) that does not induce SGs efficiently but does induce the formation of NS3 granules that persist throughout the infection. This mutant was characterized.

2'-5' oligoadenylate synthetases (OAS) are activated by viral dsRNA to produce 2-5A oligos that activate RNase L to digest viral and cellular RNAs. Resistance to flavivirus-induced disease in mice is conferred by the full-length 2'-5' oligoadenylate synthetase 1b (Oas1b) protein. Oas1b is an inactive synthetase that is able to suppress the *in vitro* synthetase activity of the active synthetase Oas1a. The ability of Oas1b to inhibit Oas1a synthetase activity *in vivo* and to form a heteromeric complex with Oas1a was investigated. Oas1b suppressed 2-5A production *in vivo*. Oas1a and Oas1b overexpressed in mammalian cells co-immunoprecipitated indicating the formation of heteromeric complexes by these proteins.

Unlike mice, humans encode a single OAS1 gene that generates alternatively spliced transcripts encoding different isoforms. Synthetase activity has previously been reported for only three of the isoforms. The *in vitro* synthetase activity of additional OAS1 isoforms was analyzed. All tested isoforms synthesized higher order 2-5A oligos. However, p44A only produced 2-5A dimers which inhibit RNase L.

INDEX WORDS: West Nile virus, PKR, dsRNA, 2'-5' oligoadenylate synthetase, Oas1b, EIF2α.

STUDY OF INNATE IMMUNE RESPONSE COMPONENTS IN WEST NILE VIRUS INFECTED CELLS

by

HUSNI MUHAMMAD HISHAM ELBAHESH

A Dissertation Submitted in Partial Fulfillment of the Requirements for the Degree of

Doctor of Philosophy

in the College of Arts and Sciences

Georgia State University

2011

STUDY OF INNATE IMMUNE RESPONSE COMPONENTS IN WEST NILE VIRUS INFECTED CELLS

by

HUSNI MUHAMMAD HISHAM ELBAHESH

Committee Chair: Margo A. Brinton

Committee: Susanna F. Greer

Zhi-Ren Liu

Electronic Version Approved:

Office of Graduate Studies

College of Arts and Sciences

Georgia State University

May 2011

DEDICATION

I dedicate this dissertation to my family. To my wife, Karen, who has stood by me through this journey and has given me the strength and support to carry out this endeavor. To my parents, Amal and Hisham, who instilled within me the desire for the pursuit of knowledge and have given me their unconditional love. To my brothers, Ehab and Ahmad, and my sister Dina for the endless and perfectly timed laughter and comedy.

"It stands to the everlasting credit of science that by acting on the human mind it has overcome man's insecurity before himself and before nature."

-- Albert Einstein

ACKNOWLEDGEMENTS

I would like to extend my sincerest appreciation to my principal advisor Dr. Margo A. Brinton who allowed me to work in her lab and complete this dissertation. I would like to thank Dr. Brinton for her support, patience, and expert advice. Thanks to the committee members Dr. Susanna Greer and Dr. Zhi-Ren Liu for their suggestions and corrections. I would especially like to thank Dr. Svetlana V. Scherbik for her technical advice, tremendous patience, and her help. I also would like to thank the rest of the Brinton lab members and colleagues at GSU for their friendship and advice.

TABLE OF CONTENTS

LIST OF FIGURES

CHAPTER 1

INTRODUCTION

General Characteristics of West Nile virus

West Nile virus (WNV) was first isolated in the West Nile region of Uganda from a febrile patient in 1937 (Gubler, 2007; Smithburn, 1940). Until 1999 WNV was limited to countries of the northern Mediterranean region, parts of Europe, the Middle East, Africa, West Asia, and Australia. In 1999, WNV extended its geographical distribution to the Western hemisphere where it has spread rapidly (Lanciotti et al., 2002). WNV is maintained in a mosquito-bird cycle in nature and virus spread follows migratory patterns of infected birds. Humans and domestic animals are susceptible to WNV infection. However, since viremia titers in these hosts are not sufficiently high enough for a mosquito to obtain virus in a blood meal, they are considered incidental, dead-end hosts (Gubler, 2007). The majority of WNV infections in humans are asymptomatic. However, flu-like symptoms are observed in about 20% of infected individuals. Less than 1% of infected persons develop severe neurologic disease, such as encephalitis, or poliomyelitis, which is sometimes fatal. (Petersen et al., 2003; Saad et al., 2005).

WNV Virion Structure

WNV virions are small, spherical, enveloped particles that are ~50 nm in diameter with nucleocapsids that range from 20 to 30 nm in diameter (Murphy, 1980). The virion envelope is a host-derived membrane in which the viral membrane (M) and envelope (E)

proteins are anchored. The C-terminal regions of these proteins are hydrophobic and span the membrane twice (Zhang et al., 2003a; Zhang et al., 2003b). During virion maturation, the M precursor (prM) is cleaved by the host protease, furin. This cleavage results in a conformational change in the associated E protein trimers that leads to the formation of E dimers that interact to form an icosohedral protein shell on the outer side of the virion envelope (Lindenbach, 2007).

Replication Cycle

Flaviviruses replicate entirely in the cytoplasm of infected cells (Fig. 1.1). The first step of the viral infection cycle is binding of the virion E protein to an unknown host receptor(s). Viral entry occurs via clathrin-mediated endocytosis. Acidification of the virus-containing endosomal vesicle causes a conformational change in the viral E protein that leads to fusion of the viral envelope with the endocytic membrane and ultimately facilitates release of the viral nucleocapsid as well as the genomic viral RNA (Chu and Ng, 2004). In the cytoplasm, the positive-sense genomic RNA is translated into a single polyprotein that is co- and post-translationally cleaved by viral and host proteases to produce the mature viral proteins (Lindenbach, 2007). The viral genome also serves as the template for minus-strand RNA synthesis. Genome RNA synthesis is more efficient than that of the minus-strand RNA resulting in a 10 to 100:1 ratio of positive- to minus-strand RNA in infected cells (Chu and Westaway, 1985).

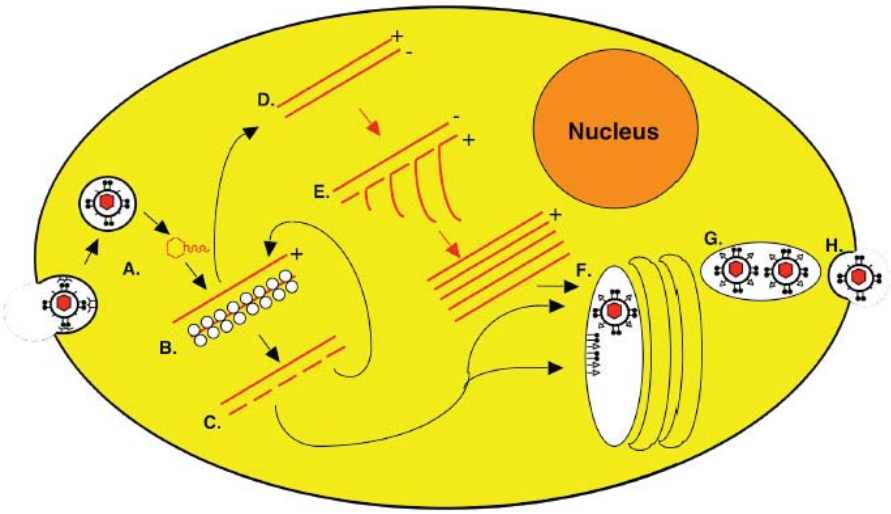

Figure 1.1. WNV replication cycle. (A) Attachment and entry of virion and uncoating of the virion RNA. (B) Translation of the virion RNA. (C) Proteolytic processing of the viral polyprotein. (D) Synthesis of minus strand RNA. (E) Synthesis of genomic RNA from the minus strand RNA. (F) Encapsidation of the viral genome and assembly of immature virions. (G) Transport of the virions to the plasma membrane. (H) Exocytosis of the virions. Figure and legend from (Brinton, 2002).

Viral RNA replication occurs inside perinuclear replication complexes that are located inside vesicles that are invaginations of rough ER membranes. Each vesicle opens to the cytoplasm via a membraneous neck (Gillespie et al., 2010). The newly transcribed genomic viral RNA exits the replication complex through the neck of these vesicles and is either translated or binds to capsid proteins associated with ER membranes leading to virion budding into the lumen of the ER (Gillespie et al., 2010). Non-infectious, immature viral particles are transported through the *trans*-Golgi network where prM is cleaved into the M protein by the host protease furin to generate mature infectious particles that are transported to the plasma membrane in vesicles (Mackenzie and Westaway, 2001; Stadler et al., 1997). Virions are released from the cell by exocytosis as

the virus-containing vesicles fuse with the plasma membrane (Mackenzie and Westaway, 2001).

Genomic RNA

The single-stranded, positive-sense WNV genome RNA is approximately 11 kb in length. The 5' end of the genome contains a type I cap but the 3' end lacks a poly(A) tail. The genomic RNA encodes a single polyprotein that is co-translationally and post-translationally cleaved by viral and host proteases to produce three structural proteins (E, M and C), and seven nonstructural proteins (NS1, NS2A, NS2B, NS3, NS4A, NS4B and NS5) (Fig. 1.2) (Lindenbach, 2007).

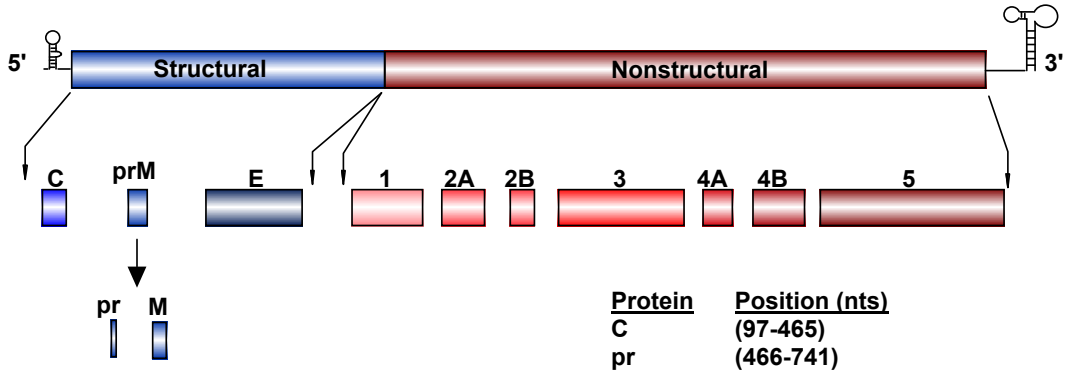

Protein	Position (nts)
C	(97-465)
pr	(466-741)
M	(742-966)
E	(967-2469)
NS1	(2470-3525)
NS2A	(3526-4218)
NS2B	(4219-4611)
NS3	(4612-6468)
NS4A	(6469-6915)
NS4B	(6916-7680)
NS5	(7681-10395)

Figure 1.2. Schematic of a flavivirus genome. The polyprotein and mature processed proteins are shown. Figure from (Brinton, 2002).

Viral Structural Proteins

Three viral structural proteins, E, prM/M and C, are encoded at the 5' end of the viral ORF and are associated with the virion (Lindenbach and Rice, 2003). The precursor of C protein, anchored C, contains a C-terminal hydrophobic domain that spans the ER membrane and targets prM for translocation to the ER prior to cleavage. Anchored C is cleaved at its C-terminus by the viral protease on the cytoplasmic side of the ER membrane to generate the mature C protein (~11 kDa) (Lindenbach, 2007; Yamshchikov and Compans, 1994). The mature C protein folds into a dimer that is composed of 2 monomers each containing 4 alpha-helices. Internal hydrophobic regions of C protein mediate association with the ER membrane while nonspecific interactions between the charged residues at the N- and C-termini of mature C protein and the viral genomic RNA are thought to facilitate assembly of the nucleocapsid around the genomic RNA (Khromykh and Westaway, 1996; Lindenbach et al., 2007). Additionally, C protein has been reported to exhibit RNA chaperoning activity that suggests it may play a role in structural rearrangements of viral RNA during WNV replication (Ivanyi-Nagy et al., 2008).

The M protein (~8 kDa) is a proteolytic fragment of its glycoprotein precursor, prM protein (~26 kDa). The C-terminal region of prM contains two transmembrane domains that anchor prM and M in the ER membrane, and may aid in the heterodimerization of prM and E. The prM protein maintains surface E proteins in a raised trimeric confirmation thus blocking premature viral fusion with the cellular

membranes during virion trafficking through acidic compartments of the *trans*-Golgi secretory pathway (Heinz et al., 1994; Zhang et al., 2003b)

The major virion surface protein is the E protein, a glycosylated type I integral membrane protein that is ~53 kDa in size. The E protein mediates viral attachment, membrane fusion as well as virion assembly (Mukhopadhyay et al., 2005). In mature virions, E protein homodimers are arranged in a head-to-tail conformation and lie parallel to the lipid bilayer (Heinz and Allison, 2000). The E protein contains the major antigenic determinants on the surface of flavivirus particles (Lindenbach, 2007).

Viral Non-Structural Proteins

The NS1 protein (~47 kDa) has been shown to exist as a monomer, homodimer and a hexamer, and is the only flaviviral nonstructural protein known to be glycosylated (Grun and Brinton, 1986; Lindenbach, 2007; Winkler et al., 1989; Winkler et al., 1988). NS1 has been reported to play a role in viral replication, and the hexameric form is secreted from infected cells and has been reported to inhibit complement activation in during WNV infection (Chung et al., 2006; Flamand et al., 1992; Flamand et al., 1999; Khromykh et al., 1999; Lindenbach and Rice, 1997). The eight C-terminal residues of NS1 and the ~140 N-terminal residues of NS2A are required for the cleavage of NS1 from NS2A by an unknown host protease (Falgout and Markoff, 1995).

The NS2A and NS2B proteins are small (23 kDa and 13 kDa, respectively) hydrophobic proteins. Mutations that prevent cleavage at the NS1/NS2A junction have proven lethal for the virus without affecting viral RNA replication, suggesting a role for

NS2A in virion assembly (Kummerer and Rice, 2002; Liu et al., 2003). In addition, mutational analysis of WNV and Kunjin NS2A demonstrated that this protein mediates attenuation of type I interferon (IFN) signaling (Liu et al., 2004; Liu et al., 2006). NS2B is a membrane-associated protein that is required as a cofactor for the activity of the serine protease of NS3 (Chambers et al., 1991; Chambers et al., 1993).

The NS3 is a large ~70 kDa protein is highly conserved among flaviviruses. The N-terminal region comprises the NS3 protease domain that forms an active complex with NS2B. NS3 autocatalytically cleaves itself from the viral polyprotein and then cleaves at multiple other sites within the polyprotein (Nall et al., 2004). RNA-stimulated NTPase and RNA helicase activities have been mapped to C-terminal regions of the NS3 protein. Additionally, the NS3 mediates dephosphorylation of the 5' end of the viral genomic RNA prior to cap addition. Collectively, the data establishes the requirement of NS3 in viral RNA replication (Borowski et al., 2000; Li et al., 1999; Wengler, 1993; Wengler and Wengler, 1991).

NS4A and NS4B are small hydrophobic proteins (16 and 27 kDa, respectively) that localize to the ER membrane. Neither of these proteins share sequence motif homology with known enzymes. The C-terminus of NS4A is cleaved by both host signal peptidase and viral serine protease (Lin et al., 1993). NS4A has been shown to interact with NS1 and colocalizes with replication complexes within vesicle packets, supporting a role for NS4A/NS1 in RNA replication (Lindenbach and Rice, 1999; Mackenzie et al., 1998). Overexpression of dengue NS4A induced membrane rearrangements similar to those observed in infected cells (Miller et al., 2007; Roosendaal et al., 2006; Welsch et

al., 2009). Kunjin NS4B can induce membrane proliferation and rearrangement and perinuclear protein accumulation when overexpressed (Westaway et al., 1997). NS4A and NS4B play a role in attenuation of the IFN antiviral response to WNV infection and NS4B was shown to inhibit STAT phosphorylation and subsequent signaling (Liu et al., 2005; Munoz-Jordan et al., 2005). NS2A, NS2B, NS3, NS4A and NS4B form ER membrane-associated complexes in infected cells (Lindenbach, 2007).

NS5 is a large (96 kDa) multifunctional protein that is the most conserved flavivirus protein. The C-terminal region of the NS5 protein contains the viral RNA-dependent RNA polymerase (RdRp) (Koonin, 1991). NS5 also has an N-terminal methyltransferase domain that methylates the cap structure of flaviviral genomic RNAs (Koonin, 1993; Lindenbach, 2007; Ray et al., 2006; Zhou et al., 2007). NS5 has been show to interact with NS3 *in vivo* as well as *in vitro* (Kapoor et al., 1995). Phosphorylation of NS5 by cellular serine/threonine kinases *in vivo* has been previously reported and this phosphorylation may regulate NS3-NS5 interactions (Kapoor et al., 1995; Mackenzie et al., 2007; Reed et al., 1998). Although predominantly cytoplasmic, the flavivirus NS5 has also been detected in the nuclei of infected cells (Buckley et al., 1992; Kapoor et al., 1995; Miller et al., 2006). In addition to RdRp and helicase functions, NS5 plays a role in modulating the antiviral host response. In cells infected with virulent strains of WNV such as, NY99, NS5 was shown to be an antagonist of IFN signaling by preventing accumulation of STAT1 phosphorylation. Interestingly, mutation of Kunjin NS5 at S653F increased the virulence of this typically attenuated

strain by making it capable of inhibiting STAT1 phosphorylation (Laurent-Rolle et al., 2010).

Genomic Untranslated Regions

The WNV 5' and 3' untranslated regions (UTRs) are 96 nt and 631 nt in length, respectively (Brinton et al., 1986; Markoff, 2003). Stable stem-loop (SL) structures are predicted to be formed by the terminal sequences of both the 5' and 3' UTRs (Brinton and Dispoto, 1988). While only short regions within the 5′ UTR sequence are conserved among different flaviviruses, the 5′ SL structure it forms shares structural homology with those of different flaviviruses (Brinton and Dispoto, 1988). The 3′ UTR of the minus-strand, used to initiate plus-strand synthesis, is complementary to the 5′ UTR. In dengue infected cells, deletions in the 5′ UTR of the viral genomic RNA proved lethal (Cahour et al., 1995). Similarly, only a few conserved sequences are present in the 3' UTR of flaviviruses (Lindenbach, 2007). However, the terminal 3′ SL forms a structure that is highly conserved among divergent flaviviruses (Brinton et al., 1986). Three hamster cell proteins were previously reported to interact with the 3′ SL of the WNV genomic RNA. One of these proteins was identified as the translation elongation factor 1A (EF1A) which is responsible for recruiting aminoacyl-tRNA to the A site of the ribosome (Blackwell and Brinton, 1995; Blackwell and Brinton, 1997; Condeelis, 1995; Grassi et al., 2007; Lewin, 2000). Mutational evidence indicated that minus-strand RNA synthesis is facilitated by the interaction between eEF1A and the WNV 3' (+) SL (Blackwell and Brinton, 1997; Davis, 2007; Khromykh et al., 2003).

Cap-Dependent Translation Initiation

Most eukaryotic mRNAs are modified in the nucleus before transport to the cytoplasm for translation. The 5' end of the mRNA is capped and a 3' poly(A) tail (~50 to 300 nts in length) is added. These terminal modifications serve to increase translational efficiency as well as stabilize the mRNA (Hall, 2002; Schoenberg and Maquat, 2009). The 5' cap of mRNAs is a molecular tag that initiates translation by recruitment of the 40S ribosomal subunit via the eIF4F cap-binding complex which consists of eIF4E, eIF4A and eIF4G (Lopez-Lastra et al., 2010; Lopez-Lastra et al., 2005). The eIF4E subunit directly binds to the 5' cap, eIF4A unwinds secondary structures within the 5' UTR of mRNAs through its ATPase and helicase activities and eIF4G serves as a scaffold protein that links the mRNA cap and the 40S ribosomal subunit via interaction with eIF4E and eIF3, respectively (Gingras et al., 1999; Lopez-Lastra et al., 2010; Lopez-Lastra et al., 2005). The poly(A) binding protein (PABP) binds to the 3' poly(A) tail of mRNAs as well as to the PABP-interacting protein-1 (PAIP-1) which is a eIF4G homologue. The eIF4G subunit bridges the 5' cap and the 3' poly(A) tail of the mRNA via interactions with PAIP-1 leading to a "closed loop" conformation of the mRNA which increases translation efficiency (Kahvejian et al., 2001). The mechanism by which mRNA circularization increases the efficiency of translation has yet to be determined. Possible explanations include efficient recycling of the 40S ribosomal subunit allowing for rapid translational re-initiation, increased stability of the mRNA and biasing translation towards full-length RNAs (Lopez-Lastra et al., 2010; Lopez-Lastra et al., 2005). Because the WNV genome does not have a 3' poly(A)

tail, it is not known whether it forms a closed loop conformation. The 43S preinitiation complex is formed at the 5' cap of the mRNA upon recruitment of the 40S ribosomal subunit bound to eIF2-GTP/Met-tRNAi, eIF3, eIF1 and eIF1A. Both eIF1 and eIF1A are required for mRNA binding and scanning of the 43S complex in a 5' to 3' direction (Lopez-Lastra et al., 2010; Pestova et al., 1998). The initiation codon recognized is usually the first AUG triplet present within the nearest Kozak consensus sequence (G/AXXAUGG) downstream of the 5' cap (Kozak, 1986). Ribosomal scanning from the 5' cap is thought to be the mechanism by which flavivirus genomes are translated (Lindenbach, 2007). Interactions between the cellular proteins binding to the 3' and 5' terminal genome RNA structures may bridge the 5' and 3' termini thereby facilitating replication of the viral RNA (Brinton, 2002). However, cellular and/or viral proteins that may be involved in translational regulation of the WNV genomic RNA have not yet been identified.

Virus Stress-Induced Genes

The virus stress-inducible genes (VSIG) are modulated in response to virus infection, dsRNA and IFN. Viral infections cause cellular stresses that result in a strong and transient induction of these genes (Sarkar and Sen, 2004). IFN responses serve as an essential first line of host defense against many viruses including flaviviruses. IFNs are classified as Type I and Type II. Both types have antiviral activity (Samuel, 2001). The two types of IFN are structurally unrelated and their actions are mediated by different and structurally unrelated cell-surface receptors (Sarkar and Sen, 2004). The Type I IFN

family includes IFN-α, IFN-β, IFN-ω and IFN-τ; while IFN-γ is the only known Type II IFN (Sarkar and Sen, 2004). A positive regulatory domain (PRD) and a PRD-like element (PRD-LE) are *cis*-acting elements present in the promoters of IFN-α and IFN-β, respectively; these elements are inducible by IFN regulatory factors (IRFs) (Nakaya et al., 2001). IFN produced in an infected cell is secreted and binds to receptors on the surface of both infected cells and uninfected cells. IFN-α/β binding to the IFN-α/β receptor (IFNAR) causes cross-activation of Jak1 and Tyk2, which phosphorylate one another along with STAT1 and STAT2. The phosphorylation of these two STATs results in the formation of IFN-stimulated gene factor 3 (ISGF3), a trimeric complex that includes STAT1, STAT2 and IRF9. The ISGF3 complex translocates to the nucleus where it binds to IFN-stimulatory response elements (ISREs) in the promoter regions of IFN-stimulated genes (ISGs) such as PKR, 2'-5' oligoadenylate synthetase (OAS) family members and IRF7, activating their transcription (Darnell et al., 1994; Nakaya et al., 2001; Stark et al., 1998). IRF7 phosphorylation in response to viral infection leads to translocation of IRF7 to the nucleus to further activate IFNα/β promoters resulting in massive IFNα/β production that is maintained via a positive feed-back loop (Au et al., 1998; Nakaya et al., 2001; Samuel, 2001). Although VSIG were initially discovered as IFN-inducible genes, their expression can be induced independently of IFN (Bandyopadhyay et al., 1995; Daly and Reich, 1995; Weaver et al., 1998).

RNA Sensor-Mediated Translational Inhibition

The IFN response to viruses is initiated at early stages of viral infection and is mediated by pattern recognition receptors (PRRs) that include retinoic acid-inducible gene I (RIG-I), melanoma differentiation associated gene 5 (MDA5) and Toll-like receptors (TLRs) that recognize viral pathogen-associated molecular patterns (PAMPs) such as single- and/or double-stranded viral RNA structures (Diamond, 2009). Engagement of these PRRs ultimately leads to activation of transcription factors including IRF3 and IRF7 that induce expression of ISGs (Li et al., 2007; Stark et al., 1998) which in turn amplify the antiviral response within infected cells and neighboring uninfected cells (Fig. 1.3).

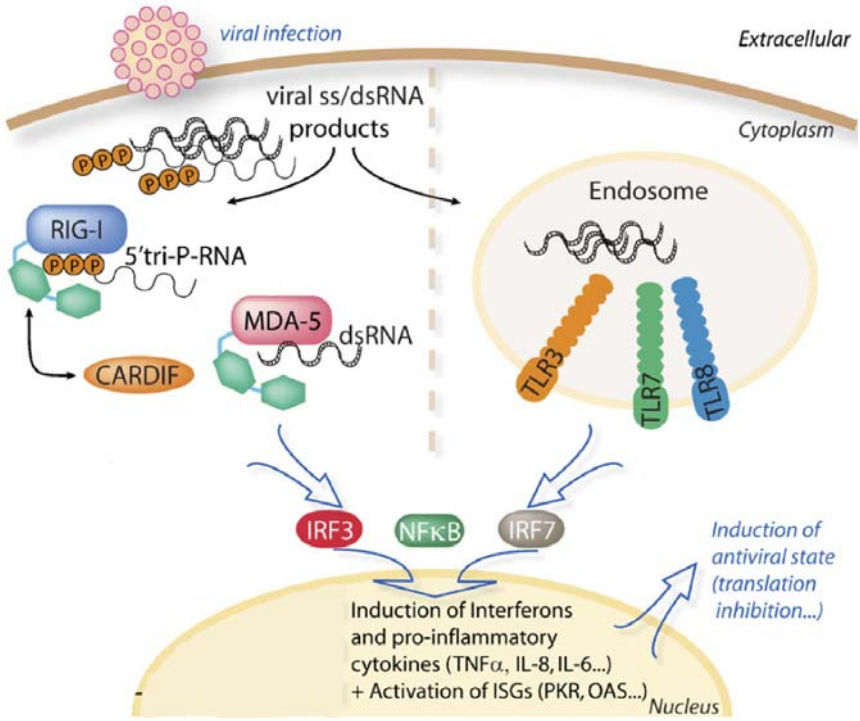

Figure 1.3. Sensing of ssRNA/dsRNA by the immune system. On the left of the diagram, sensing in non-immune cell types is represented. This relies on RIG-I (for RNAs with 5'-triphosphate) and MDA-5 (for dsRNAs). On the right of the schematic, innate immune sensing of ss/dsRNAs by endosomal TLRs in immune cells is represented. Figure and modified legend from (Gantier and Williams, 2007).

Additionally, cell-type specific (e.g. immune vs. non-immune cell) responses have previously been reported in response to viral RNAs (Gantier and Williams, 2007). In non-plasmacytoid dendritic cells and fibroblasts, the Type I IFN response to infection with ssRNA viruses is mediated through RIG-I (Kato et al., 2005). On the other hand, MDA5 was reported to be the prime sensor of poly(I:C) as well as of encephalomyocarditis virus (EMCV) RNA (Gitlin et al., 2006; Kato et al., 2006). Activation of these sensors leads to IPS-1/MAVS/CARDIF-mediated activation of transcription factors such as IRF3 and NFκB (Hiscott et al., 2006). In some immune cells, viral RNAs are initially sensed by endosomal TLRs and this results in transcriptional activation of IRFs and NFκB. Collectively, activation of these pathways confers a general antiviral state.

The PKR and the 2'-5' OAS pathways are part of the IFN-induced antiviral response and are activated by viral dsRNA structures. Unlike the cell transcriptional response mediated through the PRRs, the PKR and OAS responses limit viral protein synthesis through translational inhibition of viral mRNAs and ultimately lead to apoptosis (Gantier and Williams, 2007). Recognition of dsRNA or helical regions of hairpin structures within single-stranded RNAs by PKR promotes its dimerization and activation through subsequent autophosphorylation. Active PKR dimers bind to and phosphorylate eIF2a at S51. Phosphorylated eIF2a forms a stable complex with its guanine exchange factor, eIF2B, and this prevents efficient recycling of GDP-bound eIF2a to GTP-eIF2a leading to inhibition of translational initiation (Fig. 1.4).

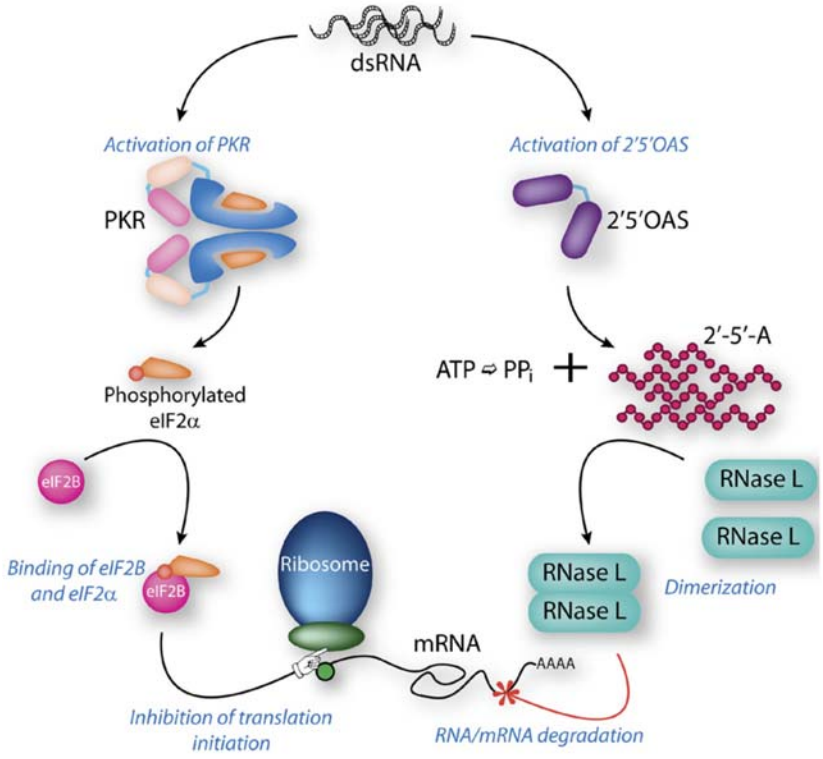

Figure 1.4. DsRNA-induced translation inhibition mechanisms. Double-stranded RNA promotes activation of PKR and 2'-5'OAS. These two events fortify the antiviral state by stopping protein synthesis. Figure and modified legend from (Gantier and Williams, 2007).

Binding of dsRNA to an OAS protein causes a conformational change that activates the enzyme. Active OASs catalyze the polymerazation of ATP into 2'-5' oligoadenylate (2-5A) that binds to RNase L and induces its dimerization and activation. Active RNase L nonspecifically degrades ssRNAs whether of cellular or viral origin which ultimately leads to apoptosis (Fig. 1.4).

GOALS OF THIS DISSERTATION

The dsRNA-induced translational inhibition in response to virus infection is largely mediated by two pathways: the dsRNA protein kinase (PKR) pathway and the 2'-5' oligoadenylate synthetase (OAS)/RNase L pathway. Both of these pathways can be activated by viral dsRNAs or secondary structures within viral ssRNAs that are produced in infected cells. Activation of the PKR pathway results in phosphorylation of eIF2a leading to an attenuation of translational initiation, whereas activation of the OAS/RNase L pathway results in degradation of virus and cellular RNAs. Components of these pathways were investigated under the following aims:

Specific Aim 1. Investigation of the mechanism of suppression of PKR phosphorylation in WNV-infected cells.

***Additional Aim*. Analysis of a spontaneous WNV infectious clone mutant.**

Specific Aim 2. Functional analysis of the mouse Oas1b protein.

Specific Aim 3. Synthetase activity analysis of human OAS1 splice variant proteins.

SUMMARY OF DISSERTATION RESULTS

PKR can be activated by viral dsRNA and then phosphorylate eIF2α leading to the formation of SGs and the attenuation of cell translation. Infections with "natural" WNV strains inefficiently induce eIF2a phosphorylation and SGs. Although total PKR was upregulated, PKR was not phosphorylated in WNV-infected MEFs and BHK cells. The low level of PKR phosphorylation observed in WNV-infected MEFs was found to be due to Type I IFN secreted in response to the infection. While PKR did not colocalize

with most of the cellular PKR inhibitor proteins tested, it did colocalize and co-immunoprecipitate with Nck in WNV-infected and uninfected cells. The association with Nck suggested PKR was inactive. In addition, even when this PKR-associated inhibitor was absent in Nck1,2-/- cells, PKR was still only minimally activated after WNV infection. Although several WNV RNAs activated PKR *in vitro*, this was not observed *in vivo*. Also, WNV infection did not interfere with the ability of intracellular PKR to respond to the non-viral dsRNA activator, poly(I:C), and virus yields were similar in control and PKR-/- cells. The results showed that PKR phosphorylation was not actively suppressed in WNV-infected BHK cells and that the PKR present did not exert an antiviral effect.

The chimeric WNV W956 IC (IC) efficiently induces SGs. Passaging the IC virus generated a mutant (IC-P) virus. IC-P virus infections did not efficiently induce SGs but did induce the formation of large NS3 granules that persisted throughout the infection. The NS3 granules localized to ER-derived membranes but did not colocalize with viral replication complexes. The data suggest that the NS3 granules are not active replication complexes and that the viral protein-directed membrane rearrangement required to form replication complexes may not occur properly/efficiently in IC-P virus-infected cells. Preliminary 454 deep sequencing identified a single mutation in the NS4B gene which may be responsible for the formation of NS3 granules and/or could change the folding of the viral RNA affecting viral RNA replication efficiency.

Murine Oas1b protein was previously shown to be an inactive synthetase and to inhibit Oas1a synthetase activity *in vitro*. Cells expressing full-length Oas1b produced

lower levels of 2-5A in response to poly(I:C) stimulation. These results show that Oas1b, but not Oas1btr, acts as a dominant negative protein for Oas1a synthetase activity, possibly to fine tune a potentially dangerous response. Co-immunoprecipitation assays demonstrated that Oas1a and Oas1b form heteromers suggesting that an interaction between these two proteins likely mediates Oas1b inhibition of Oas1a synthetase activity.

Nine alternatively spliced human OAS1 isoforms have been identified. Of the 9 isoforms, only p42, p46 and p48 were previously assayed for 2-5A synthetase activity. The various isoforms were expressed in bacteria and shown to be active synthetases. All of the isoforms synthesized higher order 2-5A except p44A, which generated 2-5A dimers. The results suggest that isoforms with different OAS1 C-termini are active 2-5A synthetases, but the C-terminus can affect the type of 2-5A produced. It is not known whether the human Oas1 isoforms are involved in regulating synthetase activity.

REFERENCES:

Au, W. C., Moore, P. A., LaFleur, D. W., Tombal, B., and Pitha, P. M. (1998). Characterization of the interferon regulatory factor-7 and its potential role in the transcription activation of interferon A genes. *J Biol Chem* **273**(44)**,** 29210-7.

Bandyopadhyay, S. K., Leonard, G. T., Jr., Bandyopadhyay, T., Stark, G. R., and Sen, G. C. (1995). Transcriptional induction by double-stranded RNA is mediated by interferon-stimulated response elements without activation of interferon-stimulated gene factor 3. *J Biol Chem* **270**(33)**,** 19624-9.

Blackwell, J. L., and Brinton, M. A. (1995). BHK cell proteins that bind to the 3' stem-loop structure of the West Nile virus genome RNA. *J Virol* **69**(9)**,** 5650-8.

Blackwell, J. L., and Brinton, M. A. (1997). Translation elongation factor-1 alpha interacts with the 3' stem-loop region of West Nile virus genomic RNA. *J Virol* **71**(9)**,** 6433-44.

Borowski, P., Mueller, O., Niebuhr, A., Kalitzky, M., Hwang, L. H., Schmitz, H., Siwecka, M. A., and Kulikowsk, T. (2000). ATP-binding domain of NTPase/helicase as a target for hepatitis C antiviral therapy. *Acta Biochim Pol* **47**(1)**,** 173-80.

Brinton, M. A. (2002). The molecular biology of West Nile Virus: a new invader of the western hemisphere. *Annu Rev Microbiol* **56,** 371-402.

Brinton, M. A., and Dispoto, J. H. (1988). Sequence and secondary structure analysis of the 5'-terminal region of flavivirus genome RNA. *Virology* **162**(2)**,** 290-9.

Brinton, M. A., Fernandez, A. V., and Dispoto, J. H. (1986). The 3'-nucleotides of flavivirus genomic RNA form a conserved secondary structure. *Virology* **153**(1)**,** 113-21.

Buckley, A., Gaidamovich, S., Turchinskaya, A., and Gould, E. A. (1992). Monoclonal antibodies identify the NS5 yellow fever virus non-structural protein in the nuclei of infected cells. *J Gen Virol* **73 (Pt 5),** 1125-30.

Cahour, A., Pletnev, A., Vazielle-Falcoz, M., Rosen, L., and Lai, C. J. (1995). Growth-restricted dengue virus mutants containing deletions in the 5' noncoding region of the RNA genome. *Virology* **207**(1)**,** 68-76.

Chambers, T. J., Grakoui, A., and Rice, C. M. (1991). Processing of the yellow fever virus nonstructural polyprotein: a catalytically active NS3 proteinase domain and NS2B are required for cleavages at dibasic sites. *J Virol* **65**(11)**,** 6042-50.

Chambers, T. J., Nestorowicz, A., Amberg, S. M., and Rice, C. M. (1993). Mutagenesis of the yellow fever virus NS2B protein: effects on proteolytic processing, NS2B-NS3 complex formation, and viral replication. *J Virol* **67**(11)**,** 6797-807.

Chu, J. J., and Ng, M. L. (2004). Infectious entry of West Nile virus occurs through a clathrin-mediated endocytic pathway. *J Virol* **78**(19)**,** 10543-55.

Chu, P. W., and Westaway, E. G. (1985). Replication strategy of Kunjin virus: evidence for recycling role of replicative form RNA as template in semiconservative and asymmetric replication. *Virology* **140**(1)**,** 68-79.

Chung, K. M., Liszewski, M. K., Nybakken, G., Davis, A. E., Townsend, R. R., Fremont, D. H., Atkinson, J. P., and Diamond, M. S. (2006). West Nile virus nonstructural

protein NS1 inhibits complement activation by binding the regulatory protein factor H. *Proc Natl Acad Sci U S A* **103**(50)**,** 19111-6.

Condeelis, J. (1995). Elongation factor 1 alpha, translation and the cytoskeleton. *Trends Biochem Sci* **20**(5)**,** 169-70.

Daly, C., and Reich, N. C. (1995). Characterization of specific DNA-binding factors activated by double-stranded RNA as positive regulators of interferon alpha/beta-stimulated genes. *J Biol Chem* **270**(40)**,** 23739-46.

Darnell, J. E., Jr., Kerr, I. M., and Stark, G. R. (1994). Jak-STAT pathways and transcriptional activation in response to IFNs and other extracellular signaling proteins. *Science* **264**(5164)**,** 1415-21.

Davis, W. G. (2007). Dissertation.

Diamond, M. S. (2009). Mechanisms of evasion of the type I interferon antiviral response by flaviviruses. *J Interferon Cytokine Res* **29**(9)**,** 521-30.

Falgout, B., and Markoff, L. (1995). Evidence that flavivirus NS1-NS2A cleavage is mediated by a membrane-bound host protease in the endoplasmic reticulum. *J Virol* **69**(11)**,** 7232-43.

Flamand, M., Deubel, V., and Girard, M. (1992). Expression and secretion of Japanese encephalitis virus nonstructural protein NS1 by insect cells using a recombinant baculovirus. *Virology* **191**(2)**,** 826-36.

Flamand, M., Megret, F., Mathieu, M., Lepault, J., Rey, F. A., and Deubel, V. (1999). Dengue virus type 1 nonstructural glycoprotein NS1 is secreted from mammalian cells as a soluble hexamer in a glycosylation-dependent fashion. *J Virol* **73**(7)**,** 6104-10.

Gantier, M. P., and Williams, B. R. (2007). The response of mammalian cells to double-stranded RNA. *Cytokine Growth Factor Rev* **18**(5-6)**,** 363-71.

Gillespie, L. K., Hoenen, A., Morgan, G., and Mackenzie, J. M. (2010). The endoplasmic reticulum provides the membrane platform for biogenesis of the flavivirus replication complex. *J Virol* **84**(20)**,** 10438-47.

Gingras, A. C., Raught, B., and Sonenberg, N. (1999). eIF4 initiation factors: effectors of mRNA recruitment to ribosomes and regulators of translation. *Annu Rev Biochem* **68,** 913-63.

Gitlin, L., Barchet, W., Gilfillan, S., Cella, M., Beutler, B., Flavell, R. A., Diamond, M. S., and Colonna, M. (2006). Essential role of mda-5 in type I IFN responses to polyriboinosinic:polyribocytidylic acid and encephalomyocarditis picornavirus. *Proc Natl Acad Sci U S A* **103**(22)**,** 8459-64.

Grassi, G., Scaggiante, B., Farra, R., Dapas, B., Agostini, F., Baiz, D., Rosso, N., and Tiribelli, C. (2007). The expression levels of the translational factors eEF1A 1/2 correlate with cell growth but not apoptosis in hepatocellular carcinoma cell lines with different differentiation grade. *Biochimie*.

Grun, J. B., and Brinton, M. A. (1986). Characterization of West Nile virus RNA-dependent RNA polymerase and cellular terminal adenylyl and uridylyl transferases in cell-free extracts. *J Virol* **60**(3)**,** 1113-24.

Gubler, D. J., Kuno, G., and Markoff, J. (2007). Flaviviruses. *In* "Fields Virology" (P. M. H. David M Knipe, Ed.), pp. 1153-1252. Lippincott Williams and Wilkins, Philadelphia.

Hall, T. M. (2002). Poly(A) tail synthesis and regulation: recent structural insights. *Curr Opin Struct Biol* **12**(1)**,** 82-8.

Heinz, F. X., and Allison, S. L. (2000). Structures and mechanisms in flavivirus fusion. *Adv Virus Res* **55,** 231-69.

Heinz, F. X., Stiasny, K., Puschner-Auer, G., Holzmann, H., Allison, S. L., Mandl, C. W., and Kunz, C. (1994). Structural changes and functional control of the tick-borne encephalitis virus glycoprotein E by the heterodimeric association with protein prM. *Virology* **198**(1)**,** 109-17.

Hiscott, J., Lin, R., Nakhaei, P., and Paz, S. (2006). MasterCARD: a priceless link to innate immunity. *Trends Mol Med* **12**(2)**,** 53-6.

Ivanyi-Nagy, R., Lavergne, J. P., Gabus, C., Ficheux, D., and Darlix, J. L. (2008). RNA chaperoning and intrinsic disorder in the core proteins of Flaviviridae. *Nucleic Acids Res* **36**(3)**,** 712-25.

Kahvejian, A., Roy, G., and Sonenberg, N. (2001). The mRNA closed-loop model: the function of PABP and PABP-interacting proteins in mRNA translation. *Cold Spring Harb Symp Quant Biol* **66,** 293-300.

Kapoor, M., Zhang, L., Ramachandra, M., Kusukawa, J., Ebner, K. E., and Padmanabhan, R. (1995). Association between NS3 and NS5 proteins of dengue virus type 2 in the putative RNA replicase is linked to differential phosphorylation of NS5. *J Biol Chem* **270**(32)**,** 19100-6.

Kato, H., Sato, S., Yoneyama, M., Yamamoto, M., Uematsu, S., Matsui, K., Tsujimura, T., Takeda, K., Fujita, T., Takeuchi, O., and Akira, S. (2005). Cell type-specific involvement of RIG-I in antiviral response. *Immunity* **23**(1)**,** 19-28.

Kato, H., Takeuchi, O., Sato, S., Yoneyama, M., Yamamoto, M., Matsui, K., Uematsu, S., Jung, A., Kawai, T., Ishii, K. J., Yamaguchi, O., Otsu, K., Tsujimura, T., Koh, C. S., Reis e Sousa, C., Matsuura, Y., Fujita, T., and Akira, S. (2006). Differential roles of MDA5 and RIG-I helicases in the recognition of RNA viruses. *Nature* **441**(7089)**,** 101-5.

Khromykh, A. A., Kondratieva, N., Sgro, J. Y., Palmenberg, A., and Westaway, E. G. (2003). Significance in replication of the terminal nucleotides of the flavivirus genome. *J Virol* **77**(19)**,** 10623-9.

Khromykh, A. A., Sedlak, P. L., Guyatt, K. J., Hall, R. A., and Westaway, E. G. (1999). Efficient trans-complementation of the flavivirus kunjin NS5 protein but not of the NS1 protein requires its coexpression with other components of the viral replicase. *J Virol* **73**(12)**,** 10272-80.

Khromykh, A. A., and Westaway, E. G. (1996). RNA binding properties of core protein of the flavivirus Kunjin. *Arch Virol* **141**(3-4)**,** 685-99.

Koonin, E. V. (1991). The phylogeny of RNA-dependent RNA polymerases of positive-strand RNA viruses. *J Gen Virol* **72 (Pt 9),** 2197-206.

Koonin, E. V. (1993). Computer-assisted identification of a putative methyltransferase domain in NS5 protein of flaviviruses and lambda 2 protein of reovirus. *J Gen Virol* **74 (Pt 4),** 733-40.

Kozak, M. (1986). Point mutations define a sequence flanking the AUG initiator codon that modulates translation by eukaryotic ribosomes. *Cell* **44**(2)**,** 283-92.

Kummerer, B. M., and Rice, C. M. (2002). Mutations in the yellow fever virus nonstructural protein NS2A selectively block production of infectious particles. *J Virol* **76**(10)**,** 4773-84.

Lanciotti, R. S., Ebel, G. D., Deubel, V., Kerst, A. J., Murri, S., Meyer, R., Bowen, M., McKinney, N., Morrill, W. E., Crabtree, M. B., Kramer, L. D., and Roehrig, J. T. (2002). Complete genome sequences and phylogenetic analysis of West Nile virus strains isolated from the United States, Europe, and the Middle East. *Virology* **298**(1)**,** 96-105.

Laurent-Rolle, M., Boer, E. F., Lubick, K. J., Wolfinbarger, J. B., Carmody, A. B., Rockx, B., Liu, W., Ashour, J., Shupert, W. L., Holbrook, M. R., Barrett, A. D., Mason, P. W., Bloom, M. E., Garcia-Sastre, A., Khromykh, A. A., and Best, S. M. (2010). The NS5 protein of the virulent West Nile virus NY99 strain is a potent antagonist of type I interferon-mediated JAK-STAT signaling. *J Virol* **84**(7)**,** 3503-15.

Lewin, B. (2000). Genes. 7 ed. Oxford University Press Inc., New York.

Li, H., Clum, S., You, S., Ebner, K. E., and Padmanabhan, R. (1999). The serine protease and RNA-stimulated nucleoside triphosphatase and RNA helicase functional domains of dengue virus type 2 NS3 converge within a region of 20 amino acids. *J Virol* **73**(4)**,** 3108-16.

Li, H., Gade, P., Xiao, W., and Kalvakolanu, D. V. (2007). The interferon signaling network and transcription factor C/EBP-beta. *Cell Mol Immunol* **4**(6)**,** 407-18.

Lin, C., Amberg, S. M., Chambers, T. J., and Rice, C. M. (1993). Cleavage at a novel site in the NS4A region by the yellow fever virus NS2B-3 proteinase is a prerequisite for processing at the downstream 4A/4B signalase site. *J Virol* **67**(4)**,** 2327-35.

Lindenbach, B. D., and Rice, C. M. (1997). trans-Complementation of yellow fever virus NS1 reveals a role in early RNA replication. *J Virol* **71**(12)**,** 9608-17.

Lindenbach, B. D., and Rice, C. M. (1999). Genetic interaction of flavivirus nonstructural proteins NS1 and NS4A as a determinant of replicase function. *J Virol* **73**(6)**,** 4611-21.

Lindenbach, B. D., Thiel, H. J., and Rice, C. M. (2007). Flaviviridae: The Viruses and Their Replication. *In* "Fields Virology" (D. M. Knipe, and Howley, P. M., Ed.), pp. 1101-1152. Lippincott Williams and Wilkins, Philadelphia.

Lindenbach, B. D., Thiel, H. J, and Rice, C. M. (2007). Flaviviridae: The Viruses and Their Replication. *In* "Fields Virology" (D. M. Knipe, and Howley, P. M., Ed.), pp. 1101-1152. Lippincott Williams and Wilkins, Philadelphia.

Liu, W. J., Chen, H. B., and Khromykh, A. A. (2003). Molecular and functional analyses of Kunjin virus infectious cDNA clones demonstrate the essential roles for NS2A in virus assembly and for a nonconservative residue in NS3 in RNA replication. *J Virol* **77**(14)**,** 7804-13.

Liu, W. J., Chen, H. B., Wang, X. J., Huang, H., and Khromykh, A. A. (2004). Analysis of adaptive mutations in Kunjin virus replicon RNA reveals a novel role for the flavivirus nonstructural protein NS2A in inhibition of beta interferon promoter-driven transcription. *J Virol* **78**(22)**,** 12225-35.

Liu, W. J., Wang, X. J., Clark, D. C., Lobigs, M., Hall, R. A., and Khromykh, A. A. (2006). A single amino acid substitution in the West Nile virus nonstructural protein NS2A disables its ability to inhibit alpha/beta interferon induction and attenuates virus virulence in mice. *J Virol* **80**(5)**,** 2396-404.

Liu, W. J., Wang, X. J., Mokhonov, V. V., Shi, P. Y., Randall, R., and Khromykh, A. A. (2005). Inhibition of interferon signaling by the New York 99 strain and Kunjin subtype of West Nile virus involves blockage of STAT1 and STAT2 activation by nonstructural proteins. *J Virol* **79**(3)**,** 1934-42.

Lopez-Lastra, M., Ramdohr, P., Letelier, A., Vallejos, M., Vera-Otarola, J., and Valiente-Echeverria, F. (2010). Translation initiation of viral mRNAs. *Rev Med Virol* **20**(3)**,** 177-95.

Lopez-Lastra, M., Rivas, A., and Barria, M. I. (2005). Protein synthesis in eukaryotes: the growing biological relevance of cap-independent translation initiation. *Biol Res* **38**(2-3)**,** 121-46.

Mackenzie, J. M., Kenney, M. T., and Westaway, E. G. (2007). West Nile virus strain Kunjin NS5 polymerase is a phosphoprotein localized at the cytoplasmic site of viral RNA synthesis. *J Gen Virol* **88**(Pt 4)**,** 1163-8.

Mackenzie, J. M., Khromykh, A. A., Jones, M. K., and Westaway, E. G. (1998). Subcellular localization and some biochemical properties of the flavivirus Kunjin nonstructural proteins NS2A and NS4A. *Virology* **245**(2)**,** 203-15.

Mackenzie, J. M., and Westaway, E. G. (2001). Assembly and maturation of the flavivirus Kunjin virus appear to occur in the rough endoplasmic reticulum and along the secretory pathway, respectively. *J Virol* **75**(22)**,** 10787-99.

Markoff, L. (2003). 5'- and 3'-noncoding regions in flavivirus RNA. *Adv Virus Res* **59,** 177-228.

Miller, S., Kastner, S., Krijnse-Locker, J., Buhler, S., and Bartenschlager, R. (2007). The non-structural protein 4A of dengue virus is an integral membrane protein inducing membrane alterations in a 2K-regulated manner. *J Biol Chem* **282**(12)**,** 8873-82.

Miller, S., Sparacio, S., and Bartenschlager, R. (2006). Subcellular localization and membrane topology of the Dengue virus type 2 Non-structural protein 4B. *J Biol Chem* **281**(13)**,** 8854-63.

Mukhopadhyay, S., Kuhn, R. J., and Rossmann, M. G. (2005). A structural perspective of the flavivirus life cycle. *Nat Rev Microbiol* **3**(1)**,** 13-22.

Munoz-Jordan, J. L., Laurent-Rolle, M., Ashour, J., Martinez-Sobrido, L., Ashok, M., Lipkin, W. I., and Garcia-Sastre, A. (2005). Inhibition of alpha/beta interferon signaling by the NS4B protein of flaviviruses. *J Virol* **79**(13)**,** 8004-13.

Murphy, F. A., Ed. (1980). Togavirus morphology and morphogenesis. In *The Togaviruses: Biology, Structure, Replication*
Edited by R. Schlesinger. New York: Academic Press.

Nakaya, T., Sato, M., Hata, N., Asagiri, M., Suemori, H., Noguchi, S., Tanaka, N., and Taniguchi, T. (2001). Gene induction pathways mediated by distinct IRFs during viral infection. *Biochem Biophys Res Commun* **283**(5)**,** 1150-6.

Nall, T. A., Chappell, K. J., Stoermer, M. J., Fang, N. X., Tyndall, J. D., Young, P. R., and Fairlie, D. P. (2004). Enzymatic characterization and homology model of a catalytically active recombinant West Nile virus NS3 protease. *J Biol Chem* **279**(47)**,** 48535-42.

Pestova, T. V., Borukhov, S. I., and Hellen, C. U. (1998). Eukaryotic ribosomes require initiation factors 1 and 1A to locate initiation codons. *Nature* **394**(6696)**,** 854-9.

Petersen, L. R., Marfin, A. A., and Gubler, D. J. (2003). West Nile virus. *Jama* **290**(4)**,** 524-8.

Ray, D., Shah, A., Tilgner, M., Guo, Y., Zhao, Y., Dong, H., Deas, T. S., Zhou, Y., Li, H., and Shi, P. Y. (2006). West Nile virus 5'-cap structure is formed by sequential guanine N-7 and ribose 2'-O methylations by nonstructural protein 5. *J Virol* **80**(17)**,** 8362-70.

Reed, K. E., Gorbalenya, A. E., and Rice, C. M. (1998). The NS5A/NS5 proteins of viruses from three genera of the family flaviviridae are phosphorylated by associated serine/threonine kinases. *J Virol* **72**(7)**,** 6199-206.

Roosendaal, J., Westaway, E. G., Khromykh, A., and Mackenzie, J. M. (2006). Regulated cleavages at the West Nile virus NS4A-2K-NS4B junctions play a major role in rearranging cytoplasmic membranes and Golgi trafficking of the NS4A protein. *J Virol* **80**(9)**,** 4623-32.

Saad, M., Youssef, S., Kirschke, D., Shubair, M., Haddadin, D., Myers, J., and Moorman, J. (2005). Acute flaccid paralysis: the spectrum of a newly recognized complication of West Nile virus infection. *J Infect* **51**(2)**,** 120-7.

Samuel, C. E. (2001). Antiviral actions of interferons. *Clin Microbiol Rev* **14**(4)**,** 778-809, table of contents.

Sarkar, S. N., and Sen, G. C. (2004). Novel functions of proteins encoded by viral stress-inducible genes. *Pharmacol Ther* **103**(3)**,** 245-59.

Schoenberg, D. R., and Maquat, L. E. (2009). Re-capping the message. *Trends Biochem Sci* **34**(9)**,** 435-42.

Smithburn, K. C., Hughes, T.P., Burke, A.W., and Paul, J.H. (1940). A neurotropic virus isolated from the blood of a native of Uganda. *Am. J. Trop. Med. Hyg.* **20,** 471-492.

Stadler, K., Allison, S. L., Schalich, J., and Heinz, F. X. (1997). Proteolytic activation of tick-borne encephalitis virus by furin. *J Virol* **71**(11)**,** 8475-81.

Stark, G. R., Kerr, I. M., Williams, B. R., Silverman, R. H., and Schreiber, R. D. (1998). How cells respond to interferons. *Annu Rev Biochem* **67,** 227-64.

Weaver, B. K., Kumar, K. P., and Reich, N. C. (1998). Interferon regulatory factor 3 and CREB-binding protein/p300 are subunits of double-stranded RNA-activated transcription factor DRAF1. *Mol Cell Biol* **18**(3)**,** 1359-68.

Welsch, S., Miller, S., Romero-Brey, I., Merz, A., Bleck, C. K., Walther, P., Fuller, S. D., Antony, C., Krijnse-Locker, J., and Bartenschlager, R. (2009). Composition and

three-dimensional architecture of the dengue virus replication and assembly sites. *Cell Host Microbe* **5**(4)**,** 365-75.

Wengler, G. (1993). The NS 3 nonstructural protein of flaviviruses contains an RNA triphosphatase activity. *Virology* **197**(1)**,** 265-73.

Wengler, G., and Wengler, G. (1991). The carboxy-terminal part of the NS 3 protein of the West Nile flavivirus can be isolated as a soluble protein after proteolytic cleavage and represents an RNA-stimulated NTPase. *Virology* **184**(2)**,** 707-15.

Westaway, E. G., Khromykh, A. A., Kenney, M. T., Mackenzie, J. M., and Jones, M. K. (1997). Proteins C and NS4B of the flavivirus Kunjin translocate independently into the nucleus. *Virology* **234**(1)**,** 31-41.

Winkler, G., Maxwell, S. E., Ruemmler, C., and Stollar, V. (1989). Newly synthesized dengue-2 virus nonstructural protein NS1 is a soluble protein but becomes partially hydrophobic and membrane-associated after dimerization. *Virology* **171**(1)**,** 302-5.

Winkler, G., Randolph, V. B., Cleaves, G. R., Ryan, T. E., and Stollar, V. (1988). Evidence that the mature form of the flavivirus nonstructural protein NS1 is a dimer. *Virology* **162**(1)**,** 187-96.

Yamshchikov, V. F., and Compans, R. W. (1994). Processing of the intracellular form of the west Nile virus capsid protein by the viral NS2B-NS3 protease: an in vitro study. *J Virol* **68**(9)**,** 5765-71.

Zhang, W., Chipman, P. R., Corver, J., Johnson, P. R., Zhang, Y., Mukhopadhyay, S., Baker, T. S., Strauss, J. H., Rossmann, M. G., and Kuhn, R. J. (2003a). Visualization of membrane protein domains by cryo-electron microscopy of dengue virus. *Nat Struct Biol* **10**(11)**,** 907-12.

Zhang, Y., Corver, J., Chipman, P. R., Zhang, W., Pletnev, S. V., Sedlak, D., Baker, T. S., Strauss, J. H., Kuhn, R. J., and Rossmann, M. G. (2003b). Structures of immature flavivirus particles. *Embo J* **22**(11)**,** 2604-13.

Zhou, Y., Ray, D., Zhao, Y., Dong, H., Ren, S., Li, Z., Guo, Y., Bernard, K. A., Shi, P. Y., and Li, H. (2007). Structure and function of flavivirus NS5 methyltransferase. *J Virol* **81**(8)**,** 3891-903.

CHAPTER 2

Investigation of the mechanism of PKR phosphorylation suppression in WNV-infected cells.

INTRODUCTION

PKR is a serine/threonine kinase composed of an N-terminal regulatory domain that contains two dsRNA binding motifs (DRBMs) and a C-terminal kinase domain (Meurs et al., 1990; Nanduri et al., 1998). These domains are connected by a spacer that provides an interface for dimerization (McKenna et al., 2007). In the unphosphorylated state, the N-terminal regulatory domain may interact with the C-terminal catalytic domain to inhibit kinase activity (Nanduri et al., 2000). Activation of PKR by dsRNA leads to the formation of dimers that are stabilized by autophosphorylation at multiple residues, including Thr446 and Thr451 which are located within the activation loop of the kinase domain and essential for PKR activation (Romano et al., 1998). Minimal PKR activation requires dsRNAs that are at least 30 bp in length. Shorter dsRNAs inhibit PKR by competitively binding to inactive PKR monomers and limiting their dimerization (Bevilacqua and Cech, 1996; Sadler and Williams, 2007). Once active PKR dimers have ejected the activating dsRNA, presumably, due to phosphorylation of N-terminal residues, they phosphorylate eIF2a (Jammi and Beal, 2001). PKR is constitutively and ubiquitously expressed at low levels due to the presence of a kinase conserved sequence (KCS) site in its promoter (Toth et al., 2006). PKR is an ISG and its expression is upregulated by Type I IFN produced in response to viral infection. The majority of

intracellular PKR is cytoplasmic where a portion is associated with ribosomes. Some PKR is also present in the nucleus (Tanaka and Samuel, 1994; Toth et al., 2006).

During translation of cellular mRNAs, a ternary complex composed of a GTP-bound eIF2 and a methionyl-tRNA delivers the charged initiator tRNA to the 40S ribosomal subunit of the 43S preinitiation complex by a process that requires the hydrolysis of GTP to GDP (Hershey, 1991; Majumdar and Maitra, 2005). Under stress conditions, the α-subunit of eIF2 is phosphorylated by one of the four eIF2α kinases: general control nonrepressed 2 (GCN2), heme-regulated inhibitor (HRI), PKR-like ER kinase (PERK), or PKR (Kaufman, 1999). The eIF2a kinases share a conserved kinase domain that mediates eIF2a phosphorylation, but each kinase responds to a different stress due to their unique regulatory domains (Kaufman, 1999). Phosphorylation of eIF2α on Ser51 leads to the formation of a high-affinity complex with the guanine exchange factor, eIF2B. This inhibits the exchange of GDP for GTP and "stalls" the preinitiation complexes on mRNAs (Sudhakar et al., 2000). Phosphorylation of as little as 20% of eIF2a significantly reduces the synthesis of most cellular proteins (Sudhakar et al., 2000). In virus-infected cells, PKR is activated by viral dsRNA. PKR can also be activated by heparin oligosaccharides, by IL-3 withdrawal, or by peroxide or arsenite treatment that leads to PKR activation via interaction with PACT (Ito et al., 1999; Patel et al., 2000).

West Nile virus, a member of the genus Flavivirus within the family *Flaviviridae*, was first isolated in 1937 from a febrile woman in the West Nile region of Uganda (Brinton, 2002). Until 1999, WNV was largely confined to Southern Europe, the Middle East, Africa, West and Central Asia, Indonesia and Australia. In 1999, WNV extended

into the Western hemisphere where it has spread rapidly. The majority of WNV infections in humans are asymptomatic. Flu-like symptoms are observed in ~20 % and meningitis, encephalitis and/or paralysis occurs in less than 1% of infected individuals (Brinton, 2002; Gubler, 2007). The WNV genome is a positive-sense, single-stranded RNA of ~11 Kb with a 5' cap but no 3' polyA tract. It encodes a single polyprotein that is co- and post-translationally cleaved to generate 3 structural proteins (E, prM and capsid) and 7 non-structural proteins (NS1, NS2a, NS2b, NS3, NS4a, NS4b and NS5). Viral replication occurs entirely in the cytoplasm where viral RNA replication occurs in vesicles formed by invaginations of the ER membranes (Lindenbach, 2007). WNV infection does not lead to shut-off of cellular protein synthesis. Viral structural proteins associated with ER membranes and newly synthesized viral RNA interact and bud into the lumen of the ER (Brinton, 2002; Gubler, 2007).

PKR has been reported to play a role in NFκB signaling and the control of cell growth through induction of p53 (Garcia et al., 2006). PKR is also involved in IFN, platelet-derived growth factor (PDGF), TNF-α, p38, JNK, STAT1 and IL-1 signaling. The involvement of PKR in multiple cellular processes requires its phosphorylation (Garcia et al., 2006). A number of cellular inhibitors have been identified that modulate PKR activity by forming stable heterocomplexes with PKR and interfering with the various steps of the PKR activation process: (1) dsRNA recognition (C114 and RPL18), (2) dimerization ($p58^{ipk}$) or (3) autophosphorylation (Hsp70 and Hsp90) (Garcia et al., 2007). The catalytic subunit of protein phosphatase 1 alpha (PP1a) dephosphorylates PKR resulting in dimer disruption (Tan et al., 2002). The importance of PKR in the

antiviral innate immune response is highlighted by the observation that most known viruses have evolved mechanisms for inhibiting PKR activity (Garcia et al., 2007). Consistent with our previous data demonstrating that WNV does not induce significant eIF2a phosphorylation (Emara and Brinton, 2007), the present study provides evidence that PKR activation is not induced nor actively suppressed in WNV-infected rodent cells.

RESULTS

PKR phosphorylation is not induced by WNV-infection. PKR can be activated by viral dsRNA and phosphorylate eIF2α leading to attenuation of cell translation (Garcia et al., 2007). We previously reported that WNV-Eg101 infection of BHK cells did not induce significant eIF2α phosphorylation (Emara and Brinton, 2007). To determine whether the low level of eIF2α phosphorylation observed was due to a lack of PKR activation, PKR phosphorylation was assessed in mock-infected or WNV Eg101-infected (MOI 5) C3H/He mouse embryo fibroblasts (MEFs) (IFN-responsive) and BHK cells (IFN non-responsive). As a positive control, mock-infected MEFs were treated with 100 IU/ml of Type I IFN for 24 h and BHK cells were transfected with 50 μg/ml poly(IC) for 2 h. A slight increase in PKR phosphorylation (P-PKR) above mock levels in WNV Eg101-infected MEFs starting at 24 h after infection (Fig. 2.1A) but no increase in WNV Eg101-infected BHK cells (Fig. 2.1B) was detected by immunoblotting using anti-phospho Thr451 PKR antibody. However, total PKR (T-PKR) protein levels increased significantly in both Type I IFN-treated and WNV Eg101-infected MEFs and in WNV Eg101-infected but not poly(I:C)-treated BHK cells. In both types of cells, the ratio of

phosphorylated to total PKR (P/T-PKR) decreased after WNV infection to levels below those observed in mock-infected cells indicating that the majority of the newly synthesized PKR was not phosphorylated.

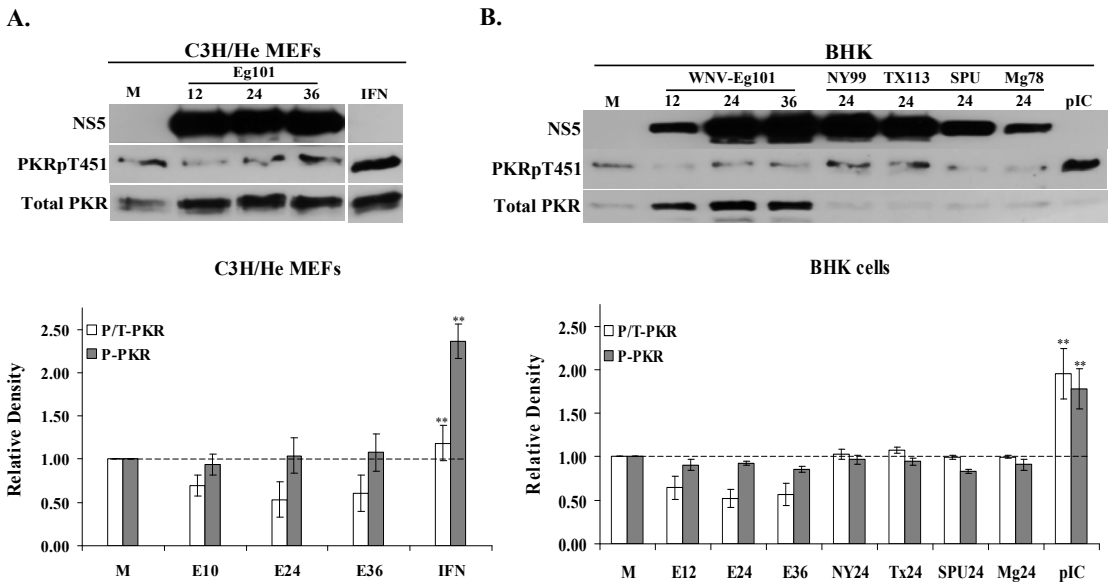

Figure 2.1. Analysis of PKR phosphorylation in WNV-infected cells. (A) C3H/He MEFs were mock infected (M), or infected with WNV-Eg101 at a MOI of 5 for the indicated times or treated with 100 U/ml universal type I IFN for 24 h (IFN). (B) BHK cells were mock-infected (M) or infected with WNV-Eg101 (MOI 5) for the indicated times or infected with various strains of WNV (NY99, TX113, SPU and Mg78) for 24 h or transfected with 50 μg/ml poly(IC) for 2 h (pIC). Total PKR, phopho-Thr451 PKR and WNV-NS5 were detected in cell lysates by Western blotting after separation of proteins by 10% SDS-PAGE. Band densities were measured, quantified using ImageJ software. The values from at least three independent experiments were expressed in relative units compared to the intensity levels present in mock-infected, untreated control lysates (value set at 1). P-PKR = level of PKR phosphorylation, P/T-PKR = ratio of phospho-PKR to total PKR. Error bars represent the standard error (SE) (n = 3 for BHK and n = 4 for C3H/He MEFs) and are based on the 95% confidence level. The dashed line denotes the baseline levels observed in mock-infected cells. Asterisks indicate a statistically significant ($p<0.05$) increase above the levels in mock-infected cells.

To determine whether the low level of PKR phosphorylation induced was virus-strain specific, BHK cells were infected with other WNV lineage 1 (NY99 or Tx113) or lineage 2 (Mg78 or SPU) strains at a MOI of 5 for 24 h. In contrast to the dramatic increase in total PKR levels in WNV Eg101-infected BHK cells, no increase in total PKR levels was observed in cells infected with the other WNV viruses (Fig. 2.1B). The

mechanism of PKR expression upregulation in WNV Eg101-infected BHK cells is not currently known. However, due to the Type I IFN insensitivity of BHK cells, the PKR upregulation is expected to be Type I IFN-independent. The ratio of phospho- to total PKR in BHK cells infected with each of the four additional WNV strains tested was similar to that in mock-infected cells (Fig. 2.1B). These data suggest that PKR phosphorylation is not induced in MEFs or BHK cells by WNV-infection.

The Low levels of PKR phosphorylation in WNV-infected MEFs is Type I IFN-dependant. PKR protein expression is upregulated in response to Type I IFN signaling (Tanaka and Samuel, 1994; Toth et al., 2006). PKR phosphorylation was also reported to be induced through direct interactions between PKR and JAK1 and/or Tyk2, two components of the Type I IFN receptor complex (Su et al., 2007). To determine whether the low level of PKR phosphorylation observed in C3H/He MEFs was due to IFN-mediated PKR activation, PKR phosphorylation was assessed in lysates from IFNR1-/- MEFs infected with WNV Eg101 at a MOI of 5 and compared to that in 129wt MEFs. Cells treated with 100 IU/ml of Type I universal IFN (PBL Biomedical laboratories, NJ) for 24 h served as a positive control. Consistent with our previous observations in C3H/He MEFs, a slight increase in P-PKR and a significant increase in T-PKR levels compared to mock-infected cells were observed in WNV-infected 129wt MEFs (Fig. 2.2). IFN treatment also resulted in an increase in PKR phosphorylation and expression. In contrast, in IFNR1-/- MEFs, neither total PKR levels nor the P/T-PKR ration increased in WNV-infected IFNR1-/- MEFs (Fig. 2.2). Although statistically significant ($p < 0.05$)

increases in P-PKR levels were observed in 129wt MEFs treated with IFN as well as at 24 and 36 h after WNV Eg101-infection, P-PKR levels were significantly higher in IFN-treated 129wt MEFs than in WNV-infected cells. These results suggest that the small increase in P/T-PKR ratio observed in WNV-infected MEFs was due to Type I IFN secreted in response to the infection. We previously reported that IFN-beta expression is upregulated in WNV-infected MEFs by 12 h after infection (Scherbik et al., 2007).

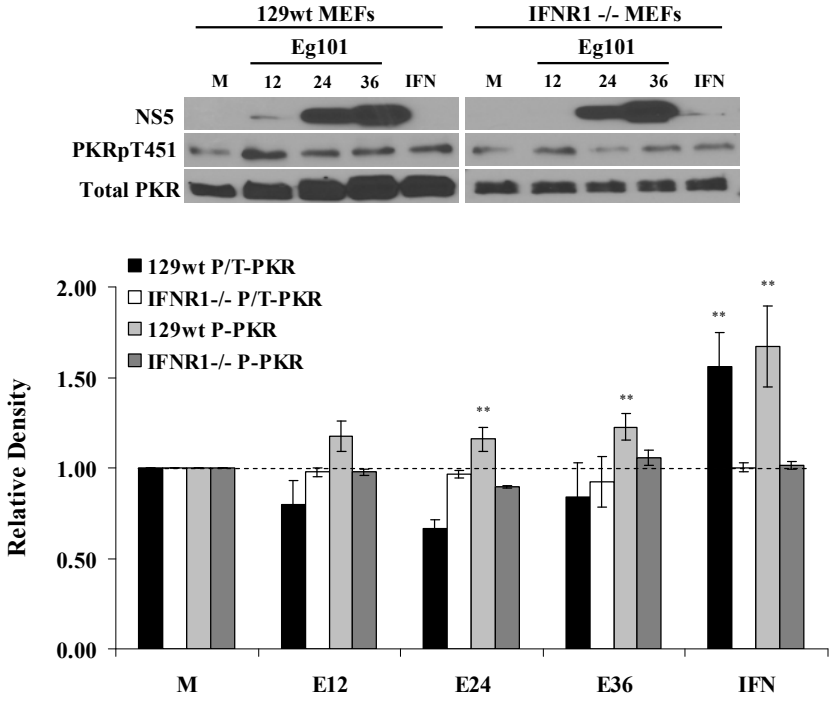

Figure 2.2. Assessment of IFN-mediated PKR phosphorylation in WNV-infected MEFs. 129wt or IFNR1-/- MEFs were mock infected (M) or infected with WNV-Eg101 at a MOI of 5 for the indicated times or treated with 100 U/ml universal Type I IFN for 24 h. The data were analyzed was done as described in the legend for Fig. 1. The dashed line denotes the baseline levels observed in mock-infected cells. Asterisks indicate statistically significant ($p<0.05$) increases above the levels in mock-infected cells.

PKR localization in WNV-infected cells. PKR is typically activated in virus-infected cells by dsRNA viral replication intermediates or hairpin structures within single-stranded viral RNAs (Garcia et al., 2006). WNV RNA replicates in the perinuclear region

of infected cells in association with ER membranes (Gillespie et al., 2010; Mackenzie, 2005). To determine whether the cellular distribution of PKR was altered in WNV-infected cells, MEFs and BHK cells were mock-infected or infected with WNV Eg101 at a MOI of 5 for 10 or 24 h. The cells were fixed, permeabilized and incubated with anti-PKR and anti-dsRNA antibody and visualized by confocal microscopy. PKR was observed to concentrate in the perinuclear region of infected cells and to co-localize with sites of viral RNA replication in both MEFs and BHK cells at 10 h and 24 h after infection (Fig. 2.3A). Because PKR serves as a sentinel of the innate immune response, viral proteins, including influenza virus NS1, reovirus σ3, Kaposi-sarcoma herpesvirus vIRF2 and LANA2, herpes simplex virus 1 (HSV-1) Us11, Epstein-Barr virus SM, vaccinia virus E3L and hepatitis C virus NS5A and E2 proteins (Garcia et al., 2007), directly interact with PKR and inhibit either its binding to viral dsRNA or its activation. To assess PKR colocalization with nonstructural protein components of the WNV replication complex, BHK cells were mock-infected or infected with WNV Eg101 at a MOI of 5 for 24 or 30 h and PKR and the viral NS1, NS3, NS5 proteins were detected by confocal microscopy using protein specific antibodies. No co-localization was observed between PKR and NS3, NS5 or NS1 (Fig. 2.3B). The observed colocalization of PKR with dsRNA but not with individual viral replication complex proteins might be due to a higher signal intensity for the viral dsRNA due to more antibody binding sites per molecule compared to the viral nonstructural proteins and also to a more restricted distribution of the viral dsRNA compared to the nonstructural proteins.

As an additional means of assessing whether PKR associates with viral protein components of the replication complexes, PKR was immunoprecipitated from mock-infected and WNV-infected BHK cells and the precipitates were immunoblotted with anti-NS3 or anti-NS5 antibodies. A species-specific IgG was used as a negative control. Neither NS3 nor NS5 co-immunoprecipitated with PKR (Fig. 2.3C). These data suggest that although PKR colocalizes with viral replication complexes, it does not interact directly with the NS3 protein, which is a marker for the membrane bound complex, nor with the NS5 (RdRp) protein. However, indirect mechanisms of PKR suppression mediated by these viral proteins were not ruled out.

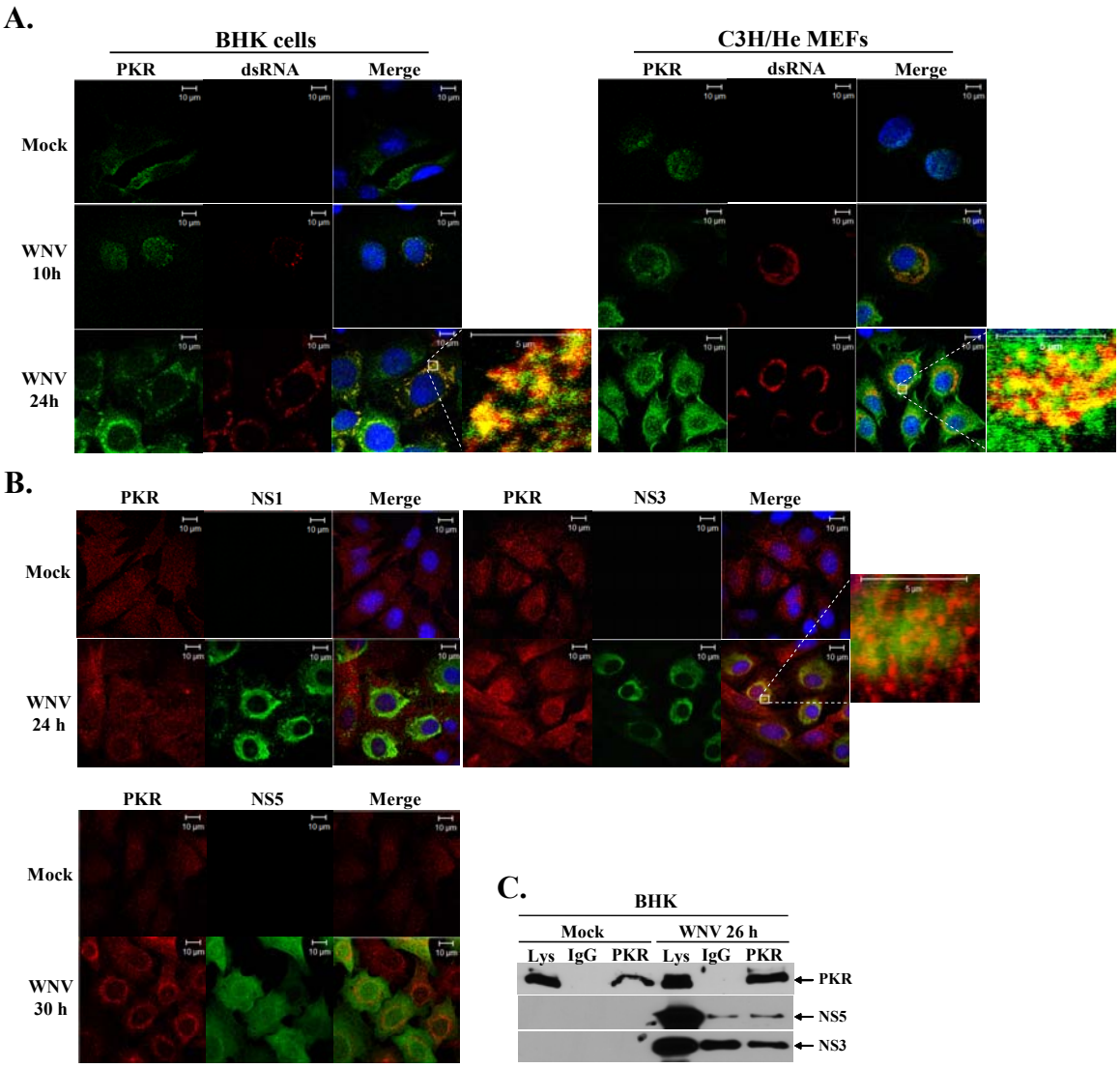

Figure 2.3. PKR colocalization with sites of WNV replication. (A) Analysis of PKR colocalization with replication complexes. BHK cells and MEFs mock-infected or infected with WNV-Eg101 at a MOI of 5. At 10 and 24 h after infection, cells were permeabilized, fixed, and blocked overnight. Cells were stained with anti-PKR and anti-dsRNA antibodies and then AlexaFluor488 (green) and AlexaFluor594 (red) conjugated secondary antibodies, respectively. Cell Nuclei were stained with Hoechst. (B) Analysis of PKR colocalization with viral proteins. BHK cells and MEFs were mock-infected or infected with WNV-Eg101 (MOI of 5). At 24 and 30 h after infection, cells were permeabilized, fixed, and blocked overnight. Cells were stained with anti-PKR and either anti-NS5, anti-NS3 or anti-NS1 antibodies and then AlexaFluor488 (green) and AlexaFluor594 (red) conjugated secondary antibodies, respectively. Cell Nuclei were stained with Hoechst. (C) Analysis of PKR interaction with viral NS3 or NS5 proteins. BHK cells were mock-infected (M), or infected with WNV-Eg101 (MOI of 5). At 26 h after infection, cells were lysed and S2 fractions were prepared. Rabbit anti-PKR antibody or a rabbit IgG was used for immunoprecipitation. Immunoprecipitated proteins were separated by 10% SDS-PAGE and detected by Western blotting using anti-NS5 or anti-NS3 antibodies.

PKR does not colocalize with known cellular PKR inhibitors in WNV-infected cells. With the exception of PP1a, known cellular PKR inhibitors must remain associated with PKR to mediate their inhibitory effect and therefore would co-localize with PKR. Hsp90 and Hsp70 have both been shown to inhibit PKR by masking its autophosphorylation sites (Donze et al., 2001; Pang et al., 2002; Pratt and Toft, 2003). In influenza infected cells, $p58^{ipk}$ is recruited by the viral NS1 protein into a complex with PKR where it binds to the PKR dimerization interface preventing activation (Lee et al., 1990). C114, an IL-11 inducible nuclear dsRNA-binding protein that shuttles between the cytoplasm and nucleus, inhibits PKR activation through interactions with the PKR DRBMs (Yin et al., 2003). To assess whether PKR is associated with a cellular PKR inhibitor in WNV-infected cells, BHK cells were infected with WNV Eg101 at a MOI of 5 and at 24 h or 30 h after infection, cells were fixed, permeabilized and incubated with anti-PKR and an antibody to a PKR inhibitor followed by incubation with fluorescent tagged secondary antibodies and visualization by confocal microscopy. Neither Hsp90, Hsp70, $p58^{ipk}$, nor C114 were observed to colocalize with PKR in WNV-infected cells (Fig. 2.4A).

The HSV protein $\gamma_1$34.5 mediates recruitment of PP1a to dephosphorylate eIF2a (He et al., 1998). PP1a has also been reported to dephosphorylate PKR (Tan et al., 2002). PP1a did not concentrate in the perinuclear regions of WNV-infected cells or colocalize with PKR (Fig. 2.4A). Overexpression of human papillomavirus E6 protein was reported to induce PKR localization to P-bodies where it was sequestered (Hebner et al., 2006). PKR did not localize to P-bodies, detected with Dcp1a antibody, in WNV-infected cells

(Fig. 2.4A). These data suggest that suppression of PKR phosphorylation in WNV-infected cells is not mediated by any of the tested cellular PKR inhibitors.

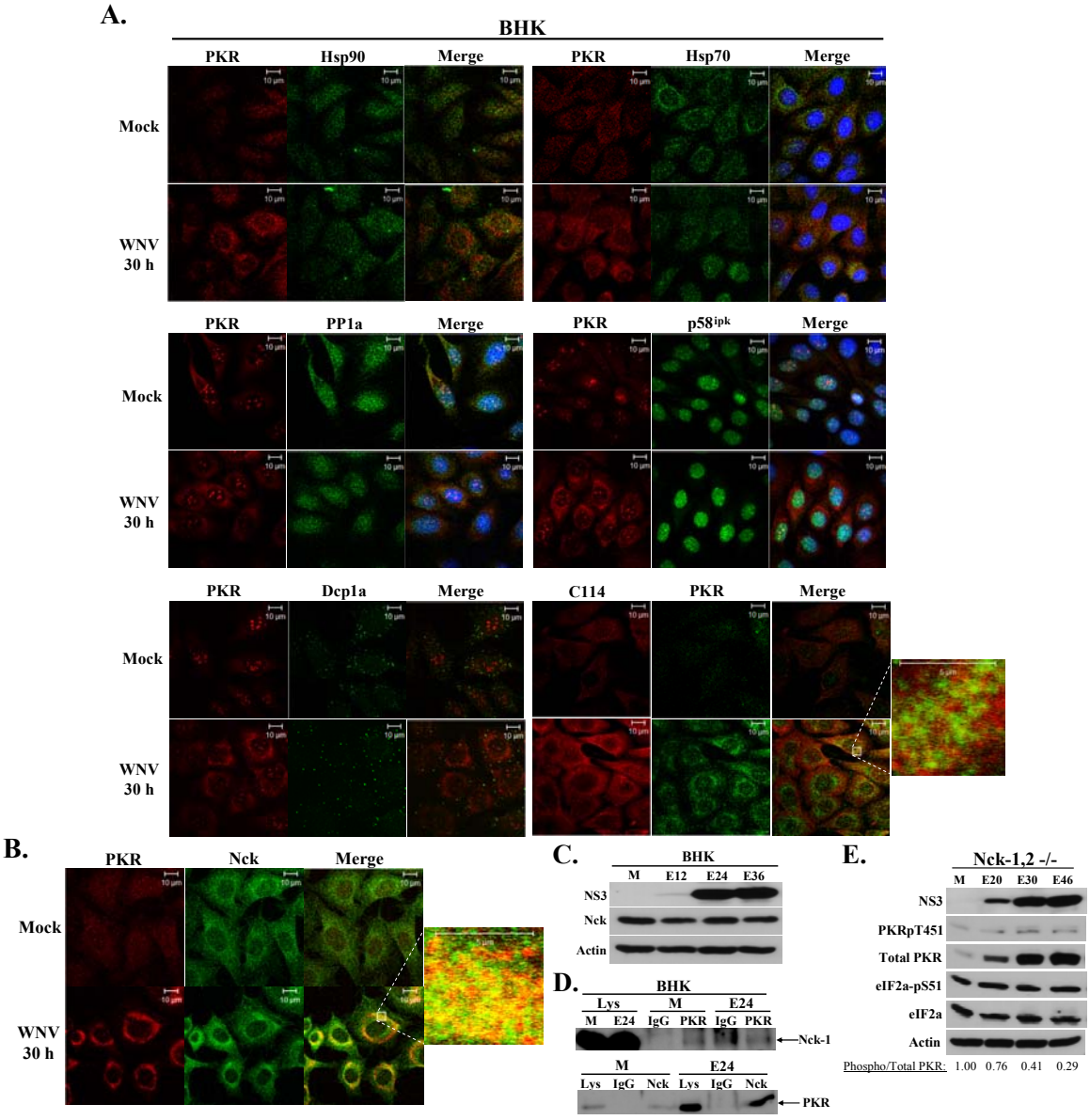

Figure 2.4. Analysis of PKR colocalization with known cellular PKR inhibitors in WNV-infected cells. (A and B) Colocalization of PKR with known cellular PKR inhibitors. BHK cells were mock-infected or infected with WNV-Eg101 (MOI of 5). At 30 h after infection, cells were permeabilized, fixed and blocked overnight. Cells were stained with anti-PKR and an antibody to a cellular PKR inhibitor and then with AlexaFluor488 (green) and AlexaFluor594/555 (red) conjugated secondary antibodies. (C) Nck protein levels in WNV-infected BHK cells. Cells were mock infected (M), or infected with WNV-Eg101 (MOI of 5) for the indicated times. NS3, Nck-1, and actin were detected by Western blotting after separation of proteins by 10% SDS-PAGE. (D) Co-immunoprecipitation of Nck and PKR. BHK cells were

mock-infected (M) or infected with WNV-Eg101 (MOI of 5). At 24 h after infection, cells were lysed and S2 fractions were prepared. Rabbit anti-PKR antibody or a rabbit IgG was used for immunoprecipitation. Immunoprecipitated proteins were separated by 10% SDS-PAGE and detected by Western blotting using anti-Nck antibody. (E) Analysis of PKR phosphorylation in WNV-infected Nck-knockout cells. Nck-1,2-/- MEFs were mock infected (M) or infected with WNV-Eg101 (MOI of 5) for the indicated times. NS3, total PKR, phopho-Thr451 PKR, total eIF2a and phospho-Ser51 eIF2a were detected by Western blotting after separation of proteins by 10% SDS-PAGE.

PKR colocalizes with the PKR inhibitor Nck in WNV-infected cells. Nck has been shown to inhibit PERK-, PKR-, and HRI- but not GCN2-mediated eIF2a phosphorylation (Cardin et al., 2007). Nck binds to inactive PKR. However, dsRNA can outcompete Nck for PKR binding (Cardin and Larose, 2008). In WNV-infected BHK cells, Nck was observed to concentrate in the perinuclear region and to colocalize with PKR (Fig. 2.4B). Nck protein levels were high in uninfected cells and did not increase in WNV-infected BHK cells (Fig. 2.4C). Interaction between Nck and PKR was analyzed by co-immunoprecipitation. Lysates made from WNV-infected BHK cells at 24 h after infection were incubated with rabbit-anti-PKR antibody or a control nonspecific rabbit IgG. The bound proteins were separated by SDS-PAGE and immunoblotted using a rabbit-anti-Nck or a mouse-anti-PKR antibody. Nck was co-immunoprecipitated by PKR antibody but not by the nonspecific IgG. Similarly, PKR was co-immunoprecipitated by Nck antibody. A higher amount of PKR was co-immunoprecipitated from WNV-infected cell lysates than from mock-infected cell lysates indicating increased Nck-PKR interaction in WNV-infected cells consistent with the increase in total PKR (Fig. 2.4D). A decrease in this interaction would be expected if WNV RNA competed with Nck for binding to PKR. The observed colocalization and association of Nck and PKR in WNV-

infected cells suggests that most of the PKR that colocalizes with viral dsRNA in infected cells is inactive.

Mammalian genomes have two Nck genes. The Nck-1 and Nck-2 proteins encoded by these genes share 68% amino acid homology and have been reported to have redundant functions based on the results of studies with single and double-knock out MEFs (Latreille and Larose, 2006). As an additional means of determining whether Nck plays a role in the inhibition of PKR activation during WNV infection, Nck1-/-, Nck2-/- (Nck1,2-/-) MEFs were infected with WNV Eg101 at a MOI of 5. Similar to what was observed with control 129wt and C3H/He MEFs, total PKR significantly increased in WNV-infected Nck1,2-/- MEFs (Fig. 2.4E). Only a minimal increase in PKR phosphorylation levels was detected in WNV-infected Nck1,2-/- MEFs (Fig. 2.4E). Similar to what was seen with control MEFs, the ratio of P/T-PKR was lower than that in mock-infected Nck1,2-/- MEFs (Fig. 2.4E). Also, no increase in eIF2a phosphorylation was observed after WNV-infection in these MEFs (Fig. 2.4E). These results indicate that even when the PKR-associated inhibitor Nck is absent, PKR is still only minimally activated in WNV-infected cells.

PKR autophosphorylation is induced by viral RNAs *in vitro*. PKR binds dsRNA in a sequence non-specific manner but the structure of the RNA plays a critical role in PKR activation. The binding of activating dsRNAs to PKR leads to the formation of active PKR dimers and release of the activating dsRNA. Activated PKR dimers have been reported to have reduced affinity to poly(I:C) (Jammi and Beal, 2001; Langland and

Jacobs, 1992; Lemaire et al., 2005). Viral PKR inhibitor RNAs, such as adenovirus VA_I RNA and Epstein-Bar virus EBER-1 RNA, bind to PKR but their structures inhibit PKR activation (Garcia et al., 2006). Neither of these RNAs induced activation of PKR *in vitro* at any of the concentrations tested (McKenna et al., 2006; McKenna et al., 2007). In competition assays with an activator RNA, optimal inhibition by either VA_I RNA or EBER-1 RNA was observed when concentrations of these RNAs were 2-10 times higher than that of an activator RNA.

A WNV genomic RNA fragment consisting of the 3' terminal 529 nts (3'sfRNA) accumulates in infected cells as well as in mouse brains (Lin et al., 2004; Scherbik et al., 2006; Urosevic et al., 1997) and is generated by XRN1 5' digestion (Pijlman et al., 2008). The 3'sfRNA is significantly larger (529 nts) than known viral PKR inhibitor RNAs (VA_I RNA 136 nts; EBER-1 RNA 157 nts). However, several regions of the mFold predicted structure of the 3'sfRNA (data not shown) are similar to the structures of the VA_I and EBER-1 RNAs (McKenna et al., 2007). The ability of the WNV 3'sfRNA to inhibit PKR activation was tested in an *in vitro* PKR autophosphorylation assay. Poly(I:C) was used as a control activator RNA. Purified recombinant PKR (a gift from Graeme Conn, Emory University) was incubated with poly(I:C) or 3'sfRNA. Both RNAs induced PKR autophosphorylation (Fig. 2.5A).

Flavivirus genome RNAs contain conserved terminal RNA structures (Brinton, 2002; Lindenbach, 2007). Since the structures of the WNV 3' and 5' terminal stem-loop (SL) RNA regions are similar to those of known viral RNA PKR inhibitors, the ability of these RNAs to inhibit PKR activation was also assessed. Both the 3'SL and 5'SL WNV

RNAs induced significant PKR autophosphorylation; the 5' SL RNA induced a 2-fold greater increase in PKR activation than the 3'SL RNA (Fig. 2.5B). Also, preincubation of either of these RNAs with PKR led to an increase not a decrease in PKR activation above that of either RNA alone. The data indicate that the WNV 3'sf, 3'SL and 5'SL RNAs can activate PKR *in vitro*.

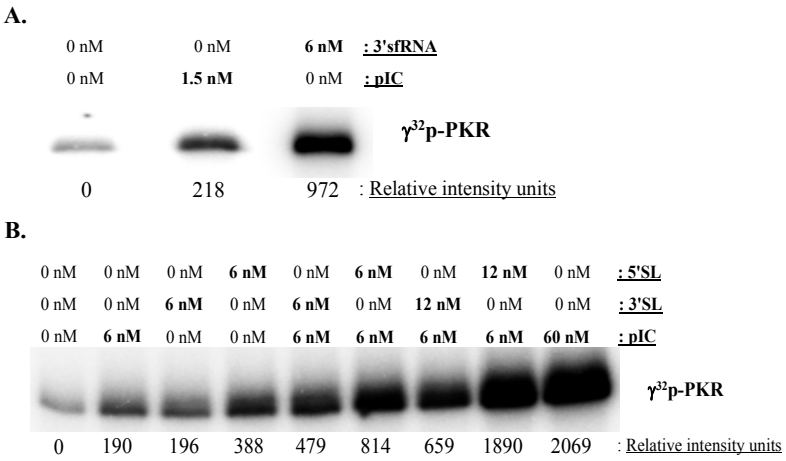

Figure 2.5. *In vitro* PKR autophosphorylation assays. (A) Reaction mixtures contained 150 ng of purified PKR alone or with the indicated concentrations of *in vitro* transcribed WNV 3'sfRNA or poly(I:C) for 30 min. (B) Reaction mixtures contained 150 ng of purified PKR alone or with the indicated concentrations of *in vitro* transcribed WNV 3'SL or 5'SL RNA and/or poly(I:C) for 30 min, or preincubated with the 3'SL or 5'SL for 10 min and then with poly(I:C) for 30 min. γ^{32}P-ATP was included in the reactions as a phosphate donor. Image Gauge 3.2 software was used to measure the relative band intensities of images acquired using a Fuji BAS 2500 analyzer. Results are representative of two independent experiments.

Poly(I:C)-mediated PKR activation in WNV-infected BHK cells. As an additional means of analyzing whether PKR is actively suppressed in WNV-infected BHK cells, the ability of poly(I:C) to activate PKR in infected cells was assessed. In preliminary experiments, the minimum concentration required for maximum intracellular PKR activation was determined to be 50 μg/ml (data not shown). BHK cells were mock-infected or infected with WNV Eg101 at a MOI of 5 and at 20 h and 30 h after infection,

cells were transfected with 50 μg/ml of poly(I:C) or incubated with transfection reagent alone for 1.5 h. An increase in total PKR levels was observed only in uninfected cells transfected with poly(I:C) (Fig. 2.6A). However, a similar increase in P-PKR, was observed in response to poly(I:C) transfection in both infected and uninfected cells (Fig. 2.6A).

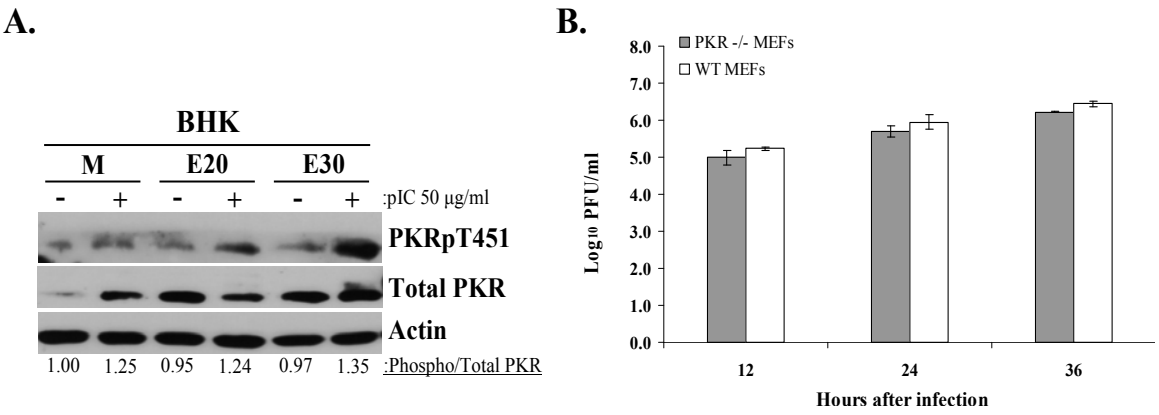

Figure 2.6. Analysis of active suppression and antiviral activities of PKR in WNV-infected cells. (A) Poly(I:C)-mediated PKR autophosphorylation in WNV-infected cells. BHK cells were mock-infected or infected with WNV-Eg101 (MOI of 5). At 20 or 30 h after infection, cells were transfected with 50 μg/ml of poly(I:C) in Celfectin II (+) or transfection reagent alone (-) for 1.5 h before cell lysis. Total PKR, phopho-Thr451 PKR and actin were detected in cell lysates by Western blotting after separation of proteins by 10% SDS-PAGE. (B) Viral yields produced by PKR-/- and wildtype MEFs infected with WNV Eg101 (MOI of 5). Samples of culture fluid were harvested at the indicated times, and infectivity titers were determined by plaque assay on BHK cells. Virus titers are expressed as $\log_{10}$ PFU/ml Error bars indicate ± standard error of the mean (SEM) (n = 3).

In additional experiments using lower poly(I:C) concentrations (10 or 25 ug/ml) similar levels of PKR activation were observed in infected and uninfected cells (data not shown). The data suggest that PKR phosphorylation is not actively suppressed in WNV-infected BHK cells and that a WNV infection does not interfere with the ability of PKR to respond to a dsRNA activator.

The antiviral effect of PKR in WNV-infected cells was assessed by comparing viral yields from WNV-infected wildtype MEFs to those from PKR-/- MEFs. Samples of

culture fluid collected at the indicated times and assayed for infectivity by plaque assay on BHK cells. Comparable virus titers were produced by both cell types at 12, 24 and 36 h after infection (Fig. 2.6B) indicating that the presence of PKR does not have an antiviral affect on WNV infection.

DISCUSSION

Infection of MEFs with WNV leads to the production of low levels of Type I IFN by 12 to 24 h after infection (Daffis et al., 2009). The initial IFN response to a WNV infection has been reported to be mediated by the RNA sensor RIG-I, while the amplified IFN response observed at later times after infection depends primarily on the MDA5 RNA sensor but also to some extent on RIG-I (Fredericksen et al., 2008). PKR is known to be an ISG (Kuhen and Samuel, 1997; Tanaka and Samuel, 1994) and PKR levels increase in cells responsive to Type I IFN with time after WNV infection. The observed increase in total PKR levels during WNV infection of Type I IFN non-responsive BHK cells indicates that PKR levels are upregulated by an IFN-independent mechanism, possibly by the NFκB pathway.

PKR is typically activated by viral dsRNA structures. PKR can also be activated in MEFs by an IFN-dependent mechanism that requires Jak1- and Tyk2-mediated phosphorylation at specific PKR tyrosine residues in addition to autophosphorylation at the Thr446 and Thr451 residues (Su et al., 2007; Su et al., 2006). IFN treatment of uninfected, wild-type (PKR+/+) MEFs but not of PKR-/- MEFs leads to PKR-mediated eIF2a phosphorylation and a reduction in protein synthesis (Su et al., 2007). The low

amount of PKR phosphorylation observed in IFN responsive, WNV-infected MEFs was not observed in WNV-infected IFNR1-/- MEFs suggesting that the observed level of PKR phosphorylation after WNV-infection of wildtype MEFs was due to IFN-induced PKR activation and not to activation by viral dsRNA. In addition, similar infectivity titers were produced by wildtype and PKR-/- MEFs infected with WNV. A previous study done with WNV virus-like particles (VLPs) containing WNV replicons concluded that PKR activation provides antiviral protection against WNV (Gilfoy and Mason, 2007). While PKR activation would be expected to have a negative effect on a flavivirus infection, similar to the data of the present study, Gilfoy and Mason (2007) observed a significant increase in total PKR but only a slight increase in PKR phosphorylation and no increase in eIF2a phosphorylation in WNV VLP-infected cells (Gilfoy and Mason, 2007). While a similar number of foci forming units (FFU) was detected in wildtype and PKR-/- MEFs 48 h after infection with WNV VLPs, IFN-treatment led to a reduction in FFUs only in wild-type MEFs suggesting that PKR was activated by IFN and not by WNV RNA replication. These results are consistent with those obtained in the present study. Another study that utilized VLPs containing a WNV replicon with a C-terminal EMCV IRES driving translation of a neomycin gene ORF (Jiang et al., 2010), reported a reduction in virus titers in cells that overexpressed PKR compared to control cells. The EMCV IRES was previously shown to activate PKR *in vitro* and *in vivo* (Arnaud et al., 2010; Shimoike et al., 2009) and this may have contributed to the PKR activation observed.

PKR exerts its antiviral effect through phosphorylation of eIF2a. Phosphorylation of as little as 20% of the eIF2a in a cell results in a significant reduction in protein synthesis (Sudhakar et al., 2000). PKR also plays a regulatory role in multiple cell signaling pathways and a number of cellular proteins have been identified that have an inhibitory effect on PKR (Garcia et al., 2006; Garcia et al., 2007). Among the cellular inhibitors tested, only Nck colocalized with the PKR that concentrated in the perinuclear region of WNV-infected cells. Since Nck interacts with inactive PKR, the detection of Nck associating with PKR in the perinuclear region of infected cells suggested that the majority of PKR is in the inactive state. An interaction between Nck and PKR in both infected and uninfected cells was indicated by co-immunoprecipitation. Nck binding to PKR can be outcompeted by dsRNA (Latreille and Larose, 2006). Even though WNV dsRNA is present in infected cells and increases with time after infection, it does not compete with Nck for binding to PKR. The minimal activation of PKR in WNV-infected Nck1,2-/- MEFs as indicated by low levels of PKR phosphorylation similar to those in wildtype MEFs provided additional evidence that PKR was not activated by viral dsRNA in infected cells. The perinuclear concentration of PKR observed in WNV-infected cells may be due to virus-directed ER membrane rearrangement.

Since eIF2a phosphorylation leads to attenuation of protein synthesis, viruses have evolved mechanisms to avoid, block or suppress PKR activation. Some viruses use alternative translational mechanisms. For example, caliciviruses encode viral proteins that act as cap-analogues while picornaviruses initiate translation from an internal ribosome entry site (IRES) in an eIF2a-independent manner (Lopez-Lastra et al., 2010).

Other viruses, such as adenoviruses and Epstein Barr virus produce small RNA inhibitors of PKR (Langland et al., 2006; Sharp et al., 1993). During influenza, reovirus, and herpes simplex virus infections, a viral protein either directly or indirectly inhibits PKR activity (Garcia et al., 2007). The WNV genome RNA utilizes cap-dependent translation and so is susceptible to eIF2a-mediated translation inhibition. However, shut-down of host translation does not occur in flavivirus infected cells (Lindenbach, 2007). We previously observed only low levels of eIF2a phosphorylation in WNV-infected BHK cells (Brinton, 2002; Emara and Brinton, 2007). Consistent with this observation, no increase in PKR phosphorylation in WNV-infected BHK cells and only a slight increase in infected MEFs mediated by IFN was observed in the present study. The observation that poly(I:C) induced similar levels of PKR phosphorylation in mock-infected and WNV-infected cells suggesting that PKR phosphorylation is not actively suppressed in WNV-infected cells. The observation that similar virus yields were produced by wildtype and PKR-/- MEFs infected with WNV confirms that the presence of PKR does not have an antiviral effect on a WNV infection.

Although terminal genomic WNV SL RNAs were able to activate PKR *in vitro*, PKR activation was not observed in WNV-infected cells even when high amount of genomic 3'sfRNA and replication intermediate RNA were present. Although the reasons why viral RNA does not bind and activate PKR in WNV-infected cells are not known, known characteristics of flavivirus infections provide possible clues. The viral capsid protein forms dimers that associate with ER membranes and viral RNA (Lindenbach, 2007) and these interactions may prevent PKR from binding to the genomic RNA. The

WNV genomic 3'SL RNA was previously reported to bind to several cellular proteins that are thought to be required for efficient initiation of viral minus strand RNA synthesis (Brinton, 2002; Davis et al., 2007). The binding of cell proteins to the 3'SL RNA in infected cells may prevent the interaction of this RNA region with PKR. The WNV genomic RNA contains a 5' cap which is an RNA modification reported to prevent PKR activation by cellular RNAs (Nallagatla et al., 2007). In addition to the 5' cap, interactions between the 5'SL and translation factors may mask this structure from detection by PKR. Alternatively, an interaction between NS5 and the 5' nts of the viral genome (Dong et al., 2008) may mask RNA structures in this region. Flaviviruses replicate in the cytoplasm and induce extensive ER membrane proliferation and rearrangement. Perinuclear vesicles that are formed by invaginations of the rough ER membrane contain the double-stranded viral RNA replication intermediates (Gillespie et al., 2010; Mackenzie, 2005; Welsch et al., 2009). The sequestering of replicating dsRNA in vesicles as well as the close proximity of viral RNA replication sites to sites of translation and packaging of genomic RNA may allow WNV dsRNA regions to evade detection by PKR. The localization of the 3'sfRNA in infected cells is not known. It is possible that it may be sequestered and inaccessible to PKR. GU wobble pairs in RNAs were previously shown to inhibit PKR activation *in vitro* (Nallagatla and Bevilacqua, 2008). Not only the number but also the clustering of GU pairs is required to sufficiently alter a dsRNA structure so that it is unable to activate PKR (Nallagatla and Bevilacqua, 2008). More than 500 GU wobble base pairs (bp) are predicted to form in a whole genome fold of the WNV Eg101 RNA (Ann Palmenberg, unpublished data). In the

context of the whole genome, 13 of the 22 GU pairs formed by the 3'sfRNA sequence are long distance interactions with nts located near the 5' end of the viral RNA. Most of these GU pairs are clustered. However, the "free" 3'sfRNA is predicted to form only 12 GU pairs and these are not clustered. The decrease in GU pairs would be expected to increase the ability of the "free" 3'sfRNA to activate PKR. However, PKR activation was not observed to increase in infected cells with the accumulation of this RNA fragment.

Although an overlap in the species of RNAs recognized by different patter recognition receptors has been reported, the RNA recognized by RIG-I, MDA5 and TLRs, which lack DRBMs, likely differs from that recognized by PKR (Nallagatla and Bevilacqua, 2008). The WNV RNA sequences or structures that can serve as targets for each of these RNA sensors have not been determined.

MATERIALS AND METHODS

Cell lines and viruses. Simian virus 40 (SV40)-transformed C3H/He and C57BL/6 mouse embryo fibroblast (MEF) lines, as well as BHK-21 WI2 cells (Vaheri et al., 1965), were grown as previously described (Scherbik et al., 2006). PKR+/+ and PKR-/- (generated by Charles Weissmann, the Scripps Research Institute; provided by Scott Kimball, Pennsylvania State University), SV40-transformed IFNR1-/- and 129 wild-type (129wt) (provided by Herbert Virgin, Washington University, St. Louis, Mo), Nck1,2-/- (provided by Tony Pawson, Samuel Lunenfield Research Institute, Ontario, Canada) MEFs were maintained at 37°C in 5% CO_2 in Dulbecco's modified Eagle medium

(DMEM) containing high glucose, 10% heat inactivated fetal bovine serum (FBS), 100 μg/ml streptomycin and 100 IU/ml penicillin.

Stocks of lineage 1 (Eg101, Tx113 and NY99) and lineage 2 (SPU and Mg78) strains of WNV were prepared by infecting BHK cells at a multiplicity of infection (MOI) of 0.1 and harvesting culture fluid 32 h after infection. Clarified culture fluid (1 x 10^8 PFU/ml, Eg101; 3 x 10^6 PFU/ml, Tx113; 5 x 10^7 PFU/ml, NY99; 2 x 10^7 PFU/ml, SPU; 3 x 10^6 PFU/ml, Mg78) was aliquoted and stored at -80°C. Plaque assays to measure virus titer were done in BHK cells as previously described (Scherbik et al., 2006).

Confocal microscopy. BHK cells (2 x 10^3 cells per well) were seeded on 12.5-mm coverslips, in 24-well plates and 24 h later, the cells were counted and infected with WNV-Eg101 at a MOI of 5. At the indicated times, cells were fixed in 4% paraformaldehyde and then permeabilized using cold 100% methanol. The cells were washed in PBS and incubated overnight at 4ºC in blocking buffer (5% heat inactivated horse serum in PBS). The cells were then incubated with a primary antibody diluted in blocking buffer for 1 h at room temperature, washed three times with PBS, and incubated for 1 h at room temperature with AlexaFluor-350, -488, -594 or -555 conjugated secondary antibodies (Invitrogen) diluted in blocking buffer. Cell nuclei were stained with 0.5 μg/ml Hoechst 33258 (Molecular Probes) added during the secondary antibody incubation. Coverslips were mounted with Prolong mounting medium (Invitrogen), and the cells were viewed and photographed with a Zeiss LSM 510 confocal microscope (Zeiss, Germany) using either a 63X or 100x oil immersion objective. The images were

merged and analyzed using Zeiss software version 3.2. The same camera settings were used for all images in an experimental series. Primary antibodies used were: mouse anti-PKR (1:100) or rabbit anti-PKR (1:100) (Santa Cruz Biotechnology), mouse anti-dsRNA (1:200) (English and Scientific Consulting, Hungary), mouse anti-Hsp90 (1:100) (Stressgen), mouse anti-Hsp70 (1:100) (Stressgen), rabbit anti-$p58^{ipk}$ (1:100) (Cell Signaling), rabbit anti-PP1a (1:100) (Cell Signaling), anti-Dcp1a (a gift from J. Lykke-Anderson, University of Colorado, Boulder, CO), rabbit anti-Nck (Millipore), mouse anti-C114 (Sigma Aldrich) and mouse-anti-RLP18 (Sigma Aldrich).

Co-immunoprecipitation assay. BHK cells (2×10^7) were mock-infected or infected with WNV at a MOI of 5. At 26 h after infection, cells were collected in NP-40 lysis buffer [50 mM sodium phosphate (pH 7.2), 150 mM NaCl, 1% Nonidet P-40, and EDTA-free Complete Mini Protease Inhibitor Cocktail (Roche)]. Cell lysates were incubated on ice for 30 min, sonicated, and then centrifuged at 2,000 × g for 5 min at 4°C to make S2 fractions. S2 lysates (500 μl per reaction containing ~500 μg of total protein) were incubated with 1 μg of rabbit anti-PKR-1 or a nonspecific rabbit IgG antibody overnight at 4°C with rotation. Protein G-magnetic beads (New England Biolabs) were added and incubation was continued for 1 h. Beads were collected magnetically, washed seven times with 1 ml of lysis buffer, and proteins were eluted by boiling for 5 min. Proteins were separated by 10% SDS/PAGE, transferred to nitrocellulose membranes, and analyzed by Western blotting using one of the following antibodies: mouse anti-PKR (Santa Cruz), rabbit anti-Nck (Millipore), mouse anti-NS5 (a gift from Pei-Yong Shi, Wadsworth Center, NY State Department of Health, NY) or goat anti-NS3 (R&D systems).

Western blot analysis. Cells were seeded into 12-well plates and grown to ~100% confluency and infected at a MOI of 5. Cells were lysed in RIPA buffer [1X PBS, 1% NP-40, 0.5% sodium deoxycholate, 1% SDS and protease inhibitor cocktail (Roche)] at the indicated times after infection, lysates were collected and 2X Sample Buffer [20% SDS, 25% glycerol, 7% 0.5M Tris-HCl (pH 6.8), 0.5% bromophenol blue,and 5% 2-mercaptoethanol] was added. The samples were boiled for 5 min and proteins were resolved by SDS-PAGE. The proteins were transferred to a nitrocellulose membrane. The membrane was blocked with 5% BSA or 5% non-fat dry milk (NFDM) in 1X TBS + 0.05% Tween-20 (TBST) for 1 h at room temperature. A primary antibody was then incubated with the membrane overnight at 4ºC, the membranes were washed 3 times in 1X TBST and then incubated with a secondary antibody diluted in 5% NFDM-TBST for 1 h at room temperature. After washing the membrane twice in 1X TBST and once in 1X TBS, membranes were processed for enhanced chemiluminescence using a Super-Signal West Pico detection kit (Pierce, Rockford, IL) according to the manufacturer's instructions. Membranes were incubated with one of the following primary antibodies: anti-p-eIF2α (Ser51) (Cell Signaling) (1:500 in 5% BSA-TBST) and anti-eIF2α (1:1000 in 5% NFDM-TBST) (Cell Signaling), anti-PKR (1:3000 in 5% NFDM-TBST) (Santa Cruz), anti-PKR-pT451 (1:500 in 5% BSA-TBST) (Millipore), anti-Nck (1:1000 in 5% NFDM-TBST) (Millipore) or anti-actin (1:40,000 in 5% NFDM-TBST) (Abcam). Anti-Rabbit-HRP (1:2000) and anti-Mouse-HRP (1:2000) (Cell Signaling) secondary antibodies were both diluted in 5% NFDM-TBST.

***In vitro* transcription of viral RNA.** WNV3'(+)SL RNA, WNV5'(+)SL RNA, and the WNV 3' small fragment RNA (3'sfRNA) were *in vitro* transcribed using a MAXIscript *in vitro* transcription kit (Ambion) in 20-µl reactions containing T7 RNA polymerase (30 U), a PCR purification kit (Qiagen)-purified PCR product (1 µg), 0.8 mM [α-^{32}P]GTP (3,000 Ci/mmol, 10 mCi/ml; Perkin Elmer), and 0.5 mM CTP, UTP, and ATP. Unlabeled viral RNA was *in vitro* transcribed as described above, except that 0.5 mM of each nucleoside triphosphate was added to the reaction mixture. The *in vitro* transcription mixture was incubated at 37°C for 2 h, and transcription was stopped by the addition of DNase I (1 U). The reaction mixture was heated at 95°C for 5 min in 2X Gel Loading Buffer II (Ambion) and the RNA transcripts were purified by electrophoresis on a 6% polyacrylamide gel containing 7 M urea. The wet gel was autoradiographed, the ^{32}P-labeled RNA band as well as unlabeled RNA bands loaded onto adjacent lanes were excised. RNA was eluted from the gel slices by rocking overnight at 4°C in elution buffer [0.5 M NH_4OAC, 1 mM EDTA, and 0.2% SDS]. Eluted RNA was filtered through a 0.45-µm cellulose acetate filter unit (Millipore), ethanol-precipitated, resuspended in water, aliquoted, and stored at -80°C. The amount of radioactivity incorporated into each RNA probe was measured in a scintillation counter (model LS6500; Beckman), and the specific activity was estimated using Ambion's specific activity calculator (Ambion). Unlabeled RNA concentrations were calculated based on UV absorbance measured at 260 nm.

RNA secondary structure prediction. The secondary structure of each RNA probe used in this study was predicted using Mfold version 3.1 software (Zuker, 2003).

PKR autophosphorylation assay. Recombinant human PKR expressed and purified from E. coli was a gift from Graem Conn, Emory University (Conn, 2003). Purified PKR (150 μg) was incubated with *in vitro* transcribed viral RNAs in kinase buffer [5 mM Tris-HCl, (pH 7.6), 1 mM $MgCl_2$, 25 mM KCl, 0.25% Triton-X 100, and RNase Inhibitor (Ambion)] on ice for 10 min. Poly(I:C), 4X Mg/ATP cocktail (Millipore) [20 mM MOPS, pH 7.2, 25 mM β-glycerophosphate, 5 mM EGTA, 1mM Na_3VO_4, 1 mM dithiothreitol, 75 mM MgCl2, and 0.5 mM ATP] and 10 μCi ^{32}p-γ-ATP (Perkin Elmer) were added to the reactions and incubated at 30°C for 20 minutes. The reactions were stopped by addition of 2X Sample Buffer [20% SDS, 25% glycerol, 7% 0.5M Tris-HCl (pH 6.8), 0.5% bromophenol blue and 5% 2-mercaptoethanol added fresh], and the proteins were resolved by SDS-PAGE. Gels were fixed in 30% methanol and 10% acetone, incubated in Autofluor image intensifier solution (National Diagnostics) and then incubated in anti-cracking buffer [7% methanol, 7% acetone and 1% glycerol] at room temperature, dried and analyzed using a Fuji BAS 2500 analyzer (Fuji Photo Film Co.) and Image Gauge software (Science Lab, 98, version 3.12; Fuji Photo Film Co.).

Poly(I:C) transfection. To activate intracellular PKR, 1 to 100 μg of poly(I:C) (Sigma Aldrich) were transfected into BHK cell monolayers in 12-well plates. Briefly, 5 μl of poly(I:C) was diluted in 95 μl OptiMEM I Reduced Serum media (Invitrogen) and incubated with 5 μl Celfectin II transfection reagent (Invitrogen) diluted in 95 μl OptiMEM for approximately 20 minutes. The poly(I:C)–Celfectin complexes were added to the cell monolayers (200 μl per well), the volume was increased to 1 ml with OptiMEM and the monolayers were incubated for 2 h at 37°C.

REFERENCES

Arnaud, N., Dabo, S., Maillard, P., Budkowska, A., Kalliampakou, K. I., Mavromara, P., Garcin, D., Hugon, J., Gatignol, A., Akazawa, D., Wakita, T., and Meurs, E. F. (2010). Hepatitis C virus controls interferon production through PKR activation. *PLoS One* **5**(5)**,** e10575.

Bevilacqua, P. C., and Cech, T. R. (1996). Minor-groove recognition of double-stranded RNA by the double-stranded RNA-binding domain from the RNA-activated protein kinase PKR. *Biochemistry* **35**(31)**,** 9983-94.

Brinton, M. A. (2002). The molecular biology of West Nile Virus: a new invader of the western hemisphere. *Annu Rev Microbiol* **56,** 371-402.

Cardin, E., and Larose, L. (2008). Nck-1 interacts with PKR and modulates its activation by dsRNA. *Biochem Biophys Res Commun* **377**(1)**,** 231-5.

Cardin, E., Latreille, M., Khoury, C., Greenwood, M. T., and Larose, L. (2007). Nck-1 selectively modulates eIF2alphaSer51 phosphorylation by a subset of eIF2alpha-kinases. *FEBS J* **274**(22)**,** 5865-75.

Conn, G. L. (2003). Expression of active RNA-activated protein kinase (PKR) in bacteria. *Biotechniques* **35**(4)**,** 682-4, 686.

Daffis, S., Suthar, M. S., Szretter, K. J., Gale, M., Jr., and Diamond, M. S. (2009). Induction of IFN-beta and the innate antiviral response in myeloid cells occurs through an IPS-1-dependent signal that does not require IRF-3 and IRF-7. *PLoS Pathog* **5**(10)**,** e1000607.

Davis, W. G., Blackwell, J. L., Shi, P. Y., and Brinton, M. A. (2007). Interaction between the cellular protein eEF1A and the 3'-terminal stem-loop of West Nile virus genomic RNA facilitates viral minus-strand RNA synthesis. *J Virol* **81**(18)**,** 10172-87.

Dong, H., Zhang, B., and Shi, P. Y. (2008). Terminal structures of West Nile virus genomic RNA and their interactions with viral NS5 protein. *Virology* **381**(1)**,** 123-35.

Donze, O., Abbas-Terki, T., and Picard, D. (2001). The Hsp90 chaperone complex is both a facilitator and a repressor of the dsRNA-dependent kinase PKR. *Embo J* **20**(14)**,** 3771-80.

Emara, M. M., and Brinton, M. A. (2007). Interaction of TIA-1/TIAR with West Nile and dengue virus products in infected cells interferes with stress granule formation and processing body assembly. *Proc Natl Acad Sci U S A* **104**(21)**,** 9041-6.

Fredericksen, B. L., Keller, B. C., Fornek, J., Katze, M. G., and Gale, M., Jr. (2008). Establishment and maintenance of the innate antiviral response to West Nile Virus involves both RIG-I and MDA5 signaling through IPS-1. *J Virol* **82**(2)**,** 609-16.

Garcia, M. A., Gil, J., Ventoso, I., Guerra, S., Domingo, E., Rivas, C., and Esteban, M. (2006). Impact of protein kinase PKR in cell biology: from antiviral to antiproliferative action. *Microbiol Mol Biol Rev* **70**(4)**,** 1032-60.

Garcia, M. A., Meurs, E. F., and Esteban, M. (2007). The dsRNA protein kinase PKR: virus and cell control. *Biochimie* **89**(6-7)**,** 799-811.

Gilfoy, F. D., and Mason, P. W. (2007). West Nile virus-induced interferon production is mediated by the double-stranded RNA-dependent protein kinase PKR. *J Virol* **81**(20)**,** 11148-58.

Gillespie, L. K., Hoenen, A., Morgan, G., and Mackenzie, J. M. (2010). The endoplasmic reticulum provides the membrane platform for biogenesis of the flavivirus replication complex. *J Virol* **84**(20)**,** 10438-47.

Gubler, D. J., Kuno, G., and Markoff, J. (2007). Flaviviruses. *In* "Fields Virology" (P. M. H. David M Knipe, Ed.), pp. 1153-1252. Lippincott Williams and Wilkins, Philadelphia.

He, B., Gross, M., and Roizman, B. (1998). The gamma134.5 protein of herpes simplex virus 1 has the structural and functional attributes of a protein phosphatase 1 regulatory subunit and is present in a high molecular weight complex with the enzyme in infected cells. *J Biol Chem* **273**(33)**,** 20737-43.

Hebner, C. M., Wilson, R., Rader, J., Bidder, M., and Laimins, L. A. (2006). Human papillomaviruses target the double-stranded RNA protein kinase pathway. *J Gen Virol* **87**(Pt 11)**,** 3183-93.

Hershey, J. W. (1991). Translational control in mammalian cells. *Annu Rev Biochem* **60,** 717-55.

Ito, T., Yang, M., and May, W. S. (1999). RAX, a cellular activator for double-stranded RNA-dependent protein kinase during stress signaling. *J Biol Chem* **274**(22)**,** 15427-32.

Jammi, N. V., and Beal, P. A. (2001). Phosphorylation of the RNA-dependent protein kinase regulates its RNA-binding activity. *Nucleic Acids Res* **29**(14)**,** 3020-9.

Jiang, D., Weidner, J. M., Qing, M., Pan, X. B., Guo, H., Xu, C., Zhang, X., Birk, A., Chang, J., Shi, P. Y., Block, T. M., and Guo, J. T. (2010). Identification of five interferon-induced cellular proteins that inhibit west nile virus and dengue virus infections. *J Virol* **84**(16)**,** 8332-41.

Kaufman, R. J. (1999). Stress signaling from the lumen of the endoplasmic reticulum: coordination of gene transcriptional and translational controls. *Genes Dev* **13**(10)**,** 1211-33.

Kuhen, K. L., and Samuel, C. E. (1997). Isolation of the interferon-inducible RNA-dependent protein kinase Pkr promoter and identification of a novel DNA element within the 5'-flanking region of human and mouse Pkr genes. *Virology* **227**(1)**,** 119-30.

Langland, J. O., Cameron, J. M., Heck, M. C., Jancovich, J. K., and Jacobs, B. L. (2006). Inhibition of PKR by RNA and DNA viruses. *Virus Res* **119**(1)**,** 100-10.

Langland, J. O., and Jacobs, B. L. (1992). Cytosolic double-stranded RNA-dependent protein kinase is likely a dimer of partially phosphorylated Mr = 66,000 subunits. *J Biol Chem* **267**(15)**,** 10729-36.

Latreille, M., and Larose, L. (2006). Nck in a complex containing the catalytic subunit of protein phosphatase 1 regulates eukaryotic initiation factor 2alpha signaling and cell survival to endoplasmic reticulum stress. *J Biol Chem* **281**(36)**,** 26633-44.

Lee, T. G., Tomita, J., Hovanessian, A. G., and Katze, M. G. (1990). Purification and partial characterization of a cellular inhibitor of the interferon-induced protein

kinase of Mr 68,000 from influenza virus-infected cells. *Proc Natl Acad Sci U S A* **87**(16)**,** 6208-12.

Lemaire, P. A., Lary, J., and Cole, J. L. (2005). Mechanism of PKR activation: dimerization and kinase activation in the absence of double-stranded RNA. *J Mol Biol* **345**(1)**,** 81-90.

Lin, K. C., Chang, H. L., and Chang, R. Y. (2004). Accumulation of a 3'-terminal genome fragment in Japanese encephalitis virus-infected mammalian and mosquito cells. *J Virol* **78**(10)**,** 5133-8.

Lindenbach, B. D., Thiel, H. J, and Rice, C. M. (2007). Flaviviridae: The Viruses and Their Replication. *In* "Fields Virology" (D. M. Knipe, and Howley, P. M., Ed.), pp. 1101-1152. Lippincott Williams and Wilkins, Philadelphia.

Lopez-Lastra, M., Ramdohr, P., Letelier, A., Vallejos, M., Vera-Otarola, J., and Valiente-Echeverria, F. (2010). Translation initiation of viral mRNAs. *Rev Med Virol* **20**(3)**,** 177-95.

Mackenzie, J. (2005). Wrapping things up about virus RNA replication. *Traffic* **6**(11)**,** 967-77.

Majumdar, R., and Maitra, U. (2005). Regulation of GTP hydrolysis prior to ribosomal AUG selection during eukaryotic translation initiation. *EMBO J* **24**(21)**,** 3737-46.

McKenna, S. A., Kim, I., Liu, C. W., and Puglisi, J. D. (2006). Uncoupling of RNA binding and PKR kinase activation by viral inhibitor RNAs. *J Mol Biol* **358**(5)**,** 1270-85.

McKenna, S. A., Lindhout, D. A., Shimoike, T., Aitken, C. E., and Puglisi, J. D. (2007). Viral dsRNA inhibitors prevent self-association and autophosphorylation of PKR. *J Mol Biol* **372**(1)**,** 103-13.

Meurs, E., Chong, K., Galabru, J., Thomas, N. S., Kerr, I. M., Williams, B. R., and Hovanessian, A. G. (1990). Molecular cloning and characterization of the human double-stranded RNA-activated protein kinase induced by interferon. *Cell* **62**(2)**,** 379-90.

Nallagatla, S. R., and Bevilacqua, P. C. (2008). Nucleoside modifications modulate activation of the protein kinase PKR in an RNA structure-specific manner. *RNA* **14**(6)**,** 1201-13.

Nallagatla, S. R., Hwang, J., Toroney, R., Zheng, X., Cameron, C. E., and Bevilacqua, P. C. (2007). 5'-triphosphate-dependent activation of PKR by RNAs with short stem-loops. *Science* **318**(5855)**,** 1455-8.

Nanduri, S., Carpick, B. W., Yang, Y., Williams, B. R., and Qin, J. (1998). Structure of the double-stranded RNA-binding domain of the protein kinase PKR reveals the molecular basis of its dsRNA-mediated activation. *EMBO J* **17**(18)**,** 5458-65.

Nanduri, S., Rahman, F., Williams, B. R., and Qin, J. (2000). A dynamically tuned double-stranded RNA binding mechanism for the activation of antiviral kinase PKR. *EMBO J* **19**(20)**,** 5567-74.

Pang, Q., Christianson, T. A., Keeble, W., Koretsky, T., and Bagby, G. C. (2002). The anti-apoptotic function of Hsp70 in the interferon-inducible double-stranded RNA-dependent protein kinase-mediated death signaling pathway requires the Fanconi anemia protein, FANCC. *J Biol Chem* **277**(51)**,** 49638-43.

Patel, C. V., Handy, I., Goldsmith, T., and Patel, R. C. (2000). PACT, a stress-modulated cellular activator of interferon-induced double-stranded RNA-activated protein kinase, PKR. *J Biol Chem* **275**(48)**,** 37993-8.

Pijlman, G. P., Funk, A., Kondratieva, N., Leung, J., Torres, S., van der Aa, L., Liu, W. J., Palmenberg, A. C., Shi, P. Y., Hall, R. A., and Khromykh, A. A. (2008). A highly structured, nuclease-resistant, noncoding RNA produced by flaviviruses is required for pathogenicity. *Cell Host Microbe* **4**(6)**,** 579-91.

Pratt, W. B., and Toft, D. O. (2003). Regulation of signaling protein function and trafficking by the hsp90/hsp70-based chaperone machinery. *Exp Biol Med (Maywood)* **228**(2)**,** 111-33.

Romano, P. R., Garcia-Barrio, M. T., Zhang, X., Wang, Q., Taylor, D. R., Zhang, F., Herring, C., Mathews, M. B., Qin, J., and Hinnebusch, A. G. (1998). Autophosphorylation in the activation loop is required for full kinase activity in vivo of human and yeast eukaryotic initiation factor 2alpha kinases PKR and GCN2. *Mol Cell Biol* **18**(4)**,** 2282-97.

Sadler, A. J., and Williams, B. R. (2007). Structure and function of the protein kinase R. *Curr Top Microbiol Immunol* **316,** 253-92.

Scherbik, S. V., Paranjape, J. M., Stockman, B. M., Silverman, R. H., and Brinton, M. A. (2006). RNase L plays a role in the antiviral response to West Nile virus. *J Virol* **80**(6)**,** 2987-99.

Scherbik, S. V., Stockman, B. M., and Brinton, M. A. (2007). Differential expression of interferon (IFN) regulatory factors and IFN-stimulated genes at early times after West Nile virus infection of mouse embryo fibroblasts. *J Virol* **81**(21)**,** 12005-18.

Sharp, T. V., Schwemmle, M., Jeffrey, I., Laing, K., Mellor, H., Proud, C. G., Hilse, K., and Clemens, M. J. (1993). Comparative analysis of the regulation of the interferon-inducible protein kinase PKR by Epstein-Barr virus RNAs EBER-1 and EBER-2 and adenovirus VAI RNA. *Nucleic Acids Res* **21**(19)**,** 4483-90.

Shimoike, T., McKenna, S. A., Lindhout, D. A., and Puglisi, J. D. (2009). Translational insensitivity to potent activation of PKR by HCV IRES RNA. *Antiviral Res* **83**(3)**,** 228-37.

Su, Q., Wang, S., Baltzis, D., Qu, L. K., Raven, J. F., Li, S., Wong, A. H., and Koromilas, A. E. (2007). Interferons induce tyrosine phosphorylation of the eIF2alpha kinase PKR through activation of Jak1 and Tyk2. *EMBO Rep* **8**(3)**,** 265-70.

Su, Q., Wang, S., Baltzis, D., Qu, L. K., Wong, A. H., and Koromilas, A. E. (2006). Tyrosine phosphorylation acts as a molecular switch to full-scale activation of the eIF2alpha RNA-dependent protein kinase. *Proc Natl Acad Sci U S A* **103**(1)**,** 63-8.

Sudhakar, A., Ramachandran, A., Ghosh, S., Hasnain, S. E., Kaufman, R. J., and Ramaiah, K. V. (2000). Phosphorylation of serine 51 in initiation factor 2 alpha (eIF2 alpha) promotes complex formation between eIF2 alpha(P) and eIF2B and causes inhibition in the guanine nucleotide exchange activity of eIF2B. *Biochemistry* **39**(42)**,** 12929-38.

Tan, S. L., Tareen, S. U., Melville, M. W., Blakely, C. M., and Katze, M. G. (2002). The direct binding of the catalytic subunit of protein phosphatase 1 to the PKR protein

kinase is necessary but not sufficient for inactivation and disruption of enzyme dimer formation. *J Biol Chem* **277**(39)**,** 36109-17.

Tanaka, H., and Samuel, C. E. (1994). Mechanism of interferon action: structure of the mouse PKR gene encoding the interferon-inducible RNA-dependent protein kinase. *Proc Natl Acad Sci U S A* **91**(17)**,** 7995-9.

Toth, A. M., Zhang, P., Das, S., George, C. X., and Samuel, C. E. (2006). Interferon action and the double-stranded RNA-dependent enzymes ADAR1 adenosine deaminase and PKR protein kinase. *Prog Nucleic Acid Res Mol Biol* **81,** 369-434.

Urosevic, N., van Maanen, M., Mansfield, J. P., Mackenzie, J. S., and Shellam, G. R. (1997). Molecular characterization of virus-specific RNA produced in the brains of flavivirus-susceptible and -resistant mice after challenge with Murray Valley encephalitis virus. *J Gen Virol* **78 (Pt 1),** 23-9.

Vaheri, A., Sedwick, W. D., Plotkin, S. A., and Maes, R. (1965). Cytopathic effect of rubella virus in RHK21 cells and growth to high titers in suspension culture. *Virology* **27**(2)**,** 239-41.

Welsch, S., Miller, S., Romero-Brey, I., Merz, A., Bleck, C. K., Walther, P., Fuller, S. D., Antony, C., Krijnse-Locker, J., and Bartenschlager, R. (2009). Composition and three-dimensional architecture of the dengue virus replication and assembly sites. *Cell Host Microbe* **5**(4)**,** 365-75.

Yin, Z., Haynie, J., Williams, B. R., and Yang, Y. C. (2003). C114 is a novel IL-11-inducible nuclear double-stranded RNA-binding protein that inhibits protein kinase R. *J Biol Chem* **278**(25)**,** 22838-45.

Zuker, M. (2003). Mfold web server for nucleic acid folding and hybridization prediction. *Nucleic Acids Res* **31**(13)**,** 3406-15.

CHAPTER 3

Analysis of a spontaneous WNV infectious clone mutant.

INTRODUCTION

A final step in the initiation of eukaryotic mRNA translation is the delivery of a methionyl-tRNA by eIF2 within a ternary complex to the 40S ribosomal subunit of the 43S preinitiation complex (Garcia et al., 2007). Under stressful conditions, phosphorylation of Ser51 of the alpha-subunit of eIF2 by one of the eIF2a kinases leads to inhibition of the exchange of GDP-bound eIF2a for GTP-eIF2a. This results in a "stalled" 43S complex and leads to an attenuation of protein synthesis (Garcia et al., 2007). Not all host translation is compromised and a subset of mRNAs escapes translation shut-off due to the presence of IRESs, multiple ATGs in close proximity to one another or the presence of unique RNA hairpin structures present within their 5' UTRs making their initiation independent of eIF2a (Mueller and Hinnebusch, 1986; Ventoso et al., 2006; Wilson et al., 2000). Ribosomes already elongating on mRNAs with a stalled 48S preinitiation complex continue translating and then fall off. RNA-binding proteins such as TIA-1, TIAR or G3BP act as nucleating proteins that bind to the stalled pre-initiation complexes and the mRNA and then aggregate to form stress granules (SGs) (Anderson and Kedersha, 2008). The mRNAs in SGs are sequestered until the cell becomes committed to either survival or death (McEwen et al., 2005). If the cellular stress is relieved or overcome, then SGs dissociate allowing eIF2a-GTP pre-initiation complexes to initiate translation of the mRNAs (Fig. 3.1). On the other hand, if the cell

is committed to death, these mRNAs will be sent to processing bodies (PBs). PBs contain proteins, including Dcp1a and Xrn1, that mediate decapping and degradation of mRNAs (Anderson and Kedersha, 2008; Buchan and Parker, 2009).

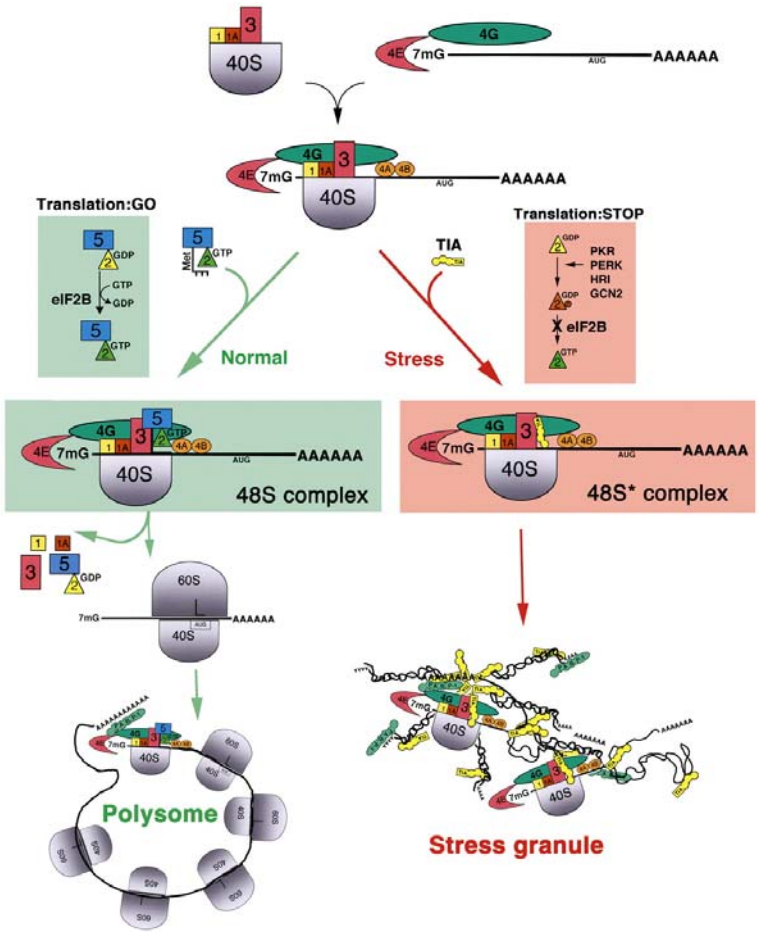

Figure 3.1. Translational initiation in the presence or absence of stress. In the absence of stress, eIF2B promotes the charging of the eIF2-GTP-tRNAMet ternary complex by exchanging GDP for GTP. When the eIF2-GTP-tRNAMet ternary complex is available, a canonical 48S preinitiation complex is assembled at the 5' end of capped transcripts and scanning begins. Upon recognition of the initiation codon by the anticodon of tRNAMet, eIF5 promotes GTP hydrolysis, and early initiation factors are displaced by the 60S ribosomal subunit. As additional ribosomes are added to the transcript, the mRNA is converted into a polysome. In stressed cells, phosphorylation of eIF2a by PKR, PERK, HRI or GCN2 converts eIF2 into a competitive antagonist of eIF2B, depleting the stores of eIF2/GTP/tRNAMet. Under these conditions, TIA-1 is included in a non-canonical, eIF2/eIF5-deficient 48S* preinitiation complex (composed of all components of the 48S pre-initiation complex except eIF2 and eIF5) that is translationally silent. TIA-1 self-aggregation then promotes the accumulation of these complexes at discrete cytoplasmic foci known as stress granules. Figure and legend modified from (Anderson and Kedersha, 2002).

Viral mRNAs compete with cellular messages for components of the translation machinery. Accordingly, many viruses have developed strategies to redirect ribosomes to selectively translate viral RNAs (Lopez-Lastra et al., 2010). Some viral components have been shown to interact with proteins found in SGs (Anderson and Kedersha, 2008). Sendai virus trailer RNAs bind to and sequesters TIAR leading to inhibition of SG assembly (Iseni et al., 2002). A stem-loop structure formed at the 3' end of the minus strand of WNV has been shown to bind to TIAR suggesting an important role for TIAR in WNV infection; these observations are further supported by the fact that the efficiency of WNV replication in TIAR -/- MEFs is reduced (Li et al., 2002).

WNV NS3 is a multifunctional protein that encodes serine protease, RNA helicase and RNA-NTPase domains (Brinton, 2002). The NS3-NS2B complex associates with the ER membrane and this association is necessary for efficient NS3 processing of the viral polyprotein (Brinton, 2002). As a component of the ER bound viral replication complex, NS3 interacts with the viral polymerase, NS5 and this interaction coordinates the helicase, polymerase and capping activities during RNA replication by the viral replication complex (Brinton, 2002; Kapoor et al., 1995).

WNV strains have been classified into two main lineages based on nucleotide sequence homology. Lineage I strains are associated with epidemics in various parts of the world while lineage II strains are primarily endemic in Africa (Gubler, 2007). The generation of a full-length cDNA infectious clone of a positive-strand RNA virus represents a powerful technique for studying these viruses. Mutations are made in DNA and then the infectious clone is used as a template to *in vitro* transcribe full-length,

infectious genomic RNA that when transfected into cells initiates an infection. Mutant viruses generated can be used to investigate the various steps of the viral replication cycle and pathogenesis (Boyer and Haenni, 1994). One obstacle in construction of many flavivirus infectious clones has been instability of the full-length cDNA in *E. coli* (Ruggli and Rice, 1999). The initial cDNA clone for yellow fever virus was maintained as separate 3' and 5' clones and ligated *in vitro* prior to RNA transcription (Rice et al., 1989).

To generate the first WNV infectious clone (IC), a lineage II virus strain (B956) that had been serially passaged multiple times and for which a sequence was available was used to construct an infectious clone cDNA (W956) (Yamshchikov et al., 2001). Because of the lack of a 3' sequence clone for the B956 passaged virus, a 3' terminal sequence (starting from within the C-terminal region of the NS5 gene to the end of 3'UTR) derived from the lineage I strain Eg101 were used to complete the cDNA clone (Fig. 3.2).

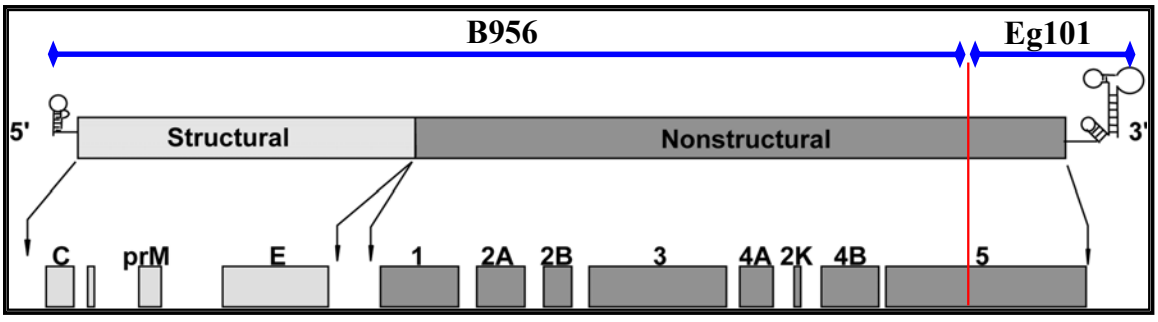

Figure 3.2. Schematic of the IC virus genome. The region comprising sequences from B956 is indicated with a blue line. The chimeric region from Eg101 is indicated with a red line.

Compared to the original B956 virus, the passaged W956 virus contains multiple nucleotide substitutions throughout the length of the genome as well as a 76 nt deletion

within the 3' UTR (Yamshchikov et al., 2004; Yamshchikov et al., 2001). W956 IC virus has been shown to efficiently induce SGs in infected cells (Courtney et al., unpublished data) but WNV Eg101 infections induce SGs inefficiently (Emara and Brinton, 2007). Virus isolated from the culture fluid of BHK cells transfected with W956 IC-derived RNA is designated IC virus in this study. When the IC virus was passaged twice in BHK cells at a MOI of 0.1, the IC-P mutant virus was generated. The current study provides data that indicate that the IC-P virus infection does not induce SGs efficiently but do induce formation of NS3 granules that persist throughout the infection.

RESULTS

SG formation in IC-P infected BHK cells. Up to 30% of BHK cells infected with WNV IC virus produced SGs while 3% or less produce SGs in response to WNV Eg101 infection (Courtney et al., unpublished data). The ability of IC-P virus to induce the formation of SGs was assessed. BHK cells were mock-infected or infected with IC virus or IC-P virus at a MOI of 5. At 30 h after infection, cells were fixed, permeabilized and incubated with anti-NS3 and anti-eIF3g antibody, followed by incubation with fluorescent tagged secondary antibodies and visualization by confocal microscopy. NS3, a viral nonstructural protein, was used as a marker of infected cells and eIF3g was used as a marker of SGs. As a positive control, mock-infected cells were treated with 0.5 mM arsenite for 30 min to induce SG formation. SGs were observed in arsenite-treated cells as well as in IC-infected cells; however, IC-P infection did not lead to the formation of SGs (Fig. 3.3). Large cytoplasmic granules were detected with anti-NS3 antibody in most

IC-P virus infected cells at all times after infection but only in a few IC virus-infected cells at early times after infection (Fig. 3.3). No colocalization was observed between NS3 and eIF3g, a marker of SGs. These results suggest that passaging of the IC virus led to the generation of a mutant that does not induce the formation of SGs but does efficiently induce NS3 "granule" formation.

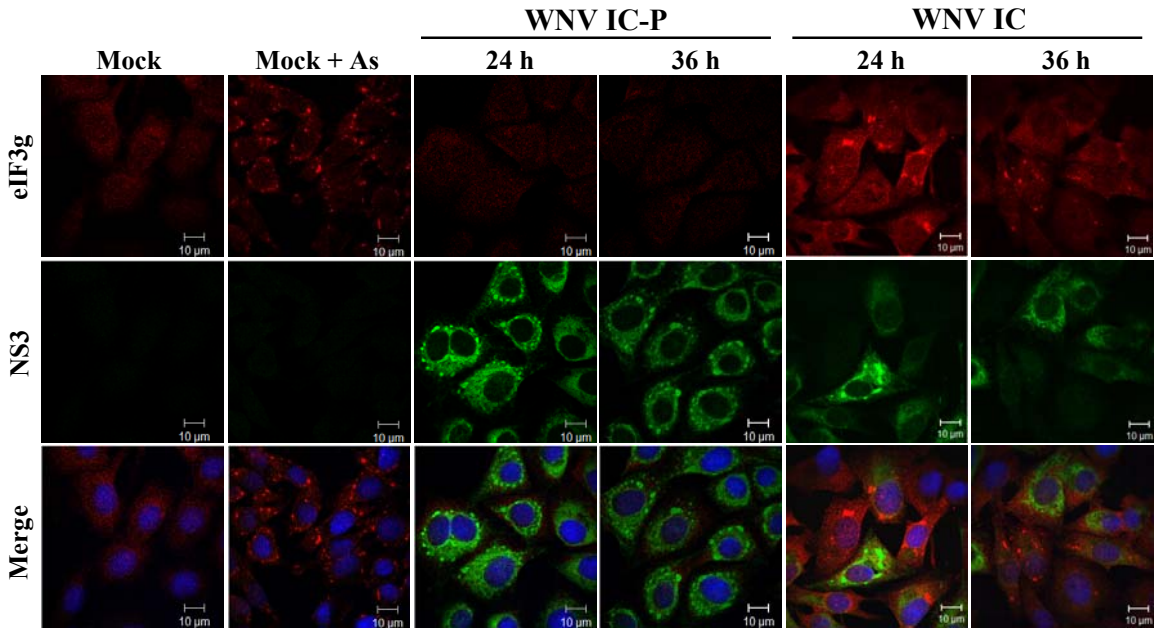

Figure 3.3. NS3 granule formation in IC-P infected BHK Cells. BHK cells were mock-infected or infected with WNV IC or WNV IC-P (MOI of 5). Positive control cells were treated with 0.5 M arsenite for 30 min. At 24 h or 36 h after infection, cells were permeabilized, fixed and blocked overnight. Cells were stained with anti-NS3 and anti-eIF3g and then with AlexaFluor488 (green) and AlexaFluor555 (red) conjugated secondary antibodies, respectively.

Formation of NS3 granules in WNV IC-P infected cells. The time course of NS3 granule formation was next investigated. BHK cells were mock-infected or infected with IC or IC-P virus. Mock-infected cells were treated with 0.5 mM arsenite for 30 min as a positive control for SGs. At 24 h or 36 h, cells were fixed, permeabilized and incubated with anti-NS3 and anti-eIF3g antibodies, followed by incubation with fluorescent tagged

secondary antibodies and visualization by confocal microscopy. SGs were observed at 24 h and 36 h in IC virus-infected cells but not in IC-P virus-infected cells at either time (Fig. 3.3). At 24 h after infection, NS3 granules were observed in most BHK cells infected with IC-P virus but only in a few cells infected with IC virus. Whereas the majority of NS3 granules had dispersed in IC virus-infected cells by 36 h, NS3 granules were still present in the majority of IC-P virus-infected cells (Fig. 3.3). The NS3 granules were mainly located at the cytoplasmic periphery of the NS3 stained area around the nucleus.

Analysis of the presence of other viral non-structural proteins in the NS3 granules. WNV replication complexes contain the viral non-structural proteins NS3, NS2A, NS2B, NS4A and NS4B in a membrane bound complex, the viral RdRpe NS5 and replicating viral RNA. Some NS1 is thought to associate with replication complexes since it has been shown to play a role in viral replication (Lindenbach, 2007). NS3 has been show to interact with NS5 (Kapoor et al., 1995). To determine whether the NS3 granules observed during IC-P virus infection also contain NS5, NS1 or viral dsRNA, BHK cells were mock-infected or infected with IC-P virus at a MOI of 5 At 26 h after infection, cells were fixed, permeabilized and incubated with anti-NS3 and anti-NS5, anti-NS1 or anti-dsRNA antibody, followed by incubation with fluorescent tagged secondary antibodies and visualization by confocal microscopy. Although perinuclear co-localization was observed between NS1 and the diffuse NS3, NS1 did not colocalize with the NS3 granules (Fig. 3.4A). The same distribution was observed for NS5 (Fig. 3.4B). Also, viral

dsRNA did not colocalize with the NS3 granules. Interestingly, dsRNA foci were detected around the NS3 granules (Fig. 3.4C and D). These data suggest that the NS3 granules are not active viral replication complexes.

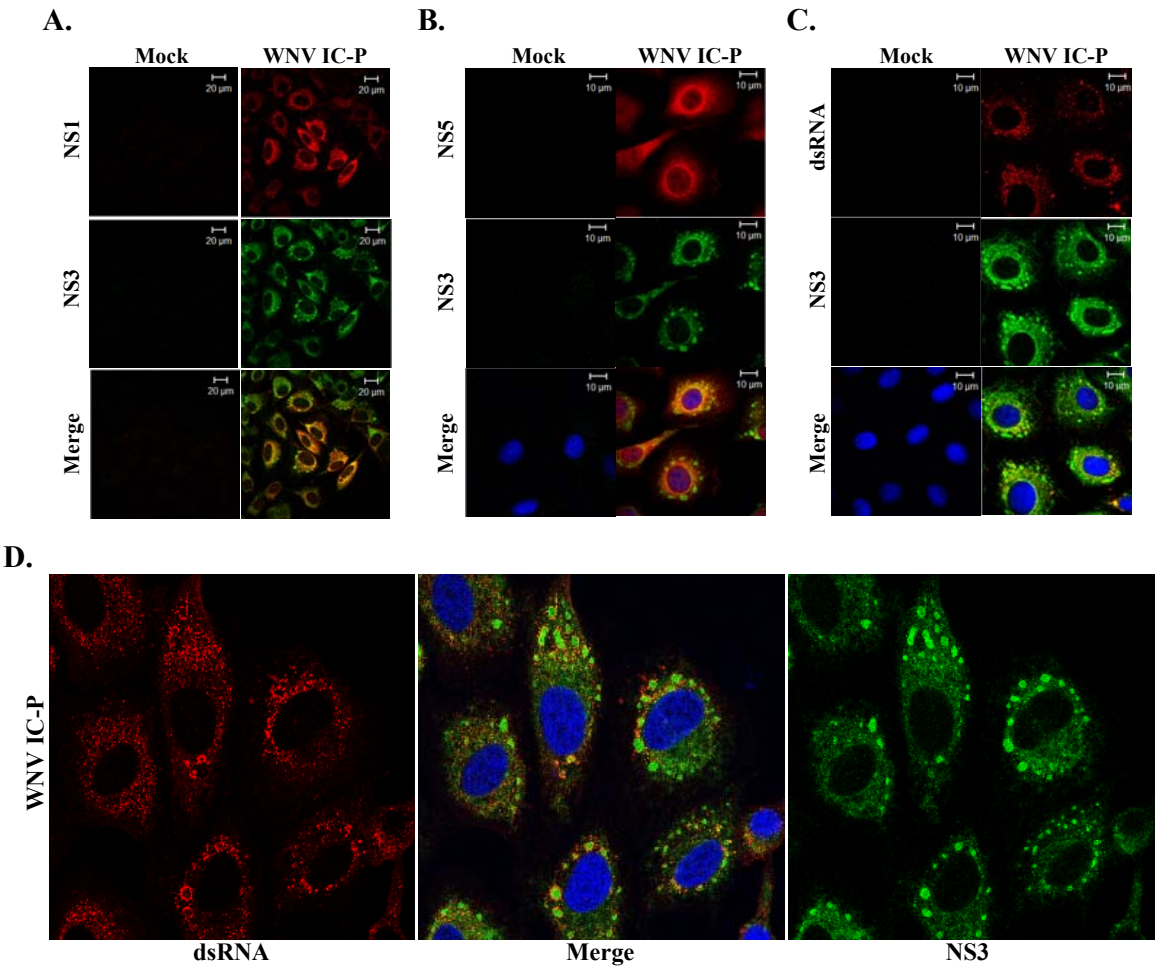

Figure 3.4. NS3 localization with IC-P viral replication sites. BHK cells were mock-infected or infected with WNV IC-P (MOI of 5). At 26 h after infection, cells were permeabilized, fixed and blocked overnight. Cells were stained with anti-NS3 and anti-NS1 (A), anti-NS5 (B) or anti-dsRNA (C and D) and then with AlexaFluor488 (green) and AlexaFluor555/594 (red) conjugated secondary antibodies.

The localization of the NS3 granules to cellular compartments within WNV IC-P virus-infected cells was next assessed. To determine whether NS3 granules colocalize with PBs, BHK cells were mock-infected or infected with WNV IC-P virus at a MOI of

5. At 26 h after infection, cells were fixed, permeabilized and incubated with anti-NS3 and anti-hDcp1a antibody, a marker of PBs, followed by incubation with fluorescent tagged secondary antibodies and visualization by confocal microscopy. As expected based on results obtained with WNV Eg101 and IC virus infections, the number of PBs decreased but the size increased with time after infection. However, PBs did not colocalize with IC-P virus-induced NS3 granules (Fig. 3.5A).

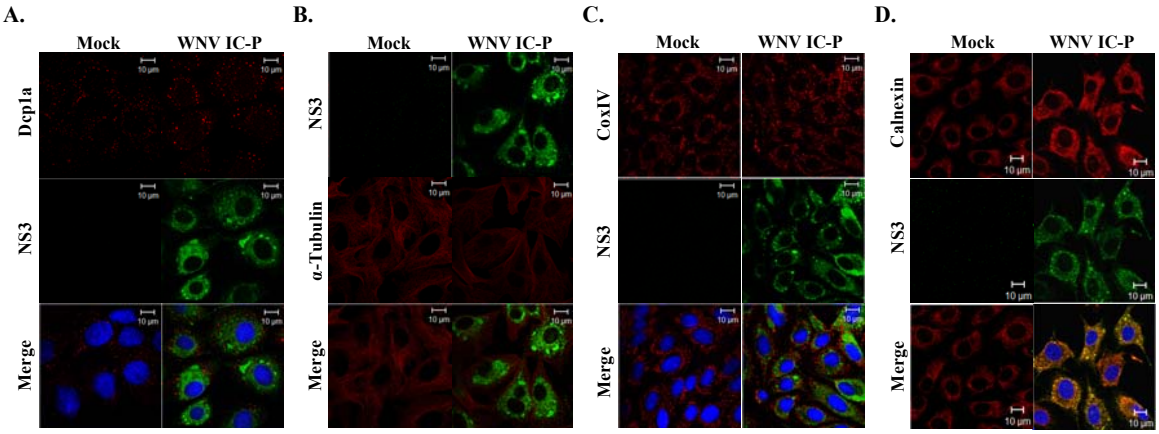

Figure 3.5. NS3 granule localization within IC-P infected cells. BHK cells were mock-infected or infected with WNV IC-P (MOI of 5). At 26 h after infection, cells were permeabilized, fixed and blocked overnight. Cells were stained with anti-NS3 and anti-Dcp1a (A), anti-α-Tubulin (B), anti-CoxIV (C) or anti-Calnexin (D) and then with AlexaFluor488 (green) and AlexaFluor555/594 (red) conjugated secondary antibodies.

The cellular localization of NS3 granules was further assessed using cellular markers specific to the mitochondria (anti-coxIV), cytoskeleton (anti-α-tubulin) and ER (anti-calnexin). BHK cells were mock-infected or infected with WNV IC-P virus at a MOI of 5. At 26 h after infection, cells were fixed, permeabilized and incubated with anti-NS3 and the indicated antibodies, followed by incubation with fluorescent tagged secondary antibodies and visualization by confocal microscopy. No colocalization was observed between the NS3 granules and mitochondria or microtubules (Fig. 3.5B and C).

In contrast, strong colocalization was observed between the NS3 granules and calnexin (Fig. 3.5D). These data suggest that the NS3 granules formed in IC-P virus-infected cells localize to ER derived membranes as do viral replication complexes but to different regions of the ER membrane.

Sequence analysis of IC-P virus. The phenotypic differences observed between the IC-P virus and the parental IC virus suggest that a mutation(s) occurred during passage of the IC virus. The genome is ~11 Kb in length. Individual nonstructural protein genes were sequenced to try to find the mutation(s) responsible for the formation of NS3 granules and the ability to suppress SG formation. BHK cells were infected with IC or IC-P virus at a MOI of 5. At 32 h, culture fluids were collected and viral genomic RNA was isolated. To generate viral gene cDNAs for sequencing, One-step RT-PCR was done using primers specific to sequences flanking each gene to be sequenced. The generated cDNAs were then subcloned into bacterial plasmids prior to amplification and 5 clones for each gene from each virus were selected for sequences. No mutations were identified in the IC-P NS1, NS2A, NS3, NS4A or NS5 genes. However, a mutation(s) may have occurred in a region of the viral RNA that has not yet been sequenced. To obtain a complete genomic sequence as well as analyze the diversity of the virus population, viral genomic RNA was extracted and purified from IC virus and IC-P virus stocks and sent to collaborators for 454 deep sequencing. The 454 sequencing analysis method is orders of magnitude more sensitive than traditional Sanger sequencing and allows identification of nucleotide frequencies at specific positions (Green et al., 2006). Initial deep sequencing

results identified a single nucleotide mutation that resulted in a coding mutation in the NS4B viral protein. The number of sequencing reads for the IC-P and IC genomic RNAs was low due to technical issues with the sequencing reaction. While there were sufficient sequencing reads to generate a consensus sequences for the IC-P virus, the number of reads was low and the sequence for the IC genomic RNA contained some gaps which may contain mutations between the two RNAs. Further deep sequencing analysis are underway to confirm our initial sequencing data.

DISCUSSION

Infectious cDNA clones of viruses have been utilized to study various aspects of viral replication. Bovine diarrhea virus and Dengue virus infectious clones were utilized to demonstrate the importance of NS3 helicase and/or NTPase activities for viral minus-strand RNA synthesis and virus viability (Gu et al., 2000; Matusan et al., 2001). Dengue virus infectious clones engineered with deletions in either the plus-strand 3' or 5' terminal structures did not replicate (Cahour et al., 1995; Lai et al., 1991; Men et al., 1996). Similarly, deletion of the 3' UTR of a Kunjin replicon was lethal (Khromykh and Westaway, 1997). Deletions within the 3' UTR regions of Dengue virus infectious clones resulted in mutant viruses that were attenuated and, in some cases, displayed altered phenotypes (Lai et al., 1991; Men et al., 1996). A WNV infectious clone harboring a mutation in the EF-1a binding site exhibited poor replication and a small plaque phenotype. Passaging of the resultant virus produced partial revertants of the mutated sequences (Davis et al., 2007) demonstrating that a selective advantage in replication

efficiency is conferred by the wild-type sequence. The WNV infectious clone used in this study is a chimeric clone composed of W956 5' and Eg101 3' sequences (Fig. 3.2). Although, WNV-IC infections in BHK cells efficiently induced SG formation, infections with the passaged WNV-IC virus did not. These results suggest that the WNV-IC virus was outcompeted by a mutant generated by a viral polymerase error.

Flavivirus replication is associated with membrane rearrangement and induction of perinuclear vesicles that enclose viral replication complexes within ER membrane invaginations (Gillespie et al., 2010; Mackenzie, 2005; Welsch et al., 2009). As the infection progresses, these vesicles accumulate and become interconnected within vesicle packets. Genomic RNA synthesized within replication complexes exit the vesicles through neck-like pores that connect the vesicles to the cytoplasm (Gillespie et al., 2010; Welsch et al., 2009). The WNV NS2B/NS3 protease complex, along with cellular proteases, cleave the viral polyprotein to generate the mature viral proteins. The NS3 protein does not contain a transmembrane domain but associates with the ER membrane-bound NS2A, NS2B, NS4A and NS4B complex via interaction with the NS3 cofactor, NS2B. Overexpression of either the hydrophobic NS4A and NS4B proteins induced membrane rearrangements similar to those observed in infected cells (Miller et al., 2007; Roosendaal et al., 2006; Welsch et al., 2009; Westaway et al., 1997a). The sequence of the IC-P virus NS4B gene has not yet been analyzed. A mutation in this protein could cause an alteration in the membrane rearrangements needed to efficiently form the final stage replication complex containing vesicles.

Some of the NS1 protein has been shown to colocalize with NS3 and dsRNA in replication complexes in WNV-infected cells (Westaway et al., 1997b). However, no colocalization was observed between the NS3 granules and NS1 in WNV IC-P infected cells. Although the viral RdRp is encoded within the NS5 protein, only 10% of NS5 was reported to be enriched in "heavy" cytoplasmic membrane fractions associated with RdRp activity (Grun and Brinton, 1987). No detectable colocalization between NS3 granules and dsRNA or NS5 was observed in WNV IC-P virus infected cells suggesting that these granules are distinct from viral replication complexes. The observation that some NS3 granules are observed in cells infected with WNV Eg101 at early times after infection suggests that these granules might represent an intermediate stage in replication complex formation.

The observed NS3 granules did not colocalize with mitochondria or PBs, nor did they colocalize with the cytoskeleton of WNV IC-P infected cells. Consistent with the formation of replication complexes within ER membrane invaginations, replication complex constituents (dsRNA, NS5 and NS3) colocalize with the ER resident protein calnexin (Mackenzie, 2005). Diffuse NS3 as well as NS3 granules colocalized with calnexin in WNV IC-P virus-infected cells suggesting that the NS3 granules are associated with ER-derived membranes. WNV-specific antibodies to NS2A, NS2B, NS4A and NS4B that work in confocal microscopy are not available to assess the presence of these proteins in NS3 granules. However, NS3 would not be expected to be membrane associated unless it interacted with one of these membrane anchor proteins. Interestingly, while dsRNA did not colocalize within the NS3 granules, it was detected in

foci located in a "ring" around the NS3 granules. These data provide further support to the hypothesis that membrane rearrangement may not occur properly or efficiently in IC-P virus-infected cells. Results obtained from preliminary 454 deep sequencing identified a single mutation in the NS4B gene which may be responsible for the formation of NS3 granules and/or could change the folding of the viral RNA affecting viral RNA replication efficiency. However, these results are yet to be confirmed by a second and more complete deep sequencing analysis

MATERIALS AND METHODS

Cell lines and viruses. Simian virus 40 (SV40)-transformed BHK-21 WI2 cells, were maintained as previously described (Scherbik et al., 2006). Stocks of virus were prepared by infecting BHK cells with WNV Eg101 at a MOI of 0.1 or transfection with *in vitro* transcribed IC RNA (1 μg) and harvesting culture fluid 32 h after infection. IC-P virus stocks were prepared by passaging of the IC virus twice in BHK cells. Clarified culture fluid (3.5×10^7 PFU/ml, IC; 3.6×10^7 PFU/ml, IC-P) was aliquoted and stored at -80°C.

Confocal microscopy. BHK cells (2×10^3 cells per well) were seeded on 12.5-mm coverslips or in 24-well plates and 24 h later, the cells were counted and infected with WNV-IC or WNV IC-P at a MOI of 5. At the indicated times, cells were fixed in 4% paraformaldehyde and then permeabilized using cold 100% methanol. The cells were washed in PBS and incubated overnight at 4ºC in blocking buffer (5% heat inactivated horse serum in PBS). The cells were then incubated with a primary antibody diluted in blocking buffer for 1 h at room temperature, washed three times with PBS, and incubated

for 1 h at room temperature with AlexaFluor-488, -594 or -555 conjugated secondary antibodies (Invitrogen) diluted in blocking buffer. Cell nuclei were stained with 0.5 µg/ml Hoechst 33258 (Molecular Probes) added during the secondary antibody incubation. Coverslips were mounted with Prolong mounting medium (Invitrogen), and the cells were viewed and photographed with a Zeiss LSM 510 confocal microscope (Zeiss, Germany) using either a 63x or 100x oil immersion objective. The images were merged and analyzed using Zeiss software version 3.2. The same camera settings were used for all images in an experimental series. Primary antibodies used were: mouse mouse anti-dsRNA (1:200) (English and Scientific Consulting), mouse anti-CoxIV (1:500) (Invitrogen), mouse anti-tubulin (1:100) (Cellsignal), rabbit anti-Calnexin (1:1000) (Sigma), goat anti-NS3 (1:300) (R & D systems), goat anti-eIF3g (1:75) (Santa Cruze) and mouse anti-Dcp1a (a gift from J. Lykke-Anderson; University of Colorado, Boulder, CO).

One-Step RT-PCR. A One-Step RT-PCR kit (Invitrogen) was used to generate cDNAs from the NS1, NS2A, NS3, NS4A or NS5 viral genes of purified IC and IC-P viral RNA. PCR products were separated by agarose-electrophoresis, purified using the MiniElute Gel extraction kit (Qiagen), subcloned into pTopoXL (Invitrogen) and transformed into Top10 chemically competent cells according to manufactures' protocols. Transformed cells were plated on LB + Kanamycin (100 µg/ml) media agar plates and incubated overnight at 37°C. Five clones from each strain were cultured and plasmids from these clones were isolated using a MiniElute DNA isolation kit according to the manufacturer's protocols (Qiagen).

Sequencing. Plasmid DNA from the various clones sequenced using M13 forward and reverse primers by the GSU Core Facility. For 454 Deep sequencing, viral RNAs were isolated using the RNeasy kit (Qiagen) according to the manufacturer's protocol. Purified RNAs were sent to collaborators for 454 sequencing.

REFERENCES:

Anderson, P., and Kedersha, N. (2002). Stressful initiations. *J Cell Sci* **115**(Pt 16)**,** 3227-34.

Anderson, P., and Kedersha, N. (2008). Stress granules: the Tao of RNA triage. *Trends Biochem Sci* **33**(3)**,** 141-50.

Boyer, J. C., and Haenni, A. L. (1994). Infectious transcripts and cDNA clones of RNA viruses. *Virology* **198**(2)**,** 415-26.

Brinton, M. A. (2002). The molecular biology of West Nile Virus: a new invader of the western hemisphere. *Annu Rev Microbiol* **56,** 371-402.

Buchan, J. R., and Parker, R. (2009). Eukaryotic stress granules: the ins and outs of translation. *Mol Cell* **36**(6)**,** 932-41.

Cahour, A., Pletnev, A., Vazielle-Falcoz, M., Rosen, L., and Lai, C. J. (1995). Growth-restricted dengue virus mutants containing deletions in the 5' noncoding region of the RNA genome. *Virology* **207**(1)**,** 68-76.

Davis, W. G., Blackwell, J. L., Shi, P. Y., and Brinton, M. A. (2007). Interaction between the cellular protein eEF1A and the 3'-terminal stem-loop of West Nile virus genomic RNA facilitates viral minus-strand RNA synthesis. *J Virol* **81**(18)**,** 10172-87.

Emara, M. M., and Brinton, M. A. (2007). Interaction of TIA-1/TIAR with West Nile and dengue virus products in infected cells interferes with stress granule formation and processing body assembly. *Proc Natl Acad Sci U S A* **104**(21)**,** 9041-6.

Garcia, M. A., Meurs, E. F., and Esteban, M. (2007). The dsRNA protein kinase PKR: Virus and cell control. *Biochimie*.

Gillespie, L. K., Hoenen, A., Morgan, G., and Mackenzie, J. M. (2010). The endoplasmic reticulum provides the membrane platform for biogenesis of the flavivirus replication complex. *J Virol* **84**(20)**,** 10438-47.

Green, R. E., Krause, J., Ptak, S. E., Briggs, A. W., Ronan, M. T., Simons, J. F., Du, L., Egholm, M., Rothberg, J. M., Paunovic, M., and Paabo, S. (2006). Analysis of one million base pairs of Neanderthal DNA. *Nature* **444**(7117)**,** 330-6.

Grun, J. B., and Brinton, M. A. (1987). Dissociation of NS5 from cell fractions containing West Nile virus-specific polymerase activity. *J Virol* **61**(11)**,** 3641-4.

Gu, B., Liu, C., Lin-Goerke, J., Maley, D. R., Gutshall, L. L., Feltenberger, C. A., and Del Vecchio, A. M. (2000). The RNA helicase and nucleotide triphosphatase activities of the bovine viral diarrhea virus NS3 protein are essential for viral replication. *J Virol* **74**(4)**,** 1794-800.

Gubler, D. J., Kuno, G., and Markoff, J. (2007). Flaviviruses. *In* "Fields Virology" (P. M. H. David M Knipe, Ed.), pp. 1153-1252. Lippincott Williams and Wilkins, Philadelphia.

Iseni, F., Garcin, D., Nishio, M., Kedersha, N., Anderson, P., and Kolakofsky, D. (2002). Sendai virus trailer RNA binds TIAR, a cellular protein involved in virus-induced apoptosis. *Embo J* **21**(19)**,** 5141-50.

Kapoor, M., Zhang, L., Ramachandra, M., Kusukawa, J., Ebner, K. E., and Padmanabhan, R. (1995). Association between NS3 and NS5 proteins of dengue

virus type 2 in the putative RNA replicase is linked to differential phosphorylation of NS5. *J Biol Chem* **270**(32)**,** 19100-6.

Khromykh, A. A., and Westaway, E. G. (1997). Subgenomic replicons of the flavivirus Kunjin: construction and applications. *J Virol* **71**(2)**,** 1497-505.

Lai, C. J., Zhao, B. T., Hori, H., and Bray, M. (1991). Infectious RNA transcribed from stably cloned full-length cDNA of dengue type 4 virus. *Proc Natl Acad Sci U S A* **88**(12)**,** 5139-43.

Li, W., Li, Y., Kedersha, N., Anderson, P., Emara, M., Swiderek, K. M., Moreno, G. T., and Brinton, M. A. (2002). Cell proteins TIA-1 and TIAR interact with the 3 ' stem-loop of the West Nile virus complementary minus-strand RNA and facilitate virus replication. *J Virol* **76**(23)**,** 11989-12000.

Lindenbach, B. D., Thiel, H. J, and Rice, C. M. (2007). Flaviviridae: The Viruses and Their Replication. *In* "Fields Virology" (D. M. Knipe, and Howley, P. M., Ed.), pp. 1101-1152. Lippincott Williams and Wilkins, Philadelphia.

Lopez-Lastra, M., Ramdohr, P., Letelier, A., Vallejos, M., Vera-Otarola, J., and Valiente-Echeverria, F. (2010). Translation initiation of viral mRNAs. *Rev Med Virol* **20**(3)**,** 177-95.

Mackenzie, J. (2005). Wrapping things up about virus RNA replication. *Traffic* **6**(11)**,** 967-77.

Matusan, A. E., Pryor, M. J., Davidson, A. D., and Wright, P. J. (2001). Mutagenesis of the Dengue virus type 2 NS3 protein within and outside helicase motifs: effects on enzyme activity and virus replication. *J Virol* **75**(20)**,** 9633-43.

McEwen, E., Kedersha, N., Song, B., Scheuner, D., Gilks, N., Han, A., Chen, J. J., Anderson, P., and Kaufman, R. J. (2005). Heme-regulated inhibitor kinase-mediated phosphorylation of eukaryotic translation initiation factor 2 inhibits translation, induces stress granule formation, and mediates survival upon arsenite exposure. *J Biol Chem* **280**(17)**,** 16925-33.

Men, R., Bray, M., Clark, D., Chanock, R. M., and Lai, C. J. (1996). Dengue type 4 virus mutants containing deletions in the 3' noncoding region of the RNA genome: analysis of growth restriction in cell culture and altered viremia pattern and immunogenicity in rhesus monkeys. *J Virol* **70**(6)**,** 3930-7.

Miller, S., Kastner, S., Krijnse-Locker, J., Buhler, S., and Bartenschlager, R. (2007). The non-structural protein 4A of dengue virus is an integral membrane protein inducing membrane alterations in a 2K-regulated manner. *J Biol Chem* **282**(12)**,** 8873-82.

Mueller, P. P., and Hinnebusch, A. G. (1986). Multiple upstream AUG codons mediate translational control of GCN4. *Cell* **45**(2)**,** 201-7.

Rice, C. M., Grakoui, A., Galler, R., and Chambers, T. J. (1989). Transcription of infectious yellow fever RNA from full-length cDNA templates produced by in vitro ligation. *New Biol* **1**(3)**,** 285-96.

Roosendaal, J., Westaway, E. G., Khromykh, A., and Mackenzie, J. M. (2006). Regulated cleavages at the West Nile virus NS4A-2K-NS4B junctions play a major role in rearranging cytoplasmic membranes and Golgi trafficking of the NS4A protein. *J Virol* **80**(9)**,** 4623-32.

Ruggli, N., and Rice, C. M. (1999). Functional cDNA clones of the Flaviviridae: strategies and applications. *Adv Virus Res* **53,** 183-207.

Scherbik, S. V., Paranjape, J. M., Stockman, B. M., Silverman, R. H., and Brinton, M. A. (2006). RNase L plays a role in the antiviral response to West Nile virus. *J Virol* **80**(6)**,** 2987-99.

Ventoso, I., Sanz, M. A., Molina, S., Berlanga, J. J., Carrasco, L., and Esteban, M. (2006). Translational resistance of late alphavirus mRNA to eIF2alpha phosphorylation: a strategy to overcome the antiviral effect of protein kinase PKR. *Genes Dev* **20**(1)**,** 87-100.

Welsch, S., Miller, S., Romero-Brey, I., Merz, A., Bleck, C. K., Walther, P., Fuller, S. D., Antony, C., Krijnse-Locker, J., and Bartenschlager, R. (2009). Composition and three-dimensional architecture of the dengue virus replication and assembly sites. *Cell Host Microbe* **5**(4)**,** 365-75.

Westaway, E. G., Khromykh, A. A., Kenney, M. T., Mackenzie, J. M., and Jones, M. K. (1997a). Proteins C and NS4B of the flavivirus Kunjin translocate independently into the nucleus. *Virology* **234**(1)**,** 31-41.

Westaway, E. G., Mackenzie, J. M., Kenney, M. T., Jones, M. K., and Khromykh, A. A. (1997b). Ultrastructure of Kunjin virus-infected cells: colocalization of NS1 and NS3 with double-stranded RNA, and of NS2B with NS3, in virus-induced membrane structures. *J Virol* **71**(9)**,** 6650-61.

Wilson, J. E., Pestova, T. V., Hellen, C. U., and Sarnow, P. (2000). Initiation of protein synthesis from the A site of the ribosome. *Cell* **102**(4)**,** 511-20.

Yamshchikov, G., Borisevich, V., Seregin, A., Chaporgina, E., Mishina, M., Mishin, V., Kwok, C. W., and Yamshchikov, V. (2004). An attenuated West Nile prototype virus is highly immunogenic and protects against the deadly NY99 strain: a candidate for live WN vaccine development. *Virology* **330**(1)**,** 304-12.

Yamshchikov, V. F., Wengler, G., Perelygin, A. A., Brinton, M. A., and Compans, R. W. (2001). An infectious clone of the West Nile flavivirus. *Virology* **281**(2)**,** 294-304.

CHAPTER 4

Functional analysis of the mouse Oas1b protein.

The majority of this chapter was published in Virology, Jan. 2011, 409(2): 262-270. The data is used with copyright permission obtained from Elsevier publishing under license #2652701163203.

An Addendum containing additional data has been added to the end of this chapter.

Results presented in Fig. 4.1A, Fig. 4.2, Fig. 4.4 and Fig. 4.5A represent data previously published as part of a Master's thesis.

INTRODUCTION

The genus *Flavivirus* includes a number of mosquito borne human pathogens, such as yellow fever virus, dengue virus, Japanese encephalitis virus, and West Nile virus (WNV). A number of factors such as the age, immune status and genetic makeup of the host as well as the route of inoculation, dose and virulence of the infecting virus can influence the outcome of flavivirus infections (Brinton, 2002). In mice, the alleles of an autosomal gene (*Flv*) determine resistance/susceptibility to flavivirus-induced disease. Mice carrying the resistant allele (Flv^r) are not resistant to flavivirus infection but produce significantly lower levels of virus compared to susceptible mice. The *Flv* gene was identified as 2′-5′ oligoadenylate synthetase 1b (Oas1b) (Mashimo et al., 2002; Perelygin et al., 2002). Resistant mice express a full-length Oas1b protein while susceptible mice express a truncated Oas1b protein (Oas1btr) generated by a premature stop-codon. The majority of inbred mouse strains used in laboratories are homozygous for the susceptibility allele (Flv^s).

In mice, the 2′-5′ oligoadenylate synthetase family consists of eight small *Oas1* genes (*Oas1a* through *Oas1h)*, an *Oas2* gene, an *Oas3* gene, and two Oas-like genes (*OasL1* and *OasL2)* (Kakuta et al., 2002). The Oas1 proteins contain a single 2′-5′ oligoadenylate synthetase unit, while two and three copies are present in the Oas2 and Oas3 proteins, respectively. The OasL proteins contain a single OAS unit as well as two C-terminal ubiquitin-like domains (Hartmann et al., 1998b; Rebouillat et al., 1998). Members of the 2′-5′ oligoadenylate synthetase family are interferon-inducible genes (ISGs) and were previously reported to be upregulated in WNV infected cells (Scherbik et al., 2007b). 2′-5′ oligoadenylate synthetases are activated by binding to dsRNA and polymerize ATP into short 2′-5′ linked oligoadenylates (2-5A) (Kerr and Brown, 1978). The 2-5A binds to RNase L in the cytosol which leads to activation and dimerization of RNase L (Floyd-Smith et al., 1981). Activated RNase L cleaves viral and cellular single-stranded RNAs after UA and UU dinucleotides (Wreschner et al., 1981). Activated RNase L was previously reported to have an antiviral effect against WNV infections in mouse embryofibroblasts (MEFs) from both flavivirus resistant and susceptible mice (Scherbik et al., 2006). The virus-nonspecific nature of 2-5A production and RNase L-mediated RNA degradation are not consistent with the flavivirus-specific phenotype of the *Flv* gene suggesting that Oas1b mediates flavivirus resistance through a novel mechanism unrelated to the 2-5A/RNase L pathway.

The N-terminal sequence of human OAS1 proteins contains an LXXXP motif previously shown to be required for synthetase activity (Ghosh et al., 1997a). The catalytic domain contains a nucleotidyltransferase fold, a P-loop motif, three catalytic

aspartic acid residues, and the substrate acceptor binding site (Yamamoto et al., 2000). The substrate donor binding site and a CFK motif are located in the C-terminal domain. The catalytic aspartic acid triad forms a Mg^{2+}-binding DAD motif. It has been suggested that the putative RNA activation site spans both the catalytic domain and C-terminal domain in the human OAS1 protein and contains a lysine/arginine rich motif (KR-rich motif). The P-loop, DAD catalytic triad, and KR-rich motif are required for the synthetase activity of OAS proteins (Saraste et al., 1990; Yamamoto et al., 2000). The CFK motif has been shown to be required for the synthetase activity of human OAS1 proteins; however, the active murine synthetases Oas1a and Oas1g contain substitutions in this motif suggesting that it is not likely to affect the structural stability of the murine proteins.

In the present study, Oas1b was shown to lack synthetase activity. This finding is consistent with previous data indicating that the flavivirus resistance phenotype mediated by Oas1b does not involve the 2-5A antiviral pathway (Scherbik et al., 2006). Full-length Oas1b, but not Oas1btr (the truncated protein encoded by *Flv*^{s}), was able to inhibit the *in vitro* synthetase activity of Oas1a in a dose-dependent manner and reduced poly(I:C)-stimulated 2-5A production *in vivo*. The results suggest that full-length Oas1b, but not the truncated protein Oas1b, functions as a dominant negative inhibitor of 2-5A oligonucleotide synthetase activity.

RESULTS

Assay of the 2-5A synthetase activity of recombinant Oas1b proteins. In a previous study, unpurified lysates from bacteria expressing individual recombinant murine Oas1 proteins fused to an N-terminal 10X histidine tag were tested for 2-5A synthetase activity and poly(I:C) binding activity (Kakuta et al., 2002). Only Oas1a and Oas1g were shown to be active 2-5A synthetases but all eight of the Oas1 proteins (Oas1a through h) tested were able to bind poly(I:C). The Oas1 cDNAs used in that study were cloned from flavivirus-susceptible C57BL/6 J mice and so Oas1btr but not Oas1b was analyzed. To test the synthetase activity of the full-length Oas1b protein, recombinant Oas1b, Oas1a (positive control) and Oas1btr (negative control) proteins fused to an N-terminal 42.5 kDa maltose binding protein (MBP) were expressed in bacteria and partially purified on amylose resin columns. Fusion proteins of the expected molecular masses, Oas1a (~ 85 kD), Oas1b (~ 86 kDa) and Oas1btr (~ 71 kDa) were detected by the Coomassie blue staining after separation of proteins by 10% SDS-PAGE (Fig. 4.1A). The average purity of Oas1a and Oas1btr was ~ 80% while that of Oas1b was ~ 60 to 75%. The identity of the recombinant proteins was confirmed by immunoblotting with anti-MBP (Fig. 4.1B) and anti-OAS antibody (Fig. 4.1C).

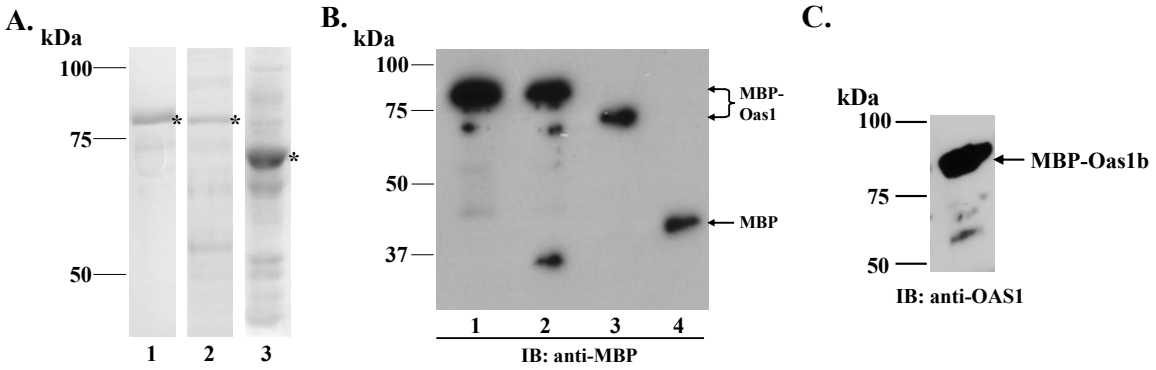

Figure 4.1. Expression and purification of recombinant MBP-Oas1 proteins. (A) MBP-Oas1 proteins were expressed in bacteria, partially purified on amylose columns, separated by 10% SDS-PAGE and visualized by Coomassie blue staining. Lane 1, MBP-Oas1a. Lane 2, MBP-Oas1b. Lane 3, MBP-Oas1btr. Asterisks indicate the positions of the MBP-Oas1 fusion proteins. (B) Immunoblot of partially purified MBP-Oas1 proteins detected with anti-MBP-HRP antibody. Lane 1, MBP-Oas1a. Lane 2, MBP-Oas1b. Lane 3, MBP-Oas1btr. Lane 4, MBP. (C) Immunoblot of partially purified MBP-Oas1b protein detected with anti-OAS1 antibody.

Some breakdown of the Oas1b protein was observed as indicated by the minor ~ 35 kDa band (N-terminal fragment) on the anti-MBP Western blot (Fig. 4.1B) and the ~ 55 kDa band (C-terminal fragment) on the anti-OAS Western blot (Fig. 4.1C).

To determine whether the MBP-tag negatively affected the enzymatic activity of Oas1a, the synthetase activity of the MBP-Oas1a fusion protein (Fig. 4.2A, lanes 4–7) was compared to that of the Oas1a protein after removal of the tag with Genenase I (Fig. 4.2A, lane 3). The proteins were incubated with poly(I:C) and α-^{32}pATP at 30 °C for 18 h. The 2-5A produced were separated by denaturing 8 M urea 20% PAGE and visualized by autoradiography. Dimer, trimer, tetramer and higher order products were produced by reactions containing MBP-Oas1a at concentrations ranging from 0.5 µg (117 nM) to 16 µg (3.76 µM) (Fig. 4.2A, lanes 4–7). The level of 2-5A synthesized by MBP-Oas1a was similar to that previously reported using a similar concentration of a His-tagged recombinant Oas1a protein under similar reaction conditions (Kakuta et al., 2002; Yan et al., 2005). The cleaved and fused Oas1a proteins produced similar levels of

2-5A, indicating that the MBP-tag did not negatively affect Oas1a synthetase activity (Fig. 4.2A, lanes 3 and 4). As expected, synthetase activity was not detected in the reaction containing MBP (Fig. 4.2A, lane 2). Neither MBP-Oas1b nor MBP-Oas1btr produced detectable 2-5A when added to the reactions at concentrations of 2.6 μg (638 nM) or 2.3 μg (605 nM), respectively (Fig. 4.2B, lanes 3 and 2). These concentrations were 4 to 5 times higher than the lowest active concentration of MBP-Oas1a tested. The results confirmed the previous finding of Kakuta et al. (2002) that Oas1a is an active 2-5A synthetase while Oas1btr is an inactive synthetase. Oas1b was also shown to be inactive. However, an additional spot migrating above the free ATP but below the position of the oligoA dimer generated by Oas1a was observed only in the Oas1b reaction (Fig. 4.2B, lane 3). This extra spot was only observed when poly(I:C) was included in the reaction mixture (Fig. 4.2C, compare lanes 3 and 4) suggesting that MBP-Oas1b, but not MBP-Oas1btr, is able to bind to and modify ATP after activation by dsRNA.

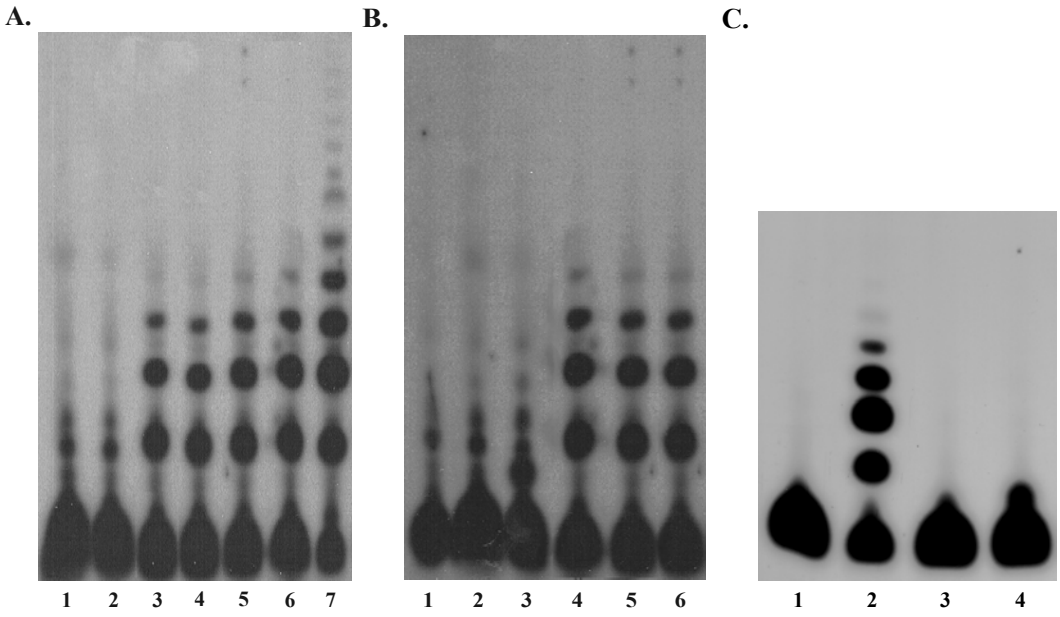

Figure 4.2. Analysis of MBP-Oas1 protein 2-5A synthetase activity. Different amounts of MBP-Oas1 proteins were incubated with α^{32}p-ATP and poly (I:C) for 18 h at 30 °C. Four µl (A) or two µl (B and C) of each reaction were then electrophoresed on a 20% polyacrylamide-urea denaturing gel. (A) Analysis of MBP-Oas1a 2-5A synthetase activity. Reactions contained: Lane 1, no protein. Lane 2, 16 µg of MBP. Lane 3, 0.75 µg of Oas1a. Lanes 4–7, 0.5 µg, 0.75 µg, 1 µg, and 16 µg of MBP-Oas1a, respectively. (B) Analysis of MBP-Oas1b 2′-5′ OAS activity. Reactions contained: Lane 1, No protein. Lane 2, 2.3 µg of MBP-Oas1btr. Lane 3, 2.6 µg of MBP-Oas1b. Lanes 4–6, 1 µg, 0.75 µg, and 0.5 µg of MBP-Oas1a, respectively. (C) Analysis of the effect of poly(I:C) on MBP–Oas1b synthetase activity. Reactions contained: Lane 1, No protein. Lane 2, 0.5 µg of MBP–Oas1a with poly(I:C). Lane 3, 1.5 µg of MBP–Oas1b without poly(I:C). Lane 4, 1.5 µg of MBP–Oas1b with 50 µg/ml poly(I:C). The data shown are representative of results obtained from at least three repeats using different pooled protein preparations.

Poly(I:C)-binding activity of recombinant Oas1b proteins. The 2-5A synthetases require dsRNA to activate them to polymerize ATP into 2-5A (Wreschner et al., 1981). In a previous study, recombinant Oas1a and Oas1btr were shown to bind poly(I:C) efficiently (Kakuta et al., 2002). Oas1b poly(I:C) binding activity was tested by incubating bacterial lysates from cells expressing recombinant MBP-Oas1b with poly(I:C)-agarose. The bound proteins were separated by SDS-PAGE and detected by immunoblotting using anti-MBP antibody. Lysates from cells expressing MBP-Oas1a

and MBP from the empty pMAL-C2g vector were used as positive and negative controls, respectively. Poly(I:C) bound efficiently to MBP-Oas1a and MBP-Oas1btr, consistent with previously published results (Kakuta et al., 2002), but less efficiently to MBP-Oas1b (Fig. 4.3). As expected, MBP did not bind to poly(I:C).

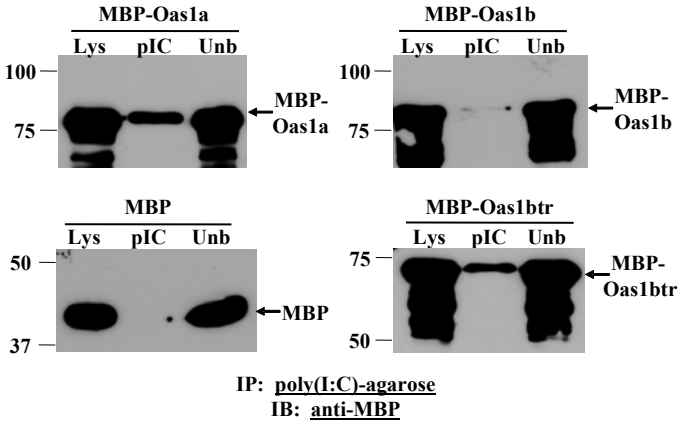

Figure 4.3. Analysis of Oas1 protein dsRNA-binding activity. The ability of MBP-Oas1a, MBP-Oas1b, MBP–Oas1btr or MBP to bind dsRNA poly(I:C)-agarose was tested. Bound RNA-protein complexes were separated by 10% SDS-PAGE. Immunoblotting was performed using anti-MBP antibody. Lys, lysate; pIC, poly(I:C)-bound fraction; Unb, unbound fraction. The data shown are representative of results obtained from at least three repetitions.

Analysis of the interaction of MBP-Oas1 proteins with WNV 3′ genomic RNA secondary structures. Single-stranded viral RNA genomes are predicted to have a significant amount of structure due to intramolecular RNA–RNA interactions and viral RNA stem-loop structures have been shown to be able to activate 2′-5′ oligoadenylate synthetases (Desai et al., 1995; Maitra and Silverman, 1998; Sharp et al., 1999). Regions of the WNV-Eg101 genome RNA predicted to form long stem-loop structures by *mfold* analysis as well as by a whole genome fold (Palmenberg and Sgro, 1997) (Fig. 4.4A, D and H) were synthesized *in vitro* and used as probes in gel mobility shift assays with MBP-Oas1a, MBP-Oas1b, and MBP-Oas1btr. Increasing concentrations of each of the

MBP-Oas1 proteins were tested with a constant amount of each probe. None of the Oas1 fusion proteins bound efficiently to Probe 1 (nts 10,931–11,029), the 3′ terminal stem-loop of the genome (Fig. 4.4A, B and C). Probe 2 (nts 10,387–10,448) was AU-rich and included the last 10 nts of the viral coding region, the viral stop-codon, and the first 57 5'nts of the 3′ UTR. MBP-Oas1b bound to Probe 2 at concentrations between 10 ng and 200 ng (Fig. 4.4E), while MBP-Oas1a RNA binding to this probe was detected starting at 50 ng (Fig. 4.4F). MBP-Oas1btr did not bind to Probe 2 at any of the concentrations tested (Fig. 4.4G). Probe 3 (nts 10,308–10,364) was also AU-rich. Only MBP-Oas1b, at concentrations of 25 ng, 50 ng and 100 ng, exhibited detectable binding to Probe 3 (Fig. 4.4I and J). The data indicate that full-length Oas1b and Oas1a, but not Oas1btr, can bind to partially dsRNAs. In contrast to its efficient binding to poly(I:C), Oas1btr did not bind to any of the viral RNAs tested.

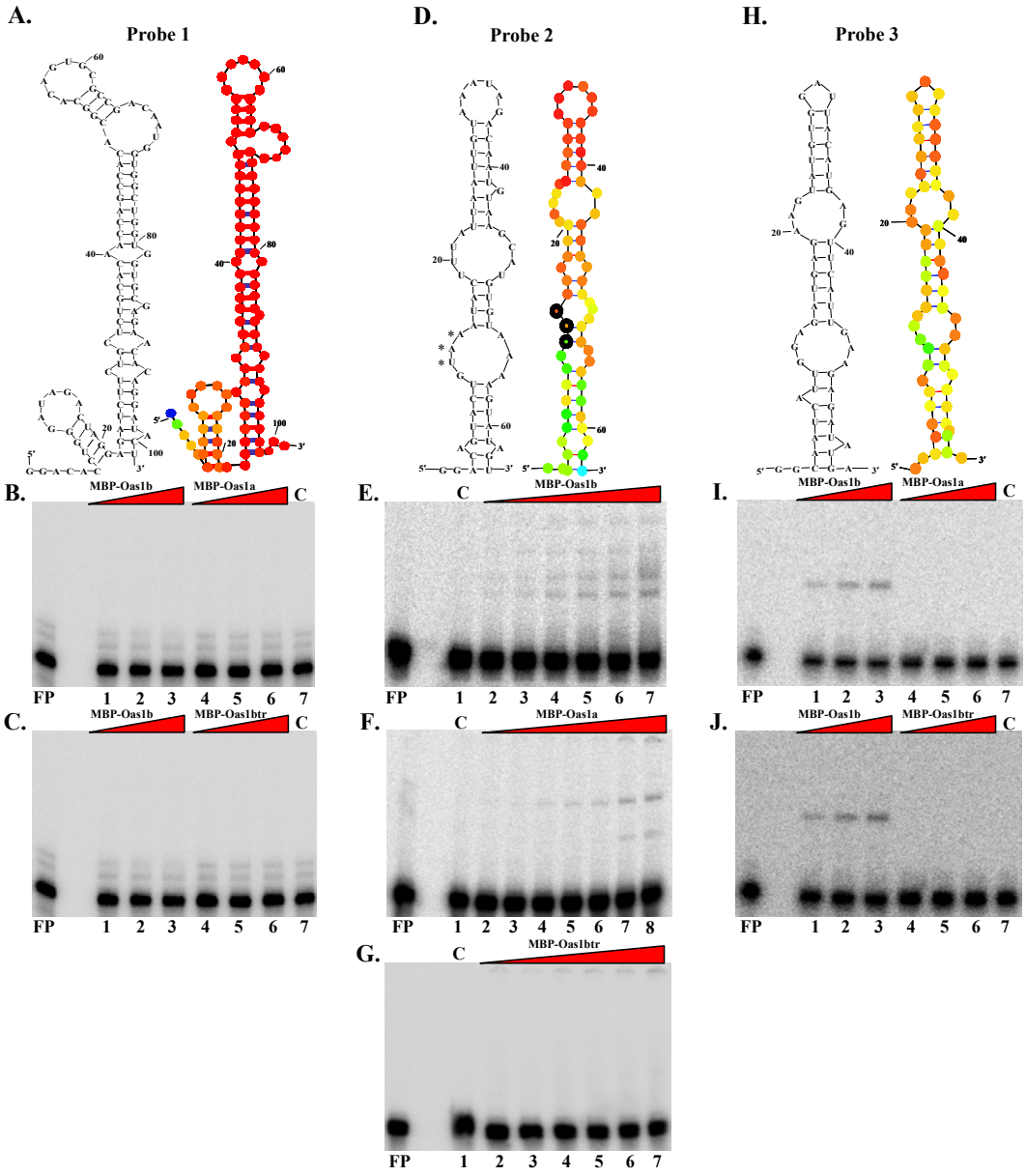

Figure 4.4. Analysis of Oas1 protein binding activity for partially dsRNA probes. (A, D, and H) WNV Eg101 genome RNA secondary structures predicted by MFOLD version 3.1 (black) of just the probe sequences or of the probe region in a whole genome fold (color). The nts with the highest probability of pairing (P–num value < 3%) are indicated in red, with orange next, then yellow, and then green. Probe 1 (A), Probe 2 (D), and Probe 3 (H) RNAs were radiolabeled by incorporation of ^{32}p-UTP during *in vitro* transcription. Gel mobility shift assays with Probe 1 (1000 cpm). (B) Lanes 1–3, MBP-Oas1b at 25, 50 and 100 ng. Lanes 4–6, MBP-Oas1a at 25, 50 and 100 ng. Lane 7, 100 ng of MBP. (C) Lanes 1–3, MBP-Oas1b at 25, 50 and 100 ng. Lanes 4–6, MBP-Oas1btr at 25, 50 and 100 ng. Lane 7, 100 ng of MBP. Gel mobility shift assays with Probe 2 (2000 cpm). (E) Lane 1, 200 ng of MBP. Lanes 2–7, MBP-Oas1b at 10, 25, 50, 75, 100, and 200 ng. (F) Lane 1, 400 ng of MBP. Lanes 2–7, MBP-Oas1a at 10, 25, 50, 75, 100, 200, and 400 ng. (G) Lane 1, 200 ng of MBP. Lanes 2–7, MBP-Oas1btr at 10, 25, 50, 75, 100, and 200 ng. Gel mobility shift assays with Probe 3 (1000 cpm). (I) Lanes 1–3, MBP-Oas1b at 25, 50 and 100 ng. Lanes 4–6,

MBP-Oas1a at 25, 50 and 100 ng. Lane 8, 100 ng of MBP. (J) Lanes 1–3, MBP-Oas1b at 25, 50 and 100 ng. Lanes 4–6, MBP-Oas1btr at 25, 50 and 100 ng. Lane 8, 100 ng of MBP. Components of binding reactions were separated on a 6% polyacrylamide non-denaturing gel. Bands on the dried gel were detected using a Bio-Image Analyzer PhosphorImager (Molecular Dynamics). FP, free probe. The data shown are representative of results obtained from at least three repeats using different pooled protein preparations.

Oas1b, but not Oas1btr, reduces Oas1a synthetase activity *in vitro*. A previous study reported that the inactive murine 2-5A synthetase, Oas1d, inhibited the *in vitro* synthetase activity of Oas1a in a dose-dependent manner (Yan et al., 2005). To investigate whether the inactive MBP-Oas1b or MBP-Oas1btr proteins could inhibit *in vitro* MBP-Oas1a synthetase activity, increasing molar ratios (0, 0.5X, 1X, 1.5X, and 2X) of these proteins were added to reactions containing a constant amount of MBP-Oas1a. MBP-Oas1b reduced MBP-Oas1a synthetase activity in a dose-dependent manner (Fig. 4.5A, lanes 2–6). In contrast, the addition of similar concentrations of MBP-Oas1btr caused no reduction in MBP-Oas1a synthetase activity (Fig. 4.5A, lanes 7–10). Both ATP and poly(I:C) were present in excess in these reactions. The data in Fig. 4.3 shows that the three Oas1 proteins studied bound poly(I:C) with different levels of efficiency: Oas1a ≥ Oas1btr > Oas1b. These data suggest that Oas1a would be expected to out-compete Oas1b for poly(I:C) binding. Also, if the inhibition were due solely to competition for poly(I:C), Oas1btr should also be expected to be able to inhibit Oas1a 2-5A synthesis. This was not observed to be the case. The results suggest that the inhibition of Oas1a synthetase activity by Oas1b is mediated through protein–protein interactions and that Oas1b, but not Oas1btr, has a dominant negative effect on *in vitro* Oas1a synthetase activity.

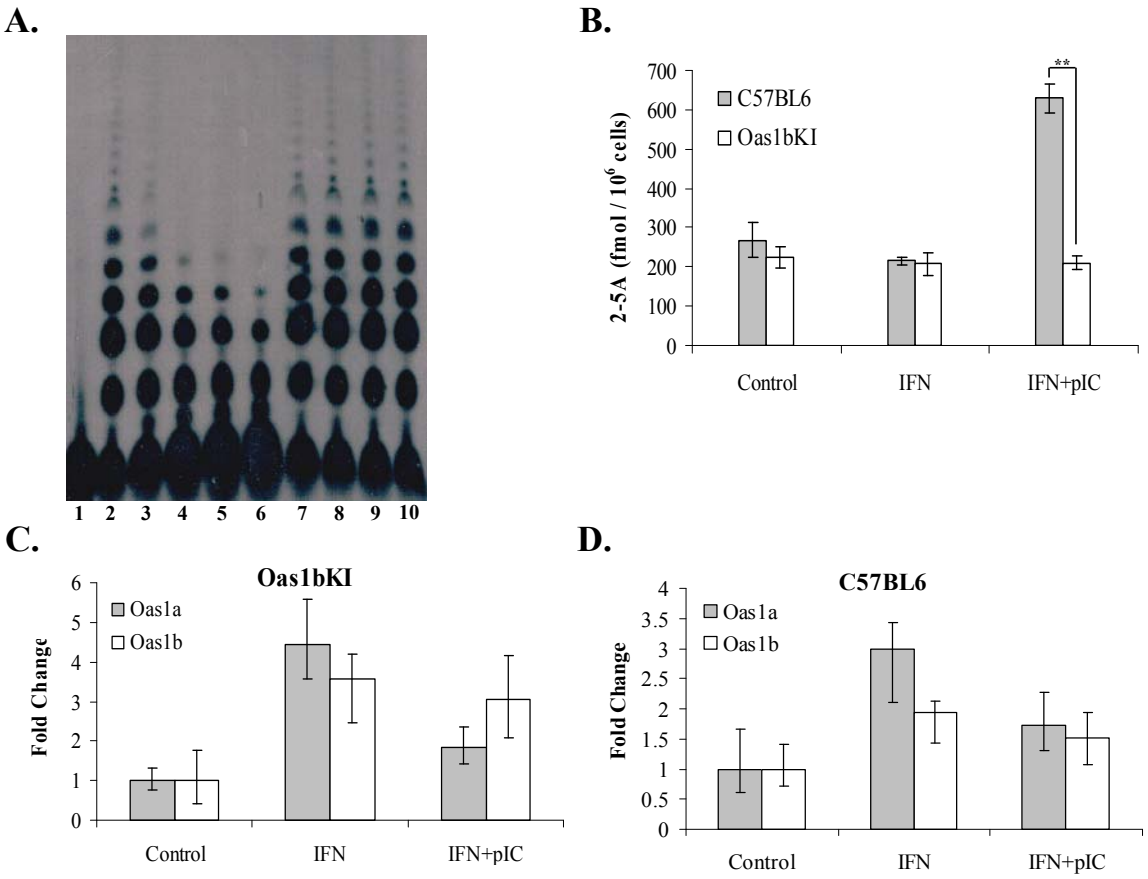

Figure 4.5. Oas1b reduces 2-5A production *in vitro* and *in vivo*. (A) *In vitro* 2-5A production. All reactions contained α^{32}p-ATP, poly (I:C), and 1 µg of MBP-Oas1a. Lane 1, no additional protein. Lanes 2–6, MBP-Oas1a and 0, 0.5X, 1X, 1.5X, or 2X of MBP-Oas1b, respectively. Lanes 7–10, MBP-Oas1a and 0, 0.5X, 1X, 1.5X, or 2X of MBP-Oas1btr, respectively. The products of each reaction were separated on a 20% polyacrylamide-urea denaturing gel. The data shown are representative of results obtained from at least three repeats using different pooled protein preparations. (B) Levels of 2-5A in C57BL6 and Oas1b-KI cells. MEFs were seeded into 6-well plates and grown overnight to about ~ 100% confluency and then incubated with 100 U/ml type I universal IFN for 24 h (IFN). No IFN was added to the media of the control cells. After 24 h, some wells of IFN treated cells were transfected with 10 µg/ml poly(I:C) for 1 h (IFN + pIC). The amounts of 2-5A in cell extracts were measured using a FRET assay of RNase L activity. Data are expressed as amount of 2-5A per 10^6 cells. The values are averages of three replicate samples each assayed in triplicate. The standard error (SE) of the mean is indicated. The results shown are representative of three experiments each done in triplicate. The data were subjected to a *Student's t-test* statistical analysis done with EXCEL software. ** denotes $p = 0.0133$. (C and D) Analysis of changes in the expression levels of the Oas1a and Oas1b genes in Oas1bKI and C57BL6 cells after IFN treatment or IFN plus poly(IC) treatment by qRT-PCR. The relative fold change in expression compared to the level of the same mRNA present in cell-type specific untreated controls (value set at 1) is expressed in RQ units. Error bars represent the SE ($n = 3$) and are based on an $RQ_{Min/Max}$ of the 95% confidence level.

Cells expressing Oas1b exhibit reduced 2-5A levels in response to poly(I:C) stimulation. The production of 2-5A in vivo in response to poly(I:C) stimulation was assessed in MEFs from transgenic C57BL/6 Oas1b knock-in mice (Oas1bKI) that express full-length Oas1b and control C57BL/6 mice that express Oas1btr (Scherbik et al., 2007a). MEFs were incubated with 100 U/ml of Type I Universal IFN for 24 h to upregulate Oas1 expression and then transfected with 10 μg/ml poly(I:C) for 1 h to induce 2-5A production. A FRET assay that measures RNase L activity based on 2-5A levels was used to determine the amount of 2-5A produced in vivo (Thakur et al., 2005). Consistent with previously published reports (Andersen et al., 2007; Knight et al., 1980), low levels of 2-5A were observed in the untreated and IFN treated MEFs. An increase in 2-5A levels was observed only in the C57BL/6 MEFs treated with IFN and poly(I:C) (Fig. 4.5B). Due to the high homology between Oas1 proteins, antibodies cannot be used to distinguish individual Oas1 proteins by Western blotting. Oas1a and Oas1b mRNA levels in Oas1bKI and C57BL/6 MEFs were therefore assessed by real-time RT-PCR. IFN treatment resulted in about a 4-fold increase of Oas1a and Oas1b mRNA in Oas1bKI cells and a 2- to 3-fold increase in C57BL/6 MEFs compared to the levels in control cells. Both Oas1a and Oas1b mRNA levels decreased after poly(I:C) transfection, possibly due to RNase L-mediated degradation of mRNA, but the levels remained higher than in control cells indicating that Oas1 mRNA was upregulated by the IFN treatment (Fig. 4.5C). Even though IFN-mediated Oas1 mRNA upregulation was less efficient in C57BL/6 MEFs compared to Oas1bKI MEFs, the levels of 2-5A production as measured by RNase L activation were higher in C57BL/6 cells expressing Oas1btr. The results are

consistent with the hypothesis that Oas1b has a dominant negative effect on Oas1a synthetase activity in vivo.

DISCUSSION

The production of 2-5A and its subsequent activation of RNase L are important components of the IFN-induced antiviral response (Samuel, 2001). Of the eight mouse Oas1 genes, only Oas1a and Oas1g are active synthetases (Kakuta et al., 2002). The alleles of the Flv gene (Oas1b) determine whether mice produce a full-length or a truncated Oas1b protein (Perelygin et al., 2002). Kakuta et al. (2002) reported that Oas1btr is an inactive synthetase and the current study showed that full-length Oas1b is also not capable of synthesizing 2-5A. Both Oas1b and Oas1btr, but none of the other inactive mouse Oas1 proteins, contain a 4 amino acid deletion in the P-loop that may prevent the folding of a catalytically functional structure as well as R90Q and R91Q substitutions in the ATP-substrate acceptor site and K195N, S203R and K209T substitutions in the ATP-substrate donor sites. The P-loop deletion as well as the substitutions in conserved residues characteristic of active synthetases are expected to be the reason for the lack of activity (Kakuta et al., 2002; Yamamoto et al., 2000).

An intact P-loop motif was previously postulated to be required for ATP binding (Saraste et al., 1990). Although both Oas1b and Oas1btr have the same 4 amino acid deletion in the 15 amino acid P-loop (VVMGGSSGKGt/aLKB, deleted residues are underlined and lower case letters indicate a sequence difference between Oas1a and

Oas1b/btr, respectively), the data from in vitro 2-5A synthetase assays suggested that Oas1b but not Oas1btr could bind and modify ATP.

The Oas1btr and Oas1b proteins also differ in their RNA binding specificities. Oas1b bound to poly(I:C) less efficiently than did either Oas1a or Oas1btr. However, the interaction of Oas1b with poly(I:C) was of sufficient strength to activate it to bind and modify ATP. It was previously reported that the RNA binding activities of OAS proteins do not correlate with their synthetase activities (Hartmann et al., 1998a). Oas1b bound to partially double-stranded viral stem-loop RNAs more efficiently than did Oas1a, while Oas1btr did not bind to any of the viral RNAs. The Oas1 dsRNA-binding domain(s) has not been identified but the crystal structure of porcine OAS, a protein that shares 56% identity with mouse Oas1b in residues important for folding, predicted a bilobal conformation with the interface between the N- and C-terminal domains forming a 35 Å long positively charged groove that could mediate interactions with RNA (Hartmann et al., 2003). Although enzymatic activity was completely abrogated by small C-terminal deletions of the human OAS1 protein, some dsRNA-binding activity was retained by truncated proteins with more than half of the protein deleted, consistent with the existence of a large RNA activation site that spans both the catalytic and C-terminal OAS1 domains (Ghosh et al., 1991; Hartmann et al., 2003). Interestingly, viral stem-loop RNA binding was observed only for the two full-length Oas1 proteins tested suggesting that the C terminus is necessary for the binding of these RNAs. However, Oas1b bound to two of the three viral RNAs while Oas1a bound to only one of these RNAs suggesting the possibility of differential RNA recognition by different Oas1 proteins. A recent study

identified the RNA consensus sequence NNWWNNNNNNNNNWGN as a recognition site for human OAS1 (Kodym et al., 2009). Although interaction between Oas1a and probe 2 was observed, no activation of Oas1a was observed after incubation of 1 μg of this protein with up to 50 μg/ml of probe 2 RNA; whereas, Oas1a activation was observed with as little as 10 μg/ml poly(I:C) (data not shown). It was previously reported that activation of human 2-5A synthetase activity in HeLa cell extracts required considerably higher concentrations (360 nM) of HCV genomic RNA than of poly(I:C) (50 μg/ml) (Han and Barton, 2002).

In addition to its antiviral role, the OAS/RNase L pathway is involved in regulating mRNA turnover during cell differentiation, division and apoptosis (Ghosh et al., 2001; Kumar et al., 1994; Salzberg et al., 1997). Because of the possibility that inappropriate or over production of 2-5A could cause significant damage, mechanisms to tightly regulate this pathway must exit in cells. Once 2-5A is synthesized, it is rapidly degraded by 2′-phosphodiesterase (Schmidt et al., 1979). However, the data from the present study and a previous study (Yan et al., 2005) indicate that inactive murine Oas1 proteins can function as dominant negative inhibitors of active synthetases (Oas1a and Oas1g) and suggest that regulation can also occur at the level of 2-5A synthesis.

The expression of the Oas1a mRNA is detected in most tissues with the highest levels in digestive and lymphoid tissues (Kakuta et al., 2002; Salzberg et al., 1997; Shibata et al., 2001). The inactive Oas1d is exclusively expressed in ovaries. It was shown to inhibit the in vitro activity of Oas1a in a dose-dependent manner and was postulated to protect oocytes from a dsRNA-induced IFN response and cell death by

reducing OAS/RNase L-mediated RNA degradation. Oas1c and Oas1e, which are also inactive synthetases, could partially compensate for this protective role in Oas1d-null mice (Yan et al., 2005) suggesting functional redundancy among the inactive synthetases. Oas1b mRNA is expressed at low levels in lung, uterus, and ovary and at higher levels in muscle tissue as well as lymphoid organs such as the thymus and spleen (Kakuta et al., 2002). Similar to Oas1d, full-length Oas1b, but not Oas1btr, inhibited in vitro Oas1a synthetase activity in a dose-dependent manner. Furthermore, 2-5A production in response to dsRNA stimulation in Oas1bKI cells, which express the full-length Oas1b, was markedly lower than in C57BL/6 cells, which express Oas1btr. These findings support a role for full-length Oas1b in the down-regulation of the Oas/RNase L pathway in vivo. Oas1b is expressed in a broad range of tissues suggesting that it is a major regulator of the Oas/RNase L pathway. However, the other inactive Oas1 proteins (Oas1c, e, f, and h) may be able to provide sufficient redundant function in mice expressing Oas1btr, which is unable to function as a dominant negative inhibitor. It has been reported that tetramer formation is required for the activity of human OAS1 proteins and that tetramerization of the human OAS1 proteins is mediated through the CFK motif (Ghosh et al., 1997b). The active mouse synthetases Oas1a and Oas1g have substitutions in the CFK motif as does Oas1d but Oas1b has an intact CFK motif. However, the gel mobility shift assay data (Fig. 4.4) suggest that Oas1b as well as Oas1a may form multimers (Fig. 4.4). Although it is not yet known whether tetramer formation is required for the synthetase activity of mouse Oas1 proteins, the dominant negative activity of

inactive mouse Oas1 proteins strongly suggests that multimer formation is required for this inhibition.

Although Oas1b functions in the OAS/RNase L pathway to reduce the level of 2-5A produced, it is paradoxically not proviral in flavivirus–infected cells because it also functions to specifically reduce the replication of flaviviruses by an alternative mechanism that is independent of RNase L (Sabin, 1952; Scherbik et al., 2006).

MATERIALS AND METHODS

Expression and purification of MBP-Oas1 proteins. Murine Oas1a cDNA (accession No. X04958) and Oas1b cDNA (accession No. AF328926) were obtained as previously described (Perelygin et al., 2002). Oas1a and Oas1b plasmid DNAs were amplified with primers that added SnaBI and BamHI restriction sites to the PCR fragment and sub-cloned into the pMAL-c2G expression vector (New England Biolabs). The resulting constructs were designated pMAL-O1a and pMAL-O1b. The pMAL-O1btr construct was generated using primers that introduced the premature codon into the Oas1b cDNA and also contained the SnaBI and BamHI restriction sites to clone the PCR fragment into pMAL-c2G. Recombinant MBP-Oas1a protein was expressed by pMAL-O1a transformed BL21 (non-D3E) cells grown in 250 ml of Rich Media containing 0.05% glucose and 75 μg/ml of carbenicillin (CRB). Expression was induced with 1 mM IPTG overnight at 16 °C. Recombinant MBP-Oas1b protein was expressed by pMAL-O1b transformed BL21 (non-D3E) cells grown in 500 ml of TB Autoinduction media (Novagen) containing 0.05% glucose and 75 μg/ml of carbenicillin (CRB). Expression

was auto-induced overnight at 16 °C. Recombinant MBP-Oas1btr protein was expressed by pMAL-O1btr transformed BL21 (non-D3E) cells grown in 250 ml of Rich Media containing 0.05% glucose and 75 μg/ml of carbenicillin (CRB). Expression was induced with 0.5 mM IPTG overnight at 16 °C. Cells were pelleted by centrifugation at 5000 ×g for 15 min in an Avanti J30-I centrifuge using a JA-10 rotor (Beckman Coulter). The cells were resuspended in 5 ml of column buffer [20 mM tris–HCl, 200 mM NaCl, 1 mM EDTA, 10 mM β-ME and Complete Mini Protease inhibitor cocktail (Roche)] and frozen at − 20 °C until use.

Purification of MBP-Oas1 proteins. Recombinant Oas1 proteins were purified by affinity column purification using amylose resin. Bacterial cells were lysed with a SLM-Aminco French pressure cell (Heinemann) at 20,000 lb/in2 and the lysate was centrifuged at 10,000 × g for 20 min. The soluble fraction was loaded onto an amylose resin column. The resin was washed with 100 ml of column buffer, and the MBP-fusion protein was then eluted from the column with 10 mM maltose in column buffer. MBP was cleaved from MBP-Oas1a using Genenase I (New England Biolabs) according to the manufacturer's protocol. The digestion mixture was loaded onto a hydroxyapatite column to remove maltose bound to MBP. Free MBP was then removed by passage through an amylose resin column. The flow-through containing Oas1a and trace amounts of the protease was collected, concentrated, and stored at − 80 °C until use. Pools of three or more partially purified recombinant Oas1 protein preparations were concentrated using a Microcon centrifugal filter device (50,000 nominal molecular weight limit) (Millipore) prior to use in vitro 2-5A synthetase and EMSA experiments.

Western blotting. MBP-Oas1 proteins were separated by 10% SDS-PAGE and transferred electrophoretically to a PVDF membrane, which was then blocked overnight at 4 °C with 5% BSA in TBS. The membrane was incubated at room temperature with a horseradish peroxidase (HRP) conjugated, monoclonal, murine anti-MBP (New England Biolabs) diluted 1:35,000 in a 5% BSA-TBS solution at room temperature for 1.5 h. The membrane was washed with 0.05% Tween-20-TBS solution (TBS-T). Alternatively, anti-OAS1 polyclonal antibody (Novus Biological) was diluted (1:1000) in a 5% milk-TBS-T solution and incubated with the membrane overnight at 4 °C. The membrane was washed with TBS-T and then incubated with anti-mouse IgG-HRP (Cell Signaling) diluted 1:2000 in 5% milk-TBS-t at room temperature for 1 h. The membrane was washed with TBS-T 3 times and once with TBS. Immunoreactive protein bands were detected by addition of West Pico Enhanced Chemiluminescence reagent (Pierce) and exposure to film.

Synthesis of RNA probes. Probe 1, Probe 2, and Probe 3 encompassed nts 10,931–11,029, 10,387–10,448, and 10,308–10,364 of the WNV Eg101 genome, respectively. RNA probes were synthesized using a MAXIscript in vitro transcription kit (Ambion) which utilizes a T7 RNA polymerase. Transcription reactions were carried out according to the manufacturer's protocol in the presence of 32P-UTP (800 mCi/mol; Perkin–Elmer). Transcription products were separated by 6 M urea PAGE. Gel slices containing RNA transcripts of the expected size were excised and the RNA was eluted from the gel slices by rocking overnight at 4 °C in elution buffer (0.5 M NH4OAC, 1 mM EDTA, and 0.2% SDS). The eluted RNA was filtered through a 0.45-μm cellulose acetate filter unit

(Millipore) to remove gel pieces, precipitated with ethanol, resuspended in water, aliquoted, and stored at − 80 °C. The amount of radioactivity incorporated into each RNA probe was measured with a scintillation counter (model LS6500; Beckman).

Genome RNA fold. A secondary structure fold of the 11,029 nt WNV-Eg101 genomic RNA (accession no. AF260968) was generated by Ann Palmenberg using version 3.1 of MFOLD (Palmenberg and Sgro, 1997). In this fold, each base was algorithmically compared with all possible partners to determine the number of pairing partners within a free-energy range. The calculated pairing numbers (P-num values) provide a quantitative measure of the pairing probability for different partners in the context of multiple sub-optimal folds. Low P-num values (< 3%) indicate high probability of pairing.

2′-5′OAS activity assay. The reaction mixture (50 µl) contained 2′-5′ OAS activity assay buffer [20 mM HEPES–KOH pH 7.5, 50 mM KCl, 25 mM Mg(OAC)2, 10 mM creatine phosphate, 1 U/µl creatine kinase, 5 mM ATP, and 7 mM β-ME], 10 µCi α32p-ATP and 50 ng/µl poly (I:C). MBP-Oas1 fusion proteins were added to reaction mixtures at increasing concentrations. Reactions were incubated at 30 °C for 18 h and stopped by addition of 50 µl of Gel Loading Buffer II (95% formamide, 18 mM EDTA, 0.025% SDS, xylene cyanol, and bromophenol blue) (Ambion). Two to four µl of each reaction were loaded onto a 20% polyacrylamide–urea gel and electrophoresed at 800 V for 3.5 h. Radiolabeled 2-5A was visualized by autoradiography.

Gel mobility shift assay. Reactions contained 1X Gel Shift Buffer (3% Ficoll-400, 20 mM sodium phosphate pH 7.2, 60 mM KCl, 1 mM MgCl2, and 0.5 mM EDTA), 0.2 µl of RNasin, 50 ng of phenol-extracted yeast tRNA as a non-specific competitor,

10 mM (DTT) dithiothreitol, Oas1 protein and radiolabeled RNA probe. Reactions were incubated at room temperature for 20 min. An equal volume of gel-shift loading buffer (0.025% bromophenol blue, 0.025% xylene cyanol, 4% sucrose, and 1X TBE) was added and the reactions were electrophoresed on non-denaturing 5% polyacrylamide gels (39:1 acrylamide:bis-acrylamide and 1X TBE) at 120 V for 2 h at 4 °C. The gel was dried and analyzed with a Fuji BAS 1800 analyzer (Fuji Photo Film Co.) and Image Gauge software (Science Lab, 98, version 3.12; Fuji Photo Film Co.).

Poly(I:C)-agarose binding assay. Recombinant MBP-Oas1a, MBP-Oas1b, MBP–Oas1btr and MBP were expressed in BL21 STAR (DE3)pLysS bacterial cells grown in 35 ml of LB Media containing 0.05% glucose and 75 μg/ml of carbenicillin (CRB) at 37 °C. At O.D600 ~ 1.0, cultures were placed on ice for 10 min. Expression was induced with 1 mM IPTG for 15 min at 20 °C. Cells were pelleted by centrifugation at 5000 ×g for 15 min in an Avanti J30-I centrifuge using a JA-10 rotor (Beckman Coulter). Cell pellets were resuspended in 1 ml of dsRNA-binding buffer [10 mM Hepes–KOH (pH 7.5), 3 mM Mg(OAc)2, 0.3 mM EDTA, 50 mM KCl, 0.5% glycerol] supplemented with protease Complete Mini EDTA-Free protease inhibitor cocktail (Roche). Cells were lysed by the addition of Cellytic cell lysis powder (Sigma-Aldrich) and incubation at 37 °C for 15 min. Cell lysates were centrifuged at 15,000 × g for 12 min in a bench-top centrifuge (model 5415 D, Eppendorf). Clarified supernatant was added to 100 μl poly(I:C)-agarose bead slurry and rotated at room temperature for 2 h. Samples were then centrifuged at 700 × g for 5 min at 4 °C and the supernatant containing the unbound protein fraction was collected. Samples were washed 5 times with 500 μl of dsRNA-binding buffer,

centrifuged at 700 × g for 5 min at 4 °C after each wash and the supernatant was discarded. The poly(I:C)-agarose bound to MBP-Oas1 proteins was resuspended in 100 µl of dsRNA-binding buffer and 100 µl of 2X SDS sample buffer (125 mM Tris–HCl pH 6.8, 4% SDS, 20% Glycerol, 0.004% bromophenol blue and 5% 2-mercaptoethanol). Whole-cell lysate, unbound fraction and poly(I:C)-agarose bound fraction proteins were separated by 10% SDS-PAGE and immunoblotted using HRP-conjugated anti-MBP antibody (New England Biolabs).

Cells. Oas1b knock-in mice were generated as previously described (Scherbik et al., 2007a). C57BL/6 and transgenic C57BL/6 Oas1b-KI MEFs were SV-40 transformed and the cell lines were maintained as previously described (Scherbik et al., 2007b).

FRET assay of RNase L activity for 2-5A levels. C57BL6 and Oas1b-KI MEFs were seeded into 6-well plates and grown overnight to about ~ 95% confluency. Cells were incubated with 100 U/ml type I universal IFN for 24 h. No IFN was added to the media for control cells. After 24 h, some of the IFN treated cells were transfected with 10 µg/ml poly(I:C) using Cellfectin (Invitrogen) for 1 h. Cells were then harvested and lysed by addition of NP-40 buffer [50 mM Tris–HCL (pH 7.2), 150 mM NaCl, 1% NP-40, 200 µM NaVO3, 2 mM EDTA, 5 mM MgCl2 and 5 mM DTT] that was pre-heated at 95 °C for 3 min. The cell suspension was heated to 95 °C for 7 min. Cell debris was removed by centrifugation and the supernatant was applied to a Microcon centrifugal filter device (3000 nominal molecular weight limit) (Millipore) and centrifuged for 45 min at 4 °C. The volume was measured and the samples stored at − 80 °C until use.

RNase L activity was determined using a fluorescence resonance energy transfer (FRET) assay (Thakur et al., 2005). Recombinant human RNase L was produced in insect cells from a baculovirus vector and purified by FPLC (Townsend et al., 2008). The cleavable substrate consisted of a 36 nucleotide synthetic oligoribonucleotide [5′(6-FAM-UUA UCA AAU UCU UAU UUG CCC CAU UUU UUU GGU UUA-BHQ-1)-3′] derived from respiratory syncytial virus (Thakur et al., 2005). The RNA sequence contains several cleavage sites for RNase L (UU or UA). Triplicate 5 µl aliquots of 1:10 dilution of each sample in DEPC-treated water were added to 96-well black polystyrene microtiter plates (Corning) on ice. The reactions (45 µl) contained 100 nM FRET probe, 25 nM RNase L, 25 mM Tris–HCl (pH 7.4), 100 mM KCl, 10 mM MgCl2, 100 µM ATP, and 7.2 mM 2-mercaptoethanol. RNase L was the last component added. The plates were incubated at 20 °C protected from light. To generate a standard curve, authentic trimeric 2-5A (> 95% purity) diluted to final concentrations of 0.05 0.1, 0.3, 1, 3, 10, and 30 nM in DEPC-treated water was used. Fluorescence was measured at 5, 30, and 60, min with a Wallac 1420 fluorimeter (Perkin–Elmer LAS Inc., USA) (excitation 485 nM/emission 535 nm with a 0.1 s integration time).

Real-time qRT-PCR. Real-time quantitative reverse transcription-PCR (qRT-PCR) analysis of mouse Oas1a and Oas1b mRNAs was performed with Assays-on-Demand 20x primer and fluorogenic TaqMan FAM/TAMRA (6-carboxyfluorescein/6-carboxytetramethylrhodamine)-labeled hybridization probe mixes (Applied Biosystems). Glyceraldehyde-3-phosphate dehydrogenase (GAPDH) mRNA was used as an endogenous control and was detected using TaqMan mouse GAPDH Control Reagents

primers and probe (Applied Biosystems). One-step RT-PCR was performed for each target gene and for the endogenous control in a singleplex format using 200 ng of RNA and the TaqMan one-step RT-PCR master mix reagent kit (Applied Biosystems). The cycling parameters were as follows: reverse transcription at 48 °C for 30 min, AmpliTaq activation at 95 °C for 10 min, denaturation at 95 °C for 15 s, and annealing/extension at 60 °C for 1 min (cycle repeated 40 times). Triplicate Ct values were analyzed with the comparative Ct(ΔΔCt) method (Applied Biosystems) using Microsoft Excel software. The amount of fold change in the target mRNA (2-ΔΔCt) was normalized to an endogenous control (GAPDH) . The relative fold change in expression compared to the level of the same mRNA present in cell–type specific, untreated controls was expressed in relative quantification (RQ) units.

REFERENCES:

Andersen, J. B., Li, X. L., Judge, C. S., Zhou, A., Jha, B. K., Shelby, S., Zhou, L., Silverman, R. H., and Hassel, B. A. (2007). Role of 2-5A-dependent RNase-L in senescence and longevity. *Oncogene* **26**(21)**,** 3081-8.

Brinton, M. A. (2002). The molecular biology of West Nile Virus: a new invader of the western hemisphere. *Annu Rev Microbiol* **56,** 371-402.

Desai, S. Y., Patel, R. C., Sen, G. C., Malhotra, P., Ghadge, G. D., and Thimmapaya, B. (1995). Activation of interferon-inducible 2'-5' oligoadenylate synthetase by adenoviral VAI RNA. *J Biol Chem* **270**(7)**,** 3454-61.

Floyd-Smith, G., Slattery, E., and Lengyel, P. (1981). Interferon action: RNA cleavage pattern of a (2'-5')oligoadenylate--dependent endonuclease. *Science* **212**(4498)**,** 1030-2.

Ghosh, A., Desai, S. Y., Sarkar, S. N., Ramaraj, P., Ghosh, S. K., Bandyopadhyay, S., and Sen, G. C. (1997a). Effects of mutating specific residues present near the amino terminus of 2'-5'-oligoadenylate synthetase. *J Biol Chem* **272**(24)**,** 15452-8.

Ghosh, A., Sarkar, S. N., Guo, W., Bandyopadhyay, S., and Sen, G. C. (1997b). Enzymatic activity of 2'-5'-oligoadenylate synthetase is impaired by specific mutations that affect oligomerization of the protein. *J Biol Chem* **272**(52)**,** 33220-6.

Ghosh, A., Sarkar, S. N., Rowe, T. M., and Sen, G. C. (2001). A specific isozyme of 2'-5' oligoadenylate synthetase is a dual function proapoptotic protein of the Bcl-2 family. *J Biol Chem* **276**(27)**,** 25447-55.

Ghosh, S. K., Kusari, J., Bandyopadhyay, S. K., Samanta, H., Kumar, R., and Sen, G. C. (1991). Cloning, sequencing, and expression of two murine 2'-5'-oligoadenylate synthetases. Structure-function relationships. *J Biol Chem* **266**(23)**,** 15293-9.

Han, J. Q., and Barton, D. J. (2002). Activation and evasion of the antiviral 2'-5' oligoadenylate synthetase/ribonuclease L pathway by hepatitis C virus mRNA. *RNA* **8**(4)**,** 512-25.

Hartmann, R., Justesen, J., Sarkar, S. N., Sen, G. C., and Yee, V. C. (2003). Crystal structure of the 2'-specific and double-stranded RNA-activated interferon-induced antiviral protein 2'-5'-oligoadenylate synthetase. *Mol Cell* **12**(5)**,** 1173-85.

Hartmann, R., Norby, P. L., Martensen, P. M., Jorgensen, P., James, M. C., Jacobsen, C., Moestrup, S. K., Clemens, M. J., and Justesen, J. (1998a). Activation of 2'-5' oligoadenylate synthetase by single-stranded and double-stranded RNA aptamers. *J Biol Chem* **273**(6)**,** 3236-46.

Hartmann, R., Olsen, H. S., Widder, S., Jorgensen, R., and Justesen, J. (1998b). p59OASL, a 2'-5' oligoadenylate synthetase like protein: a novel human gene related to the 2'-5' oligoadenylate synthetase family. *Nucleic Acids Res* **26**(18)**,** 4121-8.

Kakuta, S., Shibata, S., and Iwakura, Y. (2002). Genomic structure of the mouse 2',5'-oligoadenylate synthetase gene family. *J Interferon Cytokine Res* **22**(9)**,** 981-93.

Kerr, I. M., and Brown, R. E. (1978). pppA2'p5'A2'p5'A: an inhibitor of protein synthesis synthesized with an enzyme fraction from interferon-treated cells. *Proc Natl Acad Sci U S A* **75**(1)**,** 256-60.

Knight, M., Cayley, P. J., Silverman, R. H., Wreschner, D. H., Gilbert, C. S., Brown, R. E., and Kerr, I. M. (1980). Radioimmune, radiobinding and HPLC analysis of 2-5A and related oligonucleotides from intact cells. *Nature* **288**(5787)**,** 189-92.

Kodym, R., Kodym, E., and Story, M. D. (2009). 2'-5'-Oligoadenylate synthetase is activated by a specific RNA sequence motif. *Biochem Biophys Res Commun* **388**(2)**,** 317-22.

Kumar, R., Korutla, L., and Zhang, K. (1994). Cell cycle-dependent modulation of alpha-interferon-inducible gene expression and activation of signaling components in Daudi cells. *J Biol Chem* **269**(41)**,** 25437-41.

Maitra, R. K., and Silverman, R. H. (1998). Regulation of human immunodeficiency virus replication by 2',5'-oligoadenylate-dependent RNase L. *J Virol* **72**(2)**,** 1146-52.

Mashimo, T., Lucas, M., Simon-Chazottes, D., Frenkiel, M. P., Montagutelli, X., Ceccaldi, P. E., Deubel, V., Guenet, J. L., and Despres, P. (2002). A nonsense mutation in the gene encoding 2'-5'-oligoadenylate synthetase/L1 isoform is associated with West Nile virus susceptibility in laboratory mice. *Proc Natl Acad Sci U S A* **99**(17)**,** 11311-6.

Palmenberg, A. C., and Sgro, J. Y. (1997). Topological organization of picornaviral genomes: Statistical Prediction of RNA structural signals. *Seminars in Virology* **8**(3)**,** 231-241.

Perelygin, A. A., Scherbik, S. V., Zhulin, I. B., Stockman, B. M., Li, Y., and Brinton, M. A. (2002). Positional cloning of the murine flavivirus resistance gene. *Proc Natl Acad Sci U S A* **99**(14)**,** 9322-7.

Rebouillat, D., Marie, I., and Hovanessian, A. G. (1998). Molecular cloning and characterization of two related and interferon-induced 56-kDa and 30-kDa proteins highly similar to 2'-5' oligoadenylate synthetase. *Eur J Biochem* **257**(2)**,** 319-30.

Sabin, A. B. (1952). Nature of Inherited Resistance to Viruses Affecting the Nervous System. *Proc Natl Acad Sci U S A* **38**(6)**,** 540-6.

Salzberg, S., Hyman, T., Turm, H., Kinar, Y., Schwartz, Y., Nir, U., Lejbkowicz, F., and Huberman, E. (1997). Ectopic expression of 2-5A synthetase in myeloid cells induces growth arrest and facilitates the appearance of a myeloid differentiation marker. *Cancer Res* **57**(13)**,** 2732-40.

Samuel, C. E. (2001). Antiviral actions of interferons. *Clin Microbiol Rev* **14**(4)**,** 778-809, table of contents.

Saraste, M., Sibbald, P. R., and Wittinghofer, A. (1990). The P-loop--a common motif in ATP- and GTP-binding proteins. *Trends Biochem Sci* **15**(11)**,** 430-4.

Scherbik, S. V., Kluetzman, K., Perelygin, A. A., and Brinton, M. A. (2007a). Knock-in of the Oas1b(r) allele into a flavivirus-induced disease susceptible mouse generates the resistant phenotype. *Virology* **368**(2)**,** 232-7.

Scherbik, S. V., Paranjape, J. M., Stockman, B. M., Silverman, R. H., and Brinton, M. A. (2006). RNase L plays a role in the antiviral response to West Nile virus. *J Virol* **80**(6)**,** 2987-99.

Scherbik, S. V., Stockman, B. M., and Brinton, M. A. (2007b). Differential expression of interferon (IFN) regulatory factors and IFN-stimulated genes at early times after West Nile virus infection of mouse embryo fibroblasts. *J Virol* **81**(21)**,** 12005-18.

Schmidt, A., Chernajovsky, Y., Shulman, L., Federman, P., Berissi, H., and Revel, M. (1979). An interferon-induced phosphodiesterase degrading (2'-5') oligoisoadenylate and the C-C-A terminus of tRNA. *Proc Natl Acad Sci U S A* **76**(10)**,** 4788-92.

Sharp, T. V., Raine, D. A., Gewert, D. R., Joshi, B., Jagus, R., and Clemens, M. J. (1999). Activation of the interferon-inducible (2'-5') oligoadenylate synthetase by the Epstein-Barr virus RNA, EBER-1. *Virology* **257**(2)**,** 303-13.

Shibata, S., Kakuta, S., Hamada, K., Sokawa, Y., and Iwakura, Y. (2001). Cloning of a novel 2',5'-oligoadenylate synthetase-like molecule, Oasl5 in mice. *Gene* **271**(2)**,** 261-71.

Thakur, C. S., Xu, Z., Wang, Z., Novince, Z., and Silverman, R. H. (2005). A convenient and sensitive fluorescence resonance energy transfer assay for RNase L and 2',5' oligoadenylates. *Methods Mol Med* **116,** 103-13.

Townsend, H. L., Jha, B. K., Han, J. Q., Maluf, N. K., Silverman, R. H., and Barton, D. J. (2008). A viral RNA competitively inhibits the antiviral endoribonuclease domain of RNase L. *RNA* **14**(6)**,** 1026-36.

Wreschner, D. H., McCauley, J. W., Skehel, J. J., and Kerr, I. M. (1981). Interferon action--sequence specificity of the ppp(A2'p)nA-dependent ribonuclease. *Nature* **289**(5796)**,** 414-7.

Yamamoto, Y., Sono, D., and Sokawa, Y. (2000). Effects of specific mutations in active site motifs of 2',5'-oligoadenylate synthetase on enzymatic activity. *J Interferon Cytokine Res* **20**(3)**,** 337-44.

Yan, W., Ma, L., Stein, P., Pangas, S. A., Burns, K. H., Bai, Y., Schultz, R. M., and Matzuk, M. M. (2005). Mice deficient in oocyte-specific oligoadenylate synthetase-like protein OAS1D display reduced fertility. *Mol Cell Biol* **25**(11)**,** 4615-24.

ELSEVIER LICENSE
TERMS AND CONDITIONS

Apr 19, 2011

This is a License Agreement between Husni M Elbahesh ("You") and Elsevier ("Elsevier") provided by Copyright Clearance Center ("CCC"). The license consists of your order details, the terms and conditions provided by Elsevier, and the payment terms and conditions.

All payments must be made in full to CCC. For payment instructions, please see information listed at the bottom of this form.

Supplier	Elsevier Limited The Boulevard,Langford Lane Kidlington,Oxford,OX5 1GB,UK
Registered Company Number	1982084
Customer name	Husni M Elbahesh
Customer address	1086 North Village Dr. Decatur, GA 30032
License number	2652701163203
License date	Apr 19, 2011
Licensed content publisher	Elsevier
Licensed content publication	Virology
Licensed content title	The Flv^r-encoded murine oligoadenylate synthetase 1b (Oas1b) suppresses 2-5A synthesis in intact cells
Licensed content author	H. Elbahesh, B.K. Jha, R.H. Silverman, S.V. Scherbik, M.A. Brinton
Licensed content date	20 January 2011
Licensed content volume number	409
Licensed content issue number	2
Number of pages	9
Start Page	262
End Page	270
Type of Use	reuse in a thesis/dissertation
Portion	full article
Format	both print and electronic
Are you the author of this Elsevier article?	Yes
Will you be translating?	No
Order reference number	
Title of your thesis/dissertation	Study of Innate Immune Response Components in West Nile virus infected cells
Expected completion date	May 2011

Estimated size (number of pages)	136
Elsevier VAT number	GB 494 6272 12
Permissions price	0.00 USD
VAT/Local Sales Tax	0.0 USD / 0.0 GBP
Total	0.00 USD
Terms and Conditions	

INTRODUCTION

1. The publisher for this copyrighted material is Elsevier. By clicking "accept" in connection with completing this licensing transaction, you agree that the following terms and conditions apply to this transaction (along with the Billing and Payment terms and conditions established by Copyright Clearance Center, Inc. ("CCC"), at the time that you opened your Rightslink account and that are available at any time at http://myaccount.copyright.com).

GENERAL TERMS

2. Elsevier hereby grants you permission to reproduce the aforementioned material subject to the terms and conditions indicated.

3. Acknowledgement: If any part of the material to be used (for example, figures) has appeared in our publication with credit or acknowledgement to another source, permission must also be sought from that source. If such permission is not obtained then that material may not be included in your publication/copies. Suitable acknowledgement to the source must be made, either as a footnote or in a reference list at the end of your publication, as follows:

“Reprinted from Publication title, Vol /edition number, Author(s), Title of article / title of chapter, Pages No., Copyright (Year), with permission from Elsevier [OR APPLICABLE SOCIETY COPYRIGHT OWNER].” Also Lancet special credit - “Reprinted from The Lancet, Vol. number, Author(s), Title of article, Pages No., Copyright (Year), with permission from Elsevier.”

4. Reproduction of this material is confined to the purpose and/or media for which permission is hereby given.

5. Altering/Modifying Material: Not Permitted. However figures and illustrations may be altered/adapted minimally to serve your work. Any other abbreviations, additions, deletions and/or any other alterations shall be made only with prior written authorization of Elsevier Ltd. (Please contact Elsevier at permissions@elsevier.com)

6. If the permission fee for the requested use of our material is waived in this instance, please be advised that your future requests for Elsevier materials may attract a fee.

7. Reservation of Rights: Publisher reserves all rights not specifically granted in the combination of (i) the license details provided by you and accepted in the course of this licensing transaction, (ii) these terms and conditions and (iii) CCC's Billing and Payment terms and conditions.

8. License Contingent Upon Payment: While you may exercise the rights licensed

immediately upon issuance of the license at the end of the licensing process for the transaction, provided that you have disclosed complete and accurate details of your proposed use, no license is finally effective unless and until full payment is received from you (either by publisher or by CCC) as provided in CCC's Billing and Payment terms and conditions. If full payment is not received on a timely basis, then any license preliminarily granted shall be deemed automatically revoked and shall be void as if never granted. Further, in the event that you breach any of these terms and conditions or any of CCC's Billing and Payment terms and conditions, the license is automatically revoked and shall be void as if never granted. Use of materials as described in a revoked license, as well as any use of the materials beyond the scope of an unrevoked license, may constitute copyright infringement and publisher reserves the right to take any and all action to protect its copyright in the materials.

9. Warranties: Publisher makes no representations or warranties with respect to the licensed material.

10. Indemnity: You hereby indemnify and agree to hold harmless publisher and CCC, and their respective officers, directors, employees and agents, from and against any and all claims arising out of your use of the licensed material other than as specifically authorized pursuant to this license.

11. No Transfer of License: This license is personal to you and may not be sublicensed, assigned, or transferred by you to any other person without publisher's written permission.

12. No Amendment Except in Writing: This license may not be amended except in a writing signed by both parties (or, in the case of publisher, by CCC on publisher's behalf).

13. Objection to Contrary Terms: Publisher hereby objects to any terms contained in any purchase order, acknowledgment, check endorsement or other writing prepared by you, which terms are inconsistent with these terms and conditions or CCC's Billing and Payment terms and conditions. These terms and conditions, together with CCC's Billing and Payment terms and conditions (which are incorporated herein), comprise the entire agreement between you and publisher (and CCC) concerning this licensing transaction. In the event of any conflict between your obligations established by these terms and conditions and those established by CCC's Billing and Payment terms and conditions, these terms and conditions shall control.

14. Revocation: Elsevier or Copyright Clearance Center may deny the permissions described in this License at their sole discretion, for any reason or no reason, with a full refund payable to you. Notice of such denial will be made using the contact information provided by you. Failure to receive such notice will not alter or invalidate the denial. In no event will Elsevier or Copyright Clearance Center be responsible or liable for any costs, expenses or damage incurred by you as a result of a denial of your permission request, other than a refund of the amount(s) paid by you to Elsevier and/or Copyright Clearance Center for denied permissions.

LIMITED LICENSE

The following terms and conditions apply only to specific license types:

15. **Translation**: This permission is granted for non-exclusive world **English** rights only unless your license was granted for translation rights. If you licensed translation rights you

may only translate this content into the languages you requested. A professional translator must perform all translations and reproduce the content word for word preserving the integrity of the article. If this license is to re-use 1 or 2 figures then permission is granted for non-exclusive world rights in all languages.

16. **Website**: The following terms and conditions apply to electronic reserve and author websites:
Electronic reserve: If licensed material is to be posted to website, the web site is to be password-protected and made available only to bona fide students registered on a relevant course if:
This license was made in connection with a course,
This permission is granted for 1 year only. You may obtain a license for future website posting,
All content posted to the web site must maintain the copyright information line on the bottom of each image,
A hyper-text must be included to the Homepage of the journal from which you are licensing at http://www.sciencedirect.com/science/journal/xxxxx or the Elsevier homepage for books at http://www.elsevier.com , and
Central Storage: This license does not include permission for a scanned version of the material to be stored in a central repository such as that provided by Heron/XanEdu.

17. **Author website** for journals with the following additional clauses:

All content posted to the web site must maintain the copyright information line on the bottom of each image, and
he permission granted is limited to the personal version of your paper. You are not allowed to download and post the published electronic version of your article (whether PDF or HTML, proof or final version), nor may you scan the printed edition to create an electronic version,
A hyper-text must be included to the Homepage of the journal from which you are licensing at http://www.sciencedirect.com/science/journal/xxxxx , As part of our normal production process, you will receive an e-mail notice when your article appears on Elsevier's online service ScienceDirect (www.sciencedirect.com). That e-mail will include the article's Digital Object Identifier (DOI). This number provides the electronic link to the published article and should be included in the posting of your personal version. We ask that you wait until you receive this e-mail and have the DOI to do any posting.
Central Storage: This license does not include permission for a scanned version of the material to be stored in a central repository such as that provided by Heron/XanEdu.

18. **Author website** for books with the following additional clauses:
Authors are permitted to place a brief summary of their work online only.
A hyper-text must be included to the Elsevier homepage at http://www.elsevier.com

All content posted to the web site must maintain the copyright information line on the bottom of each image
You are not allowed to download and post the published electronic version of your chapter, nor may you scan the printed edition to create an electronic version.
Central Storage: This license does not include permission for a scanned version of the material to be stored in a central repository such as that provided by Heron/XanEdu.

19. **Website** (regular and for author): A hyper-text must be included to the Homepage of the journal from which you are licensing at http://www.sciencedirect.com/science/journal/xxxxx. or for books to the Elsevier homepage at http://www.elsevier.com

20. **Thesis/Dissertation**: If your license is for use in a thesis/dissertation your thesis may be submitted to your institution in either print or electronic form. Should your thesis be published commercially, please reapply for permission. These requirements include permission for the Library and Archives of Canada to supply single copies, on demand, of the complete thesis and include permission for UMI to supply single copies, on demand, of the complete thesis. Should your thesis be published commercially, please reapply for permission.

21. **Other Conditions**:

v1.6

Gratis licenses (referencing $0 in the Total field) are free. Please retain this printable license for your reference. No payment is required.

If you would like to pay for this license now, please remit this license along with your payment made payable to "COPYRIGHT CLEARANCE CENTER" otherwise you will be invoiced within 48 hours of the license date. Payment should be in the form of a check or money order referencing your account number and this invoice number RLNK10972734.
Once you receive your invoice for this order, you may pay your invoice by credit card. Please follow instructions provided at that time.

Make Payment To:
Copyright Clearance Center
Dept 001
P.O. Box 843006
Boston, MA 02284-3006

For suggestions or comments regarding this order, contact Rightslink Customer Support: customercare@copyright.com or +1-877-622-5543 (toll free in the US) or +1-978-646-2777.

ADDENDUM TO CHAPTER 4

Additional data -- Results and Discussion

Gel mobility shift data (Fig. 4.4) and the observation that Oas1b can inhibit Oas1a synthetase activity in a dose-dependent manner (Fig. 4.5) strongly suggest that Oas1b associates with Oas1a to mediate this inhibition. To test this hypothesis, C3H/He-1B/1A MEFs that stably express 3x FLAG-tagged Oas1b and Xpress-tagged Oas1a were made and Oas1a and Oas1b *in vivo* interactions in cell lysates were analyzed by co-immunoprecipitation. C3H/He-1B/1A S2 lysates were first incubated with rabbit anti-FLAG agarose beads or nonspecific rabbit-IgG agarose beads. Oas1a was co-immunoprecipitated by anti-FLAG antibody but not by a non-specific IgG (Fig. 4.6). These data indicate that Oas1a specifically interacts with Oas1b *in vivo*. A reciprocal immunoprecipitation using the anti-Xpress antibody proved unsuccessful because Oas1a was not efficiently immunoprecipitated (data not shown) suggesting that the use of anti-Xpress antibody for immunoprecipitation is not appropriate under the conditions used.

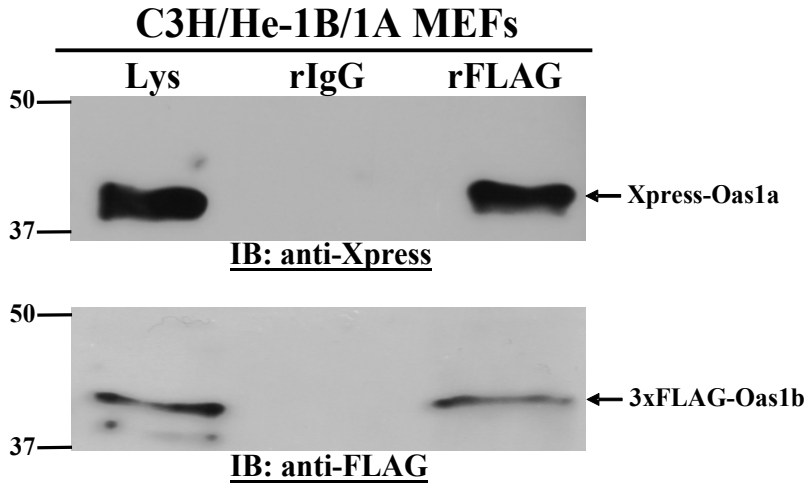

Figure 4.6. Co-immunoprecipitation of Oas1a and Oas1b. C3H/He-1B/1A cells were lysed and S2 fractions were prepared. Rabbit anti-FLAG agarose beads or rabbit control IgG agarose beads were used

for immunoprecipitation. Immunoprecipitated proteins were separated by 10% SDS-PAGE and detected by Western blotting using mouse anti-Xpress antibody or mouse anti-FLAG.

Tetramerization of the human p42 and p48 OAS1 isoforms were reported to occur and to require an intact C-F-K motif. Substitutions in this motif completely abolished human OAS1 synthetase activity (Ghosh et al., 1997a). Unlike human OAS1 proteins, the active mouse synthetases Oas1a and Oas1g have substitutions in the CFK motif predicted to inactivate their function. However, Oas1a co-immunoprecipitation with Oas1b suggests that these proteins do form multimers. This observation strongly supports the hypothesis that Oas1b inhibits Oas1a synthetase activity *in vitro* and *in vivo* through protein-protein interactions that do not require a CFK motif.

Additional data – Materials and Methods

Cells. A C3H/He-Oas1b clonal MEF cell line was generated by transfection of C3H/He MEFs with an He-Oas1b expression construct that encodes a N-terminally 3x-FLAG tagged full-length Oas1b, followed by clonal cell selection in the presence of 5 μg/ml of G418 (Gibco) (Courtney et al., unpublished data). C3H/He-1B/1A MEF cell lines were generated by transfection of C3H/He-Oas1b MEFs with a pHis/Max-Oas1a encoding a N-terminally 6X His and Xpress-tagged Oas1a followed by selection in the presence of 250 μg/ml of G418 (Gibco) and 850 μg/ml of blasticidin (Invitrogen). The resultant cell line was designated C3H/He-1B/1A. Cells were grown in minimal essential medium supplemented with 10% heat-inactivated fetal bovine serum, 10 μg/ml gentamicin and the two drugs at 37°C in 5% CO_2.

Cloning Oas1a cDNA. Oas1a cDNA was amplified by PCR using specific primers and subcloned into the pTOPO-His/Max mammalian expression vector (Invitrogen). The recombinant protein expressed has N-terminal 6X His and Xpress tags. The resultant construct was designated pHis/Max-Oas1a.

Co-immunoprecipitation assay. C3H/He-1B/1A MEFs were rinsed with cold PBS and then lysed with FLAG-lysis buffer [50 mM Tris-HCl (pH 7.4), 150 mM NaCl, 1% Triton-X 100 and 1 mM EDTA] supplemented with Complete Mini EDTA-Free Protease Inhibitor Cocktail (Roche). Cell lysates were incubated on ice for 30 min, sonicated and then centrifuged at 2000 x g for 5 min at 4°C. The supernatant was designated the S2 fraction. The protein concentrations of the S2 lysates were measured using a Bradford Assay (Bio-Rad) following the manufacturer's protocol. Protein concentration was adjusted to 1 μg/μl with FLAG-lysis buffer. S2 lysates (750 μl per reaction containing ~750 μg total protein) were incubated with 30 μl of rabbit anti-FLAG-agarose beads (10 μg of antibody) or 30 μl of agarose beads coupled to a non-specific rabbit IgG (10 μg of antibody) overnight at 4°C with rotation. Beads were collected by centrifugation at 750 x g for 2 min at 4°C, and then washed 5 times with 1 ml of FLAG-lysis buffer. Proteins were eluted by boiling in 2X SDS sample buffer for 5 min.

Western blot analysis. Proteins were separated by 10% SDS/PAGE, transferred electrophoretically to nitrocellulose membranes, and blocked with 5% non-fat dry milk (NFDM) in 1X TBS + 0.05% Tween-20 (TBST) for 1 h at room temperature. Primary antibody diluted in 5% NFDM-TBST was then incubated with the membrane overnight at 4ºC, the membranes were washed 3 times in 1X TBST and then incubated with a

secondary antibody diluted in 5% NFDM-TBST for 1 h at room temperature. After being washed twice in 1X TBST and once in 1X TBS, the membranes were processed for enhanced chemiluminescence using a Super-Signal West Pico detection kit (Pierce, Rockford, IL) according to the manufacturer's instructions. Membranes were incubated with either anti-Xpress (Invitrogen) (1:1000 in 5% NFDM-TBST) or anti-FLAG (Sigma) (1:1000 in 5% NFDM-TBST).

CHAPTER 5

Synthetase activity analysis of human OAS1 splice variants.

INTRODUCTION

Mammalian genomes encode a family of antiviral, IFN-inducible 2'-5' OAS proteins that are activated by dsRNA or hairpin structures formed by ssRNA to polymerize ATP into 2-5A that activates RNase L which cleaves cellular and viral ssRNAs after UU and UA dinucleotides (Floyd-Smith et al., 1981; Kerr and Brown, 1978; Wreschner et al., 1981). Two distinguishing features of the OAS family are their ability to form 2'-5' linked oligonucleotides and their activation by dsRNA in spite of the lack of a canonical dsRNA binding motif (Ghosh et al., 1991; Hartmann et al., 2003). In humans, small, medium and large OAS proteins are encoded by the OAS1, OAS2 and OAS3 genes, respectively. Additionally, OASL proteins, encoded by OAS-like genes, contain C-terminal ubiquitin-like domains (Hartmann et al., 1998b; Rebouillat et al., 1998). The OAS1 protein contains a single OAS unit whereas the OAS2 and OAS3 proteins are composed of 2 and 3 OAS units, respectively (Marie and Hovanessian, 1992; Rebouillat et al., 1998). Interestingly, the conserved activity motifs in the last OAS unit in OAS2 and OAS3 share the highest sequence identity with OAS1 (Hartmann et al., 2003). The catalytic activity of OAS proteins has been postulated to depend on its multimerization state. Tetramerization of the OAS1 isoforms, p42 and p48, has been reported to be required for synthetase activity (Ghosh et al., 1997). However, monomeric p42 that was expressed in insect cells was fully active (Justesen et al., 2000).

Catalytically active OAS2 and OAS3 exist as dimers and monomers, respectively (Marie and Hovanessian, 1992). Oligomerization of the OAS proteins is mediated by the CFK motif at the C-terminus of the OAS1 and OAS2 proteins; this motif is not conserved in any of the OAS domains of OAS3 (Ghosh et al., 1997). The length of 2-5A generated by the OAS proteins varies. OAS1 and OAS2 proteins are capable of synthesizing higher order 2-5A oligomers (2-5A tetramers or more), while OAS3 mainly synthesizes 2-5A dimers that do not activate RNase L (Hovanessian and Justesen, 2007).

In contrast to the 8 Oas1 genes that are present in mice, humans have a single OAS1 gene that is alternatively spliced to yield multiple isoforms. These isoforms all share the enzymatic N-terminal 346 amino acids residues but encode different C-termini due to alternative splicing (Benech et al., 1985; Ghosh et al., 2001). Polymorphisms at two positions result in the expression of different splice variants. At least 5 isoforms of human OAS1 (p42, p44, p46, p48 and p52) have been reported. Both the p42 and p44 isoforms have been reported to be produced by all genotypes (Belsher et al., 2007). An A/G SNP (rs10774671) at the intron-5/exon-6 splice acceptor site alters OAS1 splicing (Bonnevie-Nielsen et al., 2005; Ghosh et al., 1991; Justesen et al., 2000; Saunders et al., 1985). The A-allele at the intron-5/exon-6 splice acceptor site generates two transcripts, one that encodes the p48 isoform and one that encodes the p52 OAS1 isoform. The G-allele at this site leads to production of the p46 transcript (Fig. 5.1). An additional variant of the p42 isoform encodes a Ser^{162} to Gly^{162} substitution that is generated by the G-allele of an exon 3 SNP; however, this substitution is not expected to affect synthetase activity since it is not located in a catalytic region (Belsher et al., 2007).

Four novel OAS1 cDNAs have recently been identified by the Brinton lab that encode proteins designated p41, p44A, p49 and p49A (Perelygin et al., unpublished data). The p49 isoform is produced by all tested genotypes. The p41 isoform is produced when the G-allele is present in the intron-5/exon-6 splice acceptor site. The A-allele, together with an A-insertion in exon 7 that leads to a frame shift, results in premature translation termination and production of the p44 variant p44A and the p49 variant p49A (Fig. 5.1).

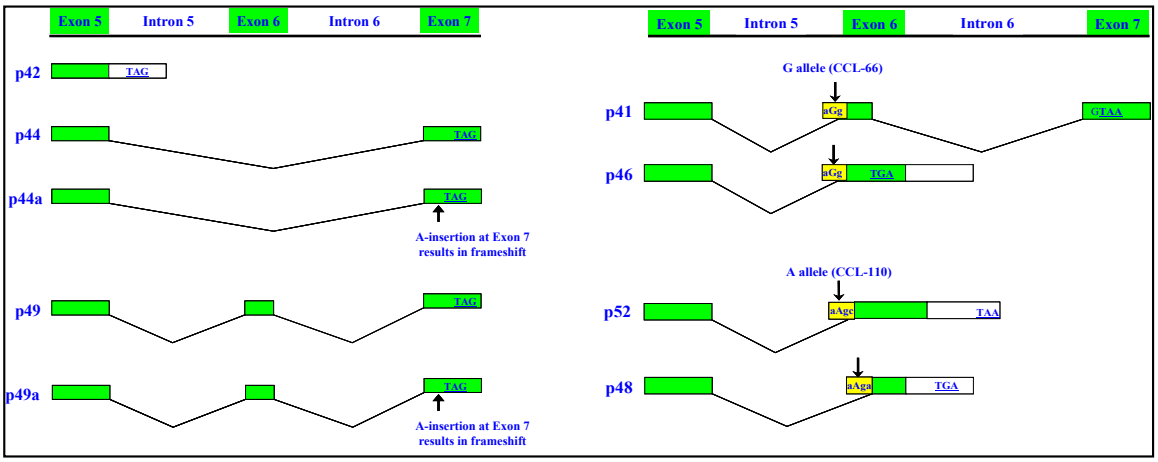

Figure 5.1. SNP-dependent generation of variant human OAS1 transcripts.

Although the p42, p44, p46, p48 and p52 transcripts were identified some time ago, the majority of the initial studies used OAS1 preparations that were presumed to contain only a single OAS1 isoform, but this was not the case according to a comprehensive review by Johnston and Torrence (1984). For instance, a previous study that reported synthetase activity for the p46 isoform (Chebath et al., 1987) used cellular extracts that contained p42 (referred to as p40) and p46, and most likely also p41, p44 and p49 all of which could have contributed to the observed synthetase activity. In addition, the antibody used to identify and/or immunoprecipitate the p46 and p42 proteins recognized a region that is present in all OAS1 isoforms as well as in OAS2 and OAS3

proteins. One study mis-identified the human p42 and p48 OAS1 isoforms as murine proteins designated 3-9 and 9-2, respectively (Ghosh et al., 1991); this was likely due to contamination of murine RNA preparations with human mRNA (Justesen et al., 2000). Most of the currently published functional studies on human OAS1 synthetase activity are limited to the p42 and p48 isoforms (Ghosh et al., 1997; Ghosh et al., 2001; Justesen et al., 2000). However, a recombinant p46 expressed in insect cells was reported to be an active synthetase (Hartmann et al., 1998a). The alternatively spliced transcripts have not yet been characterized.

The functions of most of the individual isoforms have not been tested and it is tempting to speculate that p42, which is encoded by all genotypes, provides only antiviral activity while the alternatively spliced isoforms might have additional functions. Accordingly, the p48 isoform was reported to exihibt proapoptotic activity by interacting with the anti-apoptotic Bcl-2 and $Bclx_L$ proteins via a C-terminal BH3 domain and was also reported to exhibit mitochondrial localization (Ghosh et al., 2001). Structural constraints observed in the crystal structure of the pig OAS1 protein suggest that the C-terminal alterations in the isoforms translated from alternatively spliced human OAS1 transcripts might affect enzymatic activity (Hartmann et al., 2003). The different C-termini may be responsible for alternative functions of the various OAS1 isoforms. The 2-5A synthetase activity of each of the previously described OAS1 isoforms as well as the recently identified OAS1 splice variant proteins was assessed in the current study.

RESULTS

Expression and purification of OAS1 recombinant proteins. A comprehensive analysis of the OAS1 2-5A synthetase activity of isoforms other than p42, p46 and p48 has not been reported. To assess the ability of these isoforms to polymerize ATP into 2-5A, various OAS1 isoforms as well as recombinant LacZ protein (negative control) fused to N-terminal 6X His and V5 tags were expressed in bacteria. Proteins from uninduced and IPTG-induced bacterial extracts were separated by 10% SDS-PAGE. Fusion proteins were not readily detectable in induced bacterial lysates by Coomassie blue staining (data not shown) suggesting that expression of the recombinant OAS proteins was not efficient. However, fusion proteins of the expected molecular masses were detected by immunoblotting with anti-V5 antibody only from the induced bacterial lysates confirming expression of these fusion proteins (Fig. 5.2).

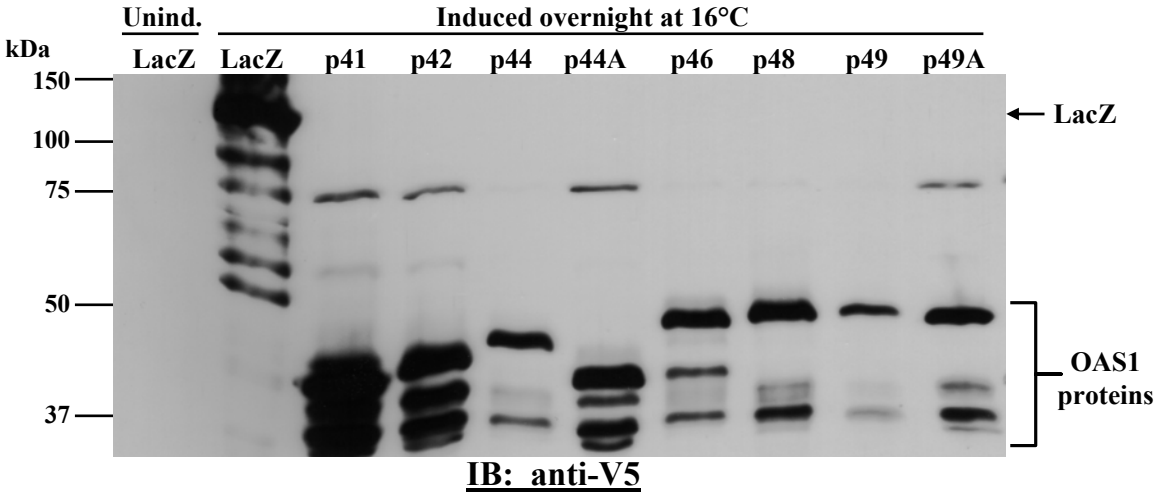

Figure 5.2. Expression of OAS1 isoform proteins. Individual human OAS1 isoform fusion proteins were expressed in bacteria. Bacteria were lysed and proteins in the crude bacterial lysates were separated by 10% SDS-PAGE, transferred to nitrocellulose membrane and immunoblotted with anti-V5 antibody.

Some breakdown of the OAS1 isoforms was observed as indicated by bands corresponding to N-terminal fragments on the anti-V5 Western blot (Fig. 5.2). Breakdown was also observed for the control protein, LacZ, which was expressed from the same plasmid and in the same cells as the OAS1 isoforms. Taken together with the poor expression levels, these data indicate some toxicity was associated with bacterial expression of the OAS1 fusion proteins; this is consistent with previously published data obtained when murine Oas1 fusion proteins were expressed in bacteria (Elbahesh et al., 2011).

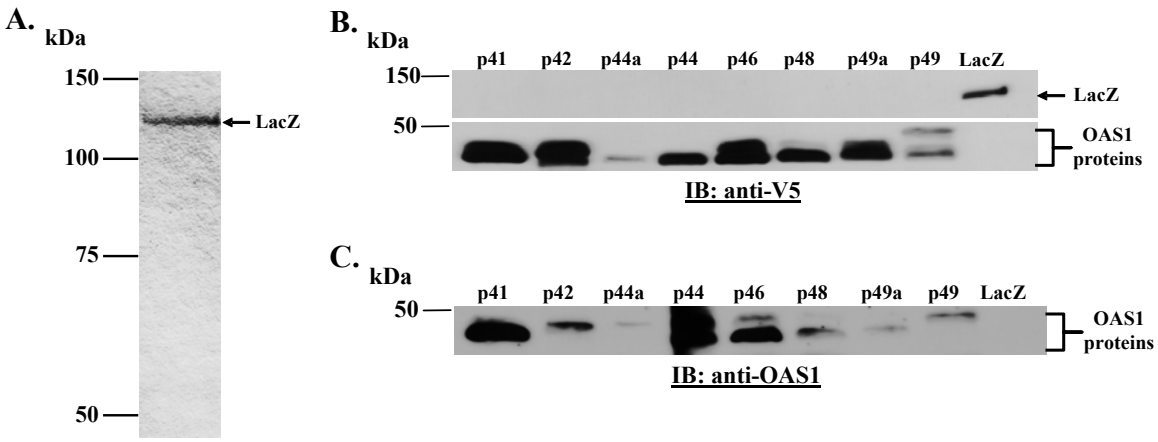

Figure 5.3. Purification of OAS1 isoform proteins. (A) Purification of the LacZ control protein. LacZ fusion was expressed in bacteria, partially purified on a metal affinity resin column, separated by 10% SDS-PAGE and visualized by Coomassie blue staining. (B and C) Immunoblot of purified OAS1 isoforms. Human OAS1 fusion proteins were expressed in bacteria, partially purified on metal affinity resin columns, separated by 10% SDS-PAGE, transferred to nitrocellulose membrane and immunoblotted for OAS1 isoforms detected with anti-V5 antibody (B) or anti-OAS1 antibody (C).

The OAS1 isoforms and recombinant LacZ were partially purified on Talon metal affinity columns and then separated by 10% SDS-PAGE. Recombinant LacZ was detectable by Coomassie staining following SDS-PAGE (Fig. 5.3A). Purified OAS1 isoform proteins were detected by Western blotting with anti-V5 antibody or anti-OAS1 antibody (Fig. 5.3B and 5.3C, respectively). As expected, LacZ was detected only by

anti-V5 antibody. The anti-V5 antibody detected a number of the OAS1 isoforms more strongly than the anti-OAS1 antibody suggesting that the anti-OAS1 antibody may not recognize all the isoforms with equal efficiency.

2-5A synthetase activity of recombinant OAS1 isoforms. To assess the ability of the human OAS1 isoforms to synthesize 2-5A, partially purified proteins were incubated with poly(I:C) and α-^{32}P-ATP at 30°C for 18 h. The 2-5A produced was separated by denaturing 8M urea 20% PAGE and visualized by autoradiography. Consistent with previous reports (Ghosh et al., 1997; Ghosh et al., 2001; Justesen et al., 2000), p42 and p48 synthesized higher order 2-5As were (2-5A tetramers or higher order products) demonstrating that the presence of N-terminal 6X His and V5 tags did not inhibit synthetase activity. Higher order 2-5A was synthesized by p41, p46, p49 and p49A (Fig. 5.4). Pig OAS1 protein (provided by Rune Hartmann, University of Aarhus, Denmark) was used as a positive control. This protein is 73% identical in sequence to human p46 OAS1 and has similar activity (Hartmann et al., 2003). As expected, the pig OAS1 efficiently produced higher order 2-5A. In contrast, p44A, which is a truncated variant of the p44 isoform, only produced 2-5A dimers (Fig. 5.4). 2-5A dimers have been reported to be very weak activators of RNase L (Dong et al., 1994). Partially purified lacZ expressed from the same vector was used as a negative control. As expected, LacZ did not produce 2-5A. A small spot that migrated above the free ATP was observed in the LacZ reaction suggesting that it might bind to ATP (Fig. 5.4). The migration of this spot

was different from that observed for p44A or any of the other isoforms indicating that synthetase activity was only observed with the OAS1 proteins.

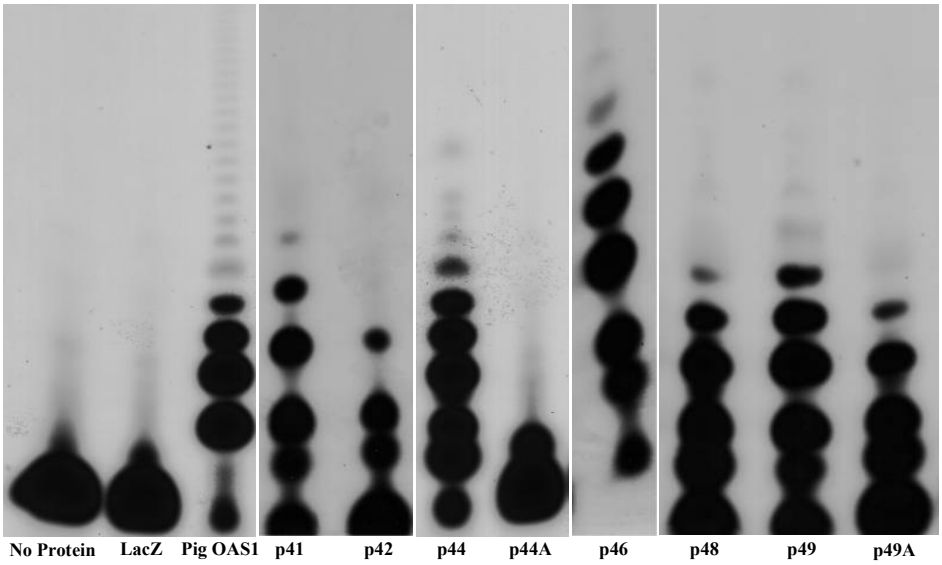

Figure 5.4. Analysis of human OAS1 isoform 2-5A synthetase activity. Each human OAS1 isoform (22 µl) was incubated with α^{32}P-ATP and poly (I:C) for 18 h at 30°C. LacZ (22 µl) was used as a negative control. Pig OAS1 (1 µg) was used as a positive control. Two µl of each reaction were then electrophoresed on a 20% polyacrylamide urea denaturing gel.

The data obtained indicate that all of the OAS1 isoforms tested, including the newly identified p41, p44A, p49 and p49A isoforms, are able to synthesize 2-5A *in vitro.* However, p44A only synthesizes dimeric 2-5A. Because the OAS1 variant proteins were expressed at low and varied levels and only partially purified, a quantitative comparison of the 2-5A activities of the various isoforms was not carried out.

DISCUSSION

The OAS/RNase L system represents an important component of the IFN-dependent antiviral response (Samuel, 2001). The proteins of the OAS family polymerize

ATP into oligoA that is uniquely linked by 2'-5' phosphodiester bonds. The only function currently identified for 2-5A is the activation of the latent cellular endoribonuclease RNase L. Activated RNase L cleaves viral and cellular ssRNAs. In humans, multiple OAS1 proteins are expressed from a single OAS1 gene due to alternatively spliced mRNAs and allelic variation. Five isoforms (p42, p44, p46, p48 and p52) were previously reported (Benech et al., 1985; Bonnevie-Nielsen et al., 2005; Ghosh et al., 2001; Ghosh et al., 1991; Justesen et al., 2000; Saunders et al., 1985). The identification of 4 new OAS1 isoforms (p41, p44A, p49 and p49A) (Perelygin et al. unpublished data) and no previous data on the synthetase activity of the majority of the OAS1 isoforms prompted the current study.

While each of the OAS1 proteins encode all of the functional motifs required for synthetase activity, the presence of different C-termini might alter the structures of some of the isoforms resulting in inactive synthetases. Of the 9 OAS1 isoforms, p42, p46 and p48 are the only ones previously characterized for their ability to synthesize 2-5A (Ghosh et al., 1997; Ghosh et al., 2001; Hartmann et al., 1998a; Justesen et al., 2000). All of the OAS1 isoforms encode an intact C-F-K motif which was reported to mediate OAS1 tetramer formation required for activation (Ghosh et al., 1997). The p41, p42, p46, p49 and p49A isoforms were observed to polymerize ATP into 2-5A oligomers in the current study. These data suggest that all of the OAS1 isoforms adopt a conformation that does not inhibit OAS synthetase activity even though different C-terminal regions are present. It is possible that sequences within the different C-terminal regions may have been selected because they form folded structures that do not impede and/or stabilize the

catalytically active structure. An alternative explanation is that short deletions of or changes in the C-terminal sequences are tolerated because they occur far enough away from the functional OAS unit. However, the p44A isoform only synthesized 2-5A dimers which suggests that deletions in the C-terminus may affect the type of 2-5A made.

Antiviral activity has been reported to be associated with the expression of specific OAS1 isoforms. For example, an A-allele in the intron-5/exon-6 splice acceptor site which leads to the expression of the p48 and p52, but not p46 or p41, OAS1 isoforms has been reported to correlate with an increased risk of infection with WNV (Lim et al., 2009). Another study reported that Dengue replication is blocked by a RNase L dependent mechanism in human cells over-expressing p42 or p46, but not p44, p48 or p52, (Lin et al., 2009). However, Lin et al. (2009) also reported an antiviral effect in cells over-expressing p100 (OAS3) which was previously reported to synthesize RNase L-inhibitory 2-5A dimers (Dong et al., 1994). Although the p100 transfected cells produced RNase L cleavage products, these may have been due to the synthesis of longer 2-5A by endogenous human OAS1 isoforms.

In addition to possible effects on protein structure and synthetase activity, the presence of different C-termini may result in differential cellular localization and/or facilitate binding of the OAS1 isoforms to unique protein partners. The p42 isoform was reported to be cytosolic as determined by subcellular fractionation (Hovanessian et al., 1987). Consistent with this observation, p42 is thought to interact with the cytosolic domain of the prolactin-receptor. This interaction was suggested to mediate inhibition of prolactin-induced STAT1 binding at the IRF-1 promoter GAS (IFN-γ activated sequence)

element observed in p42-transfected cells (McAveney et al., 2000). The p48 isoform is predicted to contain a Bcl-2 homology-3 (BH3) domain and was shown to mediate cellular apoptosis by interacting with Bcl-2 and $Bclx_L$ (Ghosh et al., 2001). Consistent with these observations, over-expressed p48 was reported to colocalize with mitochondria in osteosarcoma human cells (Ghosh et al., 2001). The fact that both the p42 and p48 isoforms have been reported to carry out alternative functions, suggests that synthetase activity does not prevent these functions. The data presented in the study provide preliminary data for future functional studies of the OAS1 isoforms.

MATERIALS AND METHODS

Cloning and expression of OAS1 isoforms. Primary human skin fibroblast cell lines, CCL-66 and CCL110, were maintained at 37°C in 5% CO_2 in Eagle's Minimum Essential Medium containing 10% heat inactivated fetal bovine serum (FBS), 100 μg/ml streptomycin and 100 IU/ml penicillin. Cell lines were treated with 1000 IU/ml of human recombinant IFN-β (Sigma) for 16 h to induce expression of OAS1 mRNA, total RNA was exctracted using RNeasy Mini Kit (Qiagen) and first-strand cDNA was generated using the ThermoScript RNase H Reverse Transcriptase kit (Invitrogen) and an oligo-dT primer. OAS1 cDNAs were cloned into the pCR-XL-TOPO TA cloning vector (Invitrogen) and plasmid DNA was amplified in One Shot TOP10 chemically competent *E. coli* cells. Plasmid DNA containing cDNA for each of the isoforms was provided by Dr. Andrey Perelygin.

Human OAS1 cDNAs for the p41, p42, p44A, p44, p46, p48, p49A and p49 isoforms was subcloned into the pET151 expression vector (Invitrogen) which encodes 6X His and V5 N-terminal tags. Plasmids were transformed into One Shot TOP10 chemically competent *E. coli* and sequenced. OAS1 isoform proteins were expressed in pET151-p41, -p42, -p44A, -p44, -p46, -p48, -p49A or -p49 transformed BL21-(DE3)-pLysS cells grown in 125 ml of LB media containing 0.05% glucose and 100 μg/ml of carbenicillin (CRB). Expression was induced with 1 mM IPTG overnight at 16°C. Cells were pelleted by centrifugation at 6,000 x g for 10 min at 4°C in a Avanti J30-I centrifuge using a JA-10 rotor (Beckman Coulter). The cells were resuspended in 10 ml of 1X Equilibration buffer [50 mM sodium phosphate (pH 7.4) and 300 mM NaCl] supplemented with Complete Mini EDTA-Free Protease inhibitor cocktail (Roche) and frozen at -80°C until use.

Purification of OAS1 isoform proteins. For cell lysis, Cellytic Express lysis powder (Sigma) was added to thawed cell suspensions and incubated at 37°C for 30 min with shaking. Samples were then clarified by centrifugation at 15,000 x g for 10 min at 4°C in a Avanti J30-I centrifuge using a JA-20 rotor (Beckman Coulter). Clarified supernatant volume was increased to 20 ml by addition of 1X Equilibration buffer and proteins were column purified by loading onto columns containing 1 ml of TALON metal affinity nickel resin (Clontech), the columns were washed with 1X Wash buffer [50 mM sodium phosphate (pH 7.4), 300 mM NaCl and 5 mM imidazole] and the bound proteins were eluted with 5 ml of 1X Elution buffer [50 mM sodium phosphate (pH 7.4), 300 mM NaCl and 150 mM imidazole. The eluted protein fractions were combined, the buffer

exchanged with protein storage buffer [20 mM Hepes-KOH (pH7.5), 50 mM KCl, 25 mM $Mg(OAc)_2$, 7 mM β-ME, 0.03 mM EDTA and 0.25% glycerol] supplemented with Complete Mini EDTA-Free Protease inhibitor cocktail (Roche) and concentrated using a Microcon centrifugal filter device (10,000 kDa cut-off) (Millipore) prior to use in *in vitro* 2-5 A synthetase assays. For short term storage, proteins were stored at 4°C or were aliquoted and stored in -80°C.

Western blotting. Proteins were resolved by SDS-PAGE, transferred to a nitrocellulose membrane and blocked with 5% non-fat dry milk (NFDM) in 1X TBS + 0.05% Tween-20 (TBST) for 1 h at room temperature. Anti-V5 (Sigma) (1:1000 in 5% NFDM-TBST) or anti-OAS1 (Novus Biological) (1:1000 in 5% NFDM-TBST) primary antibody was then incubated with the membrane overnight at 4ºC, the membranes were washed 3 times in 1X TBST and then incubated with a HRP-conjugated secondary antibody diluted in 5% NFDM-TBST for 1 h at room temperature. After washing the membrane twice in 1X TBST and once in 1X TBS, membranes were processed for enhanced chemiluminescence using a Super-Signal West Pico detection kit (ThermoScientific) according to the manufacturer's instructions.

2'-5' OAS activity assay. The reaction mixture (50 µl) contained 2′-5′ OAS activity assay buffer [20 mM HEPES-KOH pH 7.5, 50 mM KCl, 25 mM $Mg(OAC)_2$, 10 mM creatine phosphate, 1U/µl creatine kinase, 5 mM ATP, and 7 mM β-ME], 20 µCi α^{32}p-ATP and 50 ng/µl poly (I:C). Twenty-two µl of OAS1 recombinant proteins was added to the reaction mixtures, incubated at 30°C for 18 hrs and stopped by addition of 50 µl of

Gel Loading Buffer II (95% formamide, 18 mM EDTA, 0.025% SDS, xylene cyanol, and bromophenol blue) (Ambion). Two µl of each reaction were loaded onto a 20% polyacrylamide gel and electrophoresed at 800 V for 3.5 hrs. Radiolabeled 2-5A was visualized by autoradiography.

REFERENCES:

Belsher, J. L., Gay, P., Brinton, M., DellaValla, J., Ridenour, R., Lanciotti, R., Perelygin, A., Zaki, S., Paddock, C., Querec, T., Zhu, T., Pulendran, B., Eidex, R. B., and Hayes, E. (2007). Fatal multiorgan failure due to yellow fever vaccine-associated viscerotropic disease. *Vaccine* **25**(50)**,** 8480-5.

Benech, P., Mory, Y., Revel, M., and Chebath, J. (1985). Structure of two forms of the interferon-induced (2'-5') oligo A synthetase of human cells based on cDNAs and gene sequences. *Embo J* **4**(9)**,** 2249-56.

Bonnevie-Nielsen, V., Field, L. L., Lu, S., Zheng, D. J., Li, M., Martensen, P. M., Nielsen, T. B., Beck-Nielsen, H., Lau, Y. L., and Pociot, F. (2005). Variation in antiviral 2',5'-oligoadenylate synthetase (2'5'AS) enzyme activity is controlled by a single-nucleotide polymorphism at a splice-acceptor site in the OAS1 gene. *Am J Hum Genet* **76**(4)**,** 623-33.

Chebath, J., Benech, P., Hovanessian, A., Galabru, J., and Revel, M. (1987). Four different forms of interferon-induced 2',5'-oligo(A) synthetase identified by immunoblotting in human cells. *J Biol Chem* **262**(8)**,** 3852-7.

Dong, B., Xu, L., Zhou, A., Hassel, B. A., Lee, X., Torrence, P. F., and Silverman, R. H. (1994). Intrinsic molecular activities of the interferon-induced 2-5A-dependent RNase. *J Biol Chem* **269**(19)**,** 14153-8.

Elbahesh, H., Jha, B. K., Silverman, R. H., Scherbik, S. V., and Brinton, M. A. (2011). The Flvr-encoded murine oligoadenylate synthetase 1b (Oas1b) suppresses 2-5A synthesis in intact cells. *Virology* **409**(2)**,** 262-70.

Floyd-Smith, G., Slattery, E., and Lengyel, P. (1981). Interferon action: RNA cleavage pattern of a (2'-5')oligoadenylate--dependent endonuclease. *Science* **212**(4498)**,** 1030-2.

Ghosh, A., Sarkar, S. N., Guo, W., Bandyopadhyay, S., and Sen, G. C. (1997). Enzymatic activity of 2'-5'-oligoadenylate synthetase is impaired by specific mutations that affect oligomerization of the protein. *J Biol Chem* **272**(52)**,** 33220-6.

Ghosh, A., Sarkar, S. N., Rowe, T. M., and Sen, G. C. (2001). A specific isozyme of 2'-5' oligoadenylate synthetase is a dual function proapoptotic protein of the Bcl-2 family. *J Biol Chem* **276**(27)**,** 25447-55.

Ghosh, S. K., Kusari, J., Bandyopadhyay, S. K., Samanta, H., Kumar, R., and Sen, G. C. (1991). Cloning, sequencing, and expression of two murine 2'-5'-oligoadenylate synthetases. Structure-function relationships. *J Biol Chem* **266**(23)**,** 15293-9.

Hartmann, R., Justesen, J., Sarkar, S. N., Sen, G. C., and Yee, V. C. (2003). Crystal structure of the 2'-specific and double-stranded RNA-activated interferon-induced antiviral protein 2'-5'-oligoadenylate synthetase. *Mol Cell* **12**(5)**,** 1173-85.

Hartmann, R., Norby, P. L., Martensen, P. M., Jorgensen, P., James, M. C., Jacobsen, C., Moestrup, S. K., Clemens, M. J., and Justesen, J. (1998a). Activation of 2'-5' oligoadenylate synthetase by single-stranded and double-stranded RNA aptamers. *J Biol Chem* **273**(6)**,** 3236-46.

Hartmann, R., Olsen, H. S., Widder, S., Jorgensen, R., and Justesen, J. (1998b). p59OASL, a 2'-5' oligoadenylate synthetase like protein: a novel human gene

related to the 2'-5' oligoadenylate synthetase family. *Nucleic Acids Res* **26**(18)**,** 4121-8.

Hovanessian, A. G., and Justesen, J. (2007). The human 2'-5'oligoadenylate synthetase family: unique interferon-inducible enzymes catalyzing 2'-5' instead of 3'-5' phosphodiester bond formation. *Biochimie* **89**(6-7)**,** 779-88.

Hovanessian, A. G., Laurent, A. G., Chebath, J., Galabru, J., Robert, N., and Svab, J. (1987). Identification of 69-kd and 100-kd forms of 2-5A synthetase in interferon-treated human cells by specific monoclonal antibodies. *Embo J* **6**(5)**,** 1273-80.

Justesen, J., Hartmann, R., and Kjeldgaard, N. O. (2000). Gene structure and function of the 2'-5'-oligoadenylate synthetase family. *Cell Mol Life Sci* **57**(11)**,** 1593-612.

Kerr, I. M., and Brown, R. E. (1978). pppA2'p5'A2'p5'A: an inhibitor of protein synthesis synthesized with an enzyme fraction from interferon-treated cells. *Proc Natl Acad Sci U S A* **75**(1)**,** 256-60.

Lim, J. K., Lisco, A., McDermott, D. H., Huynh, L., Ward, J. M., Johnson, B., Johnson, H., Pape, J., Foster, G. A., Krysztof, D., Follmann, D., Stramer, S. L., Margolis, L. B., and Murphy, P. M. (2009). Genetic variation in OAS1 is a risk factor for initial infection with West Nile virus in man. *PLoS Pathog* **5**(2)**,** e1000321.

Lin, R. J., Yu, H. P., Chang, B. L., Tang, W. C., Liao, C. L., and Lin, Y. L. (2009). Distinct antiviral roles for human 2',5'-oligoadenylate synthetase family members against dengue virus infection. *J Immunol* **183**(12)**,** 8035-43.

Marie, I., and Hovanessian, A. G. (1992). The 69-kDa 2-5A synthetase is composed of two homologous and adjacent functional domains. *J Biol Chem* **267**(14)**,** 9933-9.

McAveney, K. M., Book, M. L., Ling, P., Chebath, J., and Yu-Lee, L. (2000). Association of 2',5'-oligoadenylate synthetase with the prolactin (PRL) receptor: alteration in PRL-inducible stat1 (signal transducer and activator of transcription 1) signaling to the IRF-1 (interferon-regulatory factor 1) promoter. *Mol Endocrinol* **14**(2)**,** 295-306.

Rebouillat, D., Marie, I., and Hovanessian, A. G. (1998). Molecular cloning and characterization of two related and interferon-induced 56-kDa and 30-kDa proteins highly similar to 2'-5' oligoadenylate synthetase. *Eur J Biochem* **257**(2)**,** 319-30.

Samuel, C. E. (2001). Antiviral actions of interferons. *Clin Microbiol Rev* **14**(4)**,** 778-809, table of contents.

Saunders, M. E., Gewert, D. R., Tugwell, M. E., McMahon, M., and Williams, B. R. (1985). Human 2-5A synthetase: characterization of a novel cDNA and corresponding gene structure. *Embo J* **4**(7)**,** 1761-8.

Wreschner, D. H., McCauley, J. W., Skehel, J. J., and Kerr, I. M. (1981). Interferon action--sequence specificity of the ppp(A2'p)nA-dependent ribonuclease. *Nature* **289**(5796)**,** 414-7.